Beyond Green Planet: A Comprehensive and Systematic Second-Generation Biomass Supply Chain Optimisation

Jixiang Zhang

Department of Chemical & Process Engineering

University of Strathclyde

A Thesis Submitted to the University of Strathclyde for the Degree of Doctor of Philosophy

2022

Jixiang Zhang

Beyond Green Planet:

A Comprehensive and Systematic Second-Generation Biomass Supply Chain Optimisation

Department of Chemical and Process Engineering

University of Strathclyde

PhD Thesis

DECLARATION

This thesis is the results of the author's original research. It has been composed by the author and has not been previously submitted for examination, which has led to the award of a degree.

Signed:

Date:

ACKNOWLEDGEMENTS

Firstly, I would like to thank my parents for financial support, encouragement and love they have sent, expanding my view and shaping my personality. Without them, this work would not have been possible.

Then I would like to thank myself that in this long period of research start thinking what I really want and what kind of person I want to be. I am really happy in my study period could slow down and enjoy life.

But most importantly, deeply thank my supervisor Dr Jun Li, Dr Xiaolei Zhang and Dr Athanasios Rentizelas for continue inspiring my research passion and insightful discussion through every stage of the research.

Last but not least, a big thank you goes to all my friends from University of Strathclyde and University of Glasgow. Their presence has made my PhD life become so enjoyable and beautiful.

Best wishes to you all,

Jixiang Zhang

February 2022

PREVIOUSLY PUBLISHED WORK

- Zhang, J., Li, J., Dong, C., Zhang, X., Rentizelas, A. and Shen, D., 2021. Comprehensive assessment of sustainable potential of agricultural residues for bioenergy based on geographical information system: A case study of China. Renewable Energy, 173, pp.466-478.
- Zhang, J., Li, J., Dong, C., Zheng, Z. and Liu, H., 2019, June. Supply chain optimization of agricultural biomass waste for centralized power generation. In ICAE2019: The 11th International Conference on Applied Energy.
- Zhang, J., Zhang, X., Rentizelas, A., Dong, C. and Li, J., Optimisation of Logistic Model Using Geographic Information Systems: A Case Study of Biomass-based Combined Heat & Power Generation in China. Revised to Applications in Energy and Combustion Science in 15-02-2022, Approved by 17-03-2022.
- Zhang, J., Rentizelas, A., Zhang, X. and Li, J., Sustainable Production of Lignocellulosic Bioethanol towards Zero Wastes. Submitted to Sustainable Energy Technologies and Assessments in 01-03-2022

ABSTRACT

Biomass energy utilization plays crucial role in both energy security and environmental production. Biomass utilization has been developed for decades, while it still considered as underutilized industry at present. One of the major restrictions is the supply chain related cost control. This thesis will analyse from three aspects (long-term, medium-term and short-term) to optimise biomass supply chain. The goal of this thesis is to establish an efficiency and low-cost integrated biomass supply chain framework, which involved modelling optimisation assisted by experiments.

Firstly, for biomass supply chain long-term optimisation, sufficient feedstock source is a key for biomass plant stable operation, thus, biomass potential assessment is necessary. A novel biomass potential assessment method was proposed in this thesis, which considered the effect of biomass feedstock removal on soil health. The thesis evaluated agricultural residues potential from three aspects (theoretical, technical and sustainable potential) in China as a case study, and analysed residues spatial distribution and production. It found that 1001.47 Mt of residue is produced annually (theoretical potential), including corn stalks (440.64 Mt), rice straw (241.45 Mt) and wheat straw (176.46 Mt). for sustainable consideration, that can be considered, 143.20 Mt residues were seen as sustainable potential, which could provide from 22.2 to 27.8 TWh power supply each year.

Secondly, biomass supply chain medium-term optimisation plays crucial role in connecting both long-term and sort-term, among that logistics cost accounts the largest proportion of biomass supply chain. The logistics algorithm modelling optimisation and pre-treatment methods characteristics experimental assessment contribute to biomass supply chain medium-term optimisation. A case study of logistic system optimisation was proposed and studied, which integrated with the decision making of long-term optimisation. The results showed that the integrated logistics related cost and greenhouse gas emission under long-term optimisation assisting reduced 0.02% and 0.01% respectively.

Thirdly, by-products valorisation is another way to reduce total biomass supply chain cost in short-term optimisation. This thesis proposed a conceptual zero waste biorefinery process network design, and investigated a novel concept of corn stalk-based ethanol production as a case study. The results showed that the optimised ethanol production cost and greenhouse gas emission reduce 20.5% and 73.1% respectively.

At the end of this thesis, variable future work of biomass supply chain optimisation is presented for consideration. This thesis provide a comprehensive solution for the problem of biomass supply chain cost control and efficiency improvement, which various stakeholders benefit from this thesis. For example, long-term optimisation, the investigation of biomass potential assessment provide an overview not only to policymaker for decision making, but also to investors for avoiding disorderly competition. Medium-term optimisation, the robust logistic model saved logistic cost for investor, meanwhile, reduced CO_2 emission further contributing to public health. Short-term optimisation, the conceptual zero waste biorefinery process design for by-product valorisation is another three birds one stone conception which benefits investors, environment and human well-being.

TABLE OF CONTENTS

LIST OF TABLES

LIST OF FIGURES

ABBREVIATIONS

AFEX	Ammonia Fibre Explosion
C	Carbon
CEPCI	Chemical Engineering Plant Cost Index
CH_4	Methane
CHN Analyser	Carbon Hydrogen and Nitrogen Analyser
CHP	Combined Heat and Power
CO	Carbon Monoxide
CO2	Carbon Dioxide
CP	Crop Production
DTG	Derivative Thermogravimetric
EIA	Energy Information Administration
FAOSTAT	Food And Agriculture Organization Statistical Database
GIS	Geographic Information System
H	Hydrogen
HHV	Higher Heating Value
HI	Harvest Index
IRR	Internal Rate of Return
LHV	Lower Heating Value
LP	Linear Programming
MESP	Minimum Ethanol Selling Price
MILP	Mixed-Integer Linear Programming
MINLP	Mixed Integer Non-Linear Programming

N	Nitrogen
NBSC	National Bureau of Statistics of China
NLP	Non-Linear Programming
NPV	Net Present Value
NREL	National Renewable Energy Laboratory
O	Oxygen
PI	Profitability Index
PPI	Producer Price Index
RFA	Renewable Fuel Association
RPR	Residue To Product Ratio
RRA	Residue Retention Amount
RRR	Residue Retention Rate
S	Sulphur
SE	Soil Erosion
SOM	Soil Organic Matter
TGA	Thermogravimetric Analyzer

NOMENCLATURE LIST

Q_0	Biomass demand for power generation
P_n	Power generation capacity
h	Operation time
η	Power generation efficiency (%)
ρ	Biomass feedstocks distribution density
R	Collection radius
r	Distance from field to storage depot
$L2$	Distance from storage depot to power plant
∂	Agriculture residues available collection index
μ	Dry matter loss coefficient
M	Moisture content of received residues
C_c	Biomass purchasing cost
C_{pt}	Biomass pre-treatment cost
C_t	Transportation cost
C_s	Storage cost
C_{ash}	Ash disposal cost
C_p	Power plant cost
P_c	Purchasing price
C_{d1}	Equipment purchasing cost
C_{m1}	Maintain cost
C_{em1}	Employees' cost
C_{ful1}	Operation cost (fuel cost)

β	Equipment working capability
C_{e1}	Purchasing price for each equipment
n_1	Equipment utilization life
RV_1	Rest value of equipment
C_{om1}	Fixed percentage 0.2%
N_1	The number of employees
C_{sal}	The salary of each worker each year.
O_{con1}	Energy consumption
C_{oil}	Oil price
C_{ele}	Electricity price
O_{con2}	Energy consumption
$C_{e2refer}$	Reference size of torrefaction plant
RV_2	Rest value of equipment
F	Scale factor
n_2	Torrefaction equipment utilization life
C_{om2}	Fixed percentage
N_2	The number of employees
C_{t1}	The cost from filed to collection depot
C_{t2}	The cost from collection depot to power station
C_{t3}	Handing cost
f	Road tortuosity factor
P_t	Transport price
V_v	Transportation vehicle volume
ρ_1	Biomass loss bulk density from filed to storage depot

n	The number of storage depots
P_L	Two times loading and unloading cost
C_{s1}	Storage fixed cost
S_s	Storage area
C_{sm}	Management cost for storage.
H	The height for storage
ρ_i	Biomass bulk density in storage
C_{s2}	Storage facility cost
C_c	Storage facility construction cost
RV_4	Net salvage value of storage facility
n_4	Storage depot utilization life
C_{s3}	Storage variable cost
P_{os}	Operation cost
M_{ash}	Ash content of biomass (%)
P_{ash}	Ash disposal cost (£/t)
Q_{ash}	Ash quantity
C_{pi}	Total investment cost for biomass plant
n_5	Power plant operation period (year)
RV_5	Net salvage value of power plant
$C_{pi\ refer}$	Power plant investment cost under referred size
γ	Maintain cost factor
λ	Salary and welfare factor
θ	Power plant scale factor
C_{bg}	Biomass grinding cost

E_{bg}	Electricity consumption for grinding
R_{pg}	Power plant power generation revenue
P_{ele}	Electricity on-grid sealing price
P_s	Subsidy from government
P_h	Heating sealing price
T_h	Heating sealing period
H_{LHV}	Lower heating value for heating supply (MJ/kg)
E_h	Power plant heating efficiency
E_t	CO_2 emission in transportation
E_{CO2}	Total CO_2 emission
E_{pt}	CO_2 emission in pre-treatment
E_s	CO_2 emission in storage
E_{diesel}	CO_2 emission for diesel
Q_{carbon}	Carbon content in diesel
φ_{carbon}	Carbon oxidation rate in diesel
δ_{carbon}	Carbon and carbon dioxide mass ratio
LHV_{carbon}	Diesel lower heating value (kJ/kg)
E_{t1}	CO_2 emission in transportation from field to storage depot
E_{t2}	CO_2 emission in transportation from storage depot to power plant
E_{t3}	CO_2 emission in transportation handling
$Q_{c_{full}}$	Full loaded truck diesel consumption in collection
$Q_{c_{emp}}$	Empty truck diesel consumption in collection
$Q_{p_{full}}$	Full loaded truck diesel consumption to power station
$Q_{p_{emp}}$	Empty truck diesel consumption to power station

β_4	Loading and unloading equipment working capacity (t/hr)
O_{con4}	Diesel consumption (l/hr)
E_{ele}	Electricity CO_2 emission (renewable)
O_{con2}	Electricity consumption
β_5	Stacking equipment capacity
P_{stack}	Stacking equipment power
β_6	Unstacking equipment capacity
$P_{unstack}$	Unstacking equipment power

CHAPTER 1:
INTRODUCTION

Globalisation promotes the efficient flow of products, labours, and capital worldwide, which, however, is fragile since partial mistakes can lead to a series of problems, especially in the field of energy transportation. During the Covid-19 pandemic, due to labour shortage and various anti-epidemic inspects, the supply of long-distance foil fuel (such as oil and natural gas) faced significant challenges. In the UK, primary petroleum (crude oil and natural gas liquids) accounts for the largest proportion (43%) of energy production [1]. According to the Paris Agreement, developing renewable energy is an effective way to prevent global warming. COP26 reaffirms temperature goal in the Paris Agreement and phased out low-efficiency fossil fuel subsidies [2]. Biomass can store carbon from the atmosphere into plants through photosynthesis, which can be seen as a carbon-free energy source.

Energy security has been globally acknowledged as a crucial factor for a national development strategy. The rapid growth in global energy consumption has already heightened concerns over supply difficulties, depletion of resources and environmental impacts [3]. In recent years, the renewable energy sector has developed rapidly, and bioenergy has been identified as one of the major renewable energy sources [4]. The EU has established its renewable energy strategy with the goal of reducing greenhouse gas emissions by 80-95% in 2050 compared with 1990 levels with renewable energy accounting for at least 55% of the gross final energy consumption [5]. Biomass has been anticipated as a major source of renewable energy. By 2020, China had installed over 29.5 GW of biomass-based power plants and 13.3 GW of this are powered by agricultural residues, which contribute 51 TWh of power supply a year [6].

Although biofuel is a renewable and biodegradable with the potential to replace fossil fuels, its output is very limited. One of the biggest concerns is the cost control. According to Ekşioğlu et al. [7], costs related to biomass supply account for approximately 20% to 40% of ethanol costs, with logistics costs occupying the largest proportion of supply costs, approximately 90%. In order to further reduce the production cost of biofuel, it is imperative to design a low-cost and high-efficiency supply chain. Biomass supply chain applications and related optimisation are to be discussed in the following section.

1.1 Supply chain

A supply chain is a system composed of different entities that deliver products and/or services to end-users through upstream and downstream channels [8, 9]. Increasing demand and consumption have put pressure on industrial output and supply chains, leading to a high degree of complexity and diversity in decision making. Thus, an effective, sustainable and economical supply chain is imperative. In this case, supply chain management comes into being. The concept of supply chain management is to coordinate core business entities into a unified decision-making structure in order to minimise costs or improve system efficiency [10, 11]. To put it in another way, supply chain management aims to synthesise and distribute products or services that meet the required quantity and quality while maximising revenue (profit, efficiency and effective value-added movement). The principle of supply chain is to move material or information from source to end-users, while supply chain management is to build a highly efficient and low-cost system integrating all the entities in the supply chain.

1.2 Biomass supply chain

Biomass supply chain can be simply described as the movement of biomass from source to end-users, such as energy and chemical production related biorefinery plants [12]. The structure of biomass supply chain varies with feedstock type, conversion technologies and final bioproducts. A whole biomass supply chain is composed of many entities, including feedstocks producing field, processing infrastructure, biorefinery plant and end-users [13]. The six major sub-processes, namely, harvest, collection, transportation, pre-treatment, storage and handling, which connect these entities and contribute to a complete integrated biomass supply chain [14], as demonstrated in Figure 1- 1, showing that these processing activities in relation to entities are highly symbiotic and interconnected to each other.

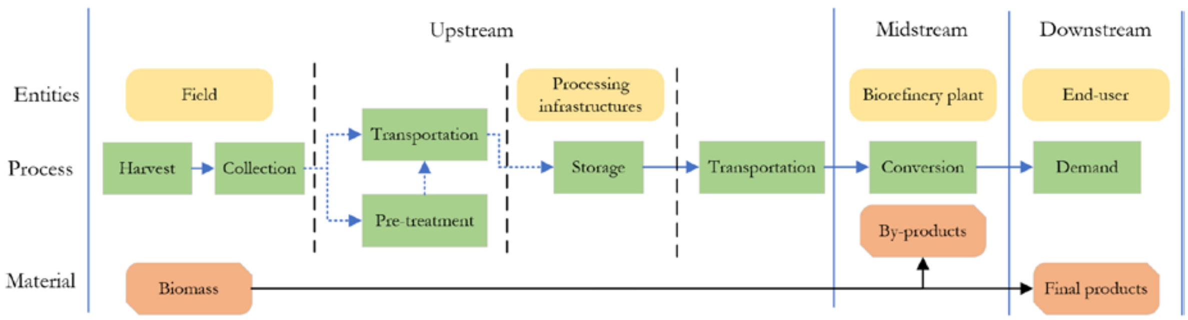

Figure 1- 1: Sketch of biomass supply chain

Due to the features of biomass, biomass supply chain differs from traditional supply chain. The availability and supply uncertainty of biomass feedstocks may be severely affected by weather and seasons [15, 16], which requires a large amount of biomass to be stored for a longer period throughout the year, leading to a significant increase in storage infrastructure. Furthermore, biomass materials normally have high moisture contents and low bulk density, which are easily broken, putting a great pressure on the transportation, storage and related infrastructure construction of biomass supply chain [17, 18]. Therefore, it is necessary to provide adequate storage facilities, handling equipment and transportation means in accordance with local conditions. Such characteristics (i.e., long period storage and low bulk density) increase the complexity of biomass supply chain in terms of cost control and operation, especially when biomass is used as an energy source, logistics operations account for the largest proportion of bioenergy costs [19, 20]. There is a great demand for a stable, sustainable and economical supply chain system for feedstocks.

A well-designed and managed supply chain system plays a vital role in reducing biomass supplying costs and biofuel production costs. Various decision-making strategies are adopted depending on the contribution of biomass supply chain sub-components, such as the combination of transportation, storage, collection and pre-treatment. In order to develop a cost-effective supply chain model, decision-making strategies and levels are essential, involving long-term strategies at the strategic decision-making level, medium-term strategies at the tactical decision-making level, and short-term decision-making strategies at the operational level [7, 21]. The design of a biomass supply chain model includes determining: 1) biomass demand, biorefinery plant location and capacity based on local biomass potential; 2) number and location of biomass processing infrastructure; 3) stable biomass supply farm; 4) biorefinery collection facilities and 5) daily operation planning. Long-term strategies help to reduce the external uncertainties of biorefinery companies in the supply of feedstocks, such as feedstocks related potential assessment, infrastructure location and production capacity. Flexible medium-term decision-making strategies at the operational level have advantages in terms of logistic management and transportation patten. In daily operations, short-term strategies are greatly beneficial to handle uncertainties in production. Figure 1- 2 depicts the decision making at each level of biomass supply chain. It can be seen that each decision-making level (strategy) in the biomass supply chain has different priorities, in which each solution is related to another. Comprehensive optimisation of the biomass supply chain requires a combination of these three kinds of decision-making strategies. Well-designed strategies are likely to create value for the biomass supply chain. However, coordinating three types of decision strategies is challenging. For example, optimising transportation process (one goal of the medium-term strategies) needs to consider infrastructure location and production capacity (one goal of the long-term strategies), whereas infrastructure and production capacity rely on local biomass potential, which depends on the assessment of local conditions. To design an effective logistics system, it is necessary to consider operation strategies and technologies used in each sub-process. A good operational strategy is critical to the coordinated operation of all processes in the supply chain and to ensure that the entire supply chain functions as efficiently as possibly [22].

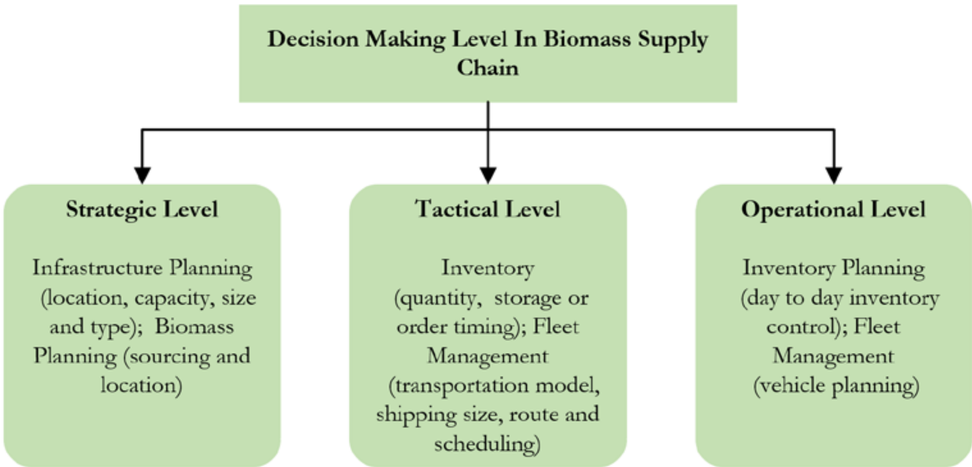

Figure 1- 2: Decision making levels of a biomass supply chain

The main challenge of biomass to bioenergy conversion supply chain is biomass logistics operation [23], which is embodied in biomass transportation, feedstock quality stability, distribution and tactical operation programme [24]. Biomass feedstocks logistic system can be described the period that feedstocks transfer from field to biorefinery plant, Referring upstream in figure 1-1. Biomass is a material with low bulk density which occupies a lot of storage and transportation space. As stated above, biomass logistics is a highly symbiotic system, in which one factor would affect the efficiency and cost control of the entire supply chain system, thereby it requiring proper management and strategic planning to reduce negative impact on financial benefits and minimise the impact on the environment. For example, Figure 1- 3 shows two types of biomass collection modes with and without pre-treatment (e.g., densification) in biomass logistics. The application and strategy of pre-treatment (a supply chain sub-process) technologies affect further sub-process operation strategy as well as the cost and efficiency related to integrated supply chain. Therefore, it is significant to design a biomass logistic system comprehensively, as each sub-process is greatly influenced by the other.

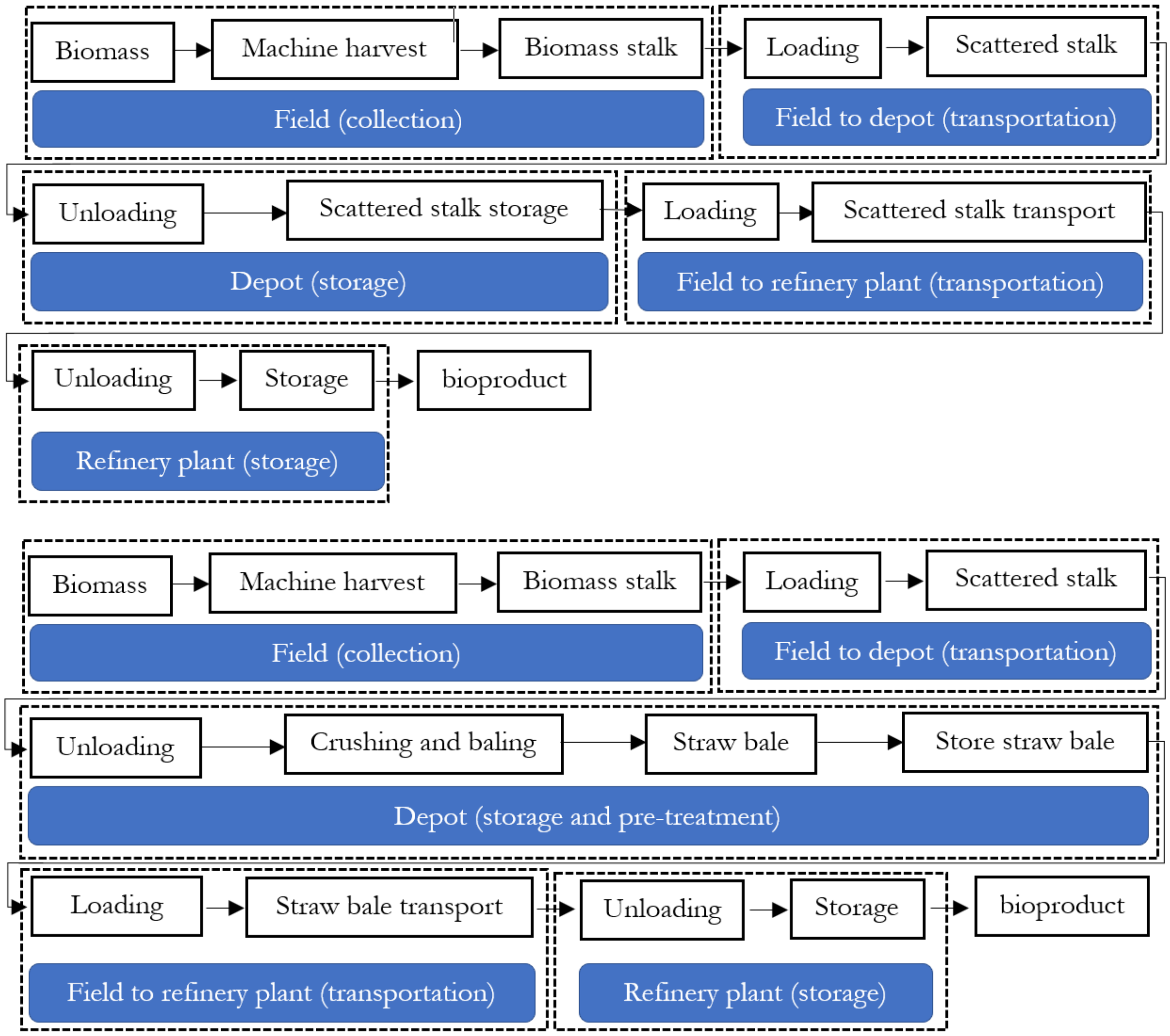

Figure 1- 3: Biomass logistic modes. Top (a) scattered biomass collection mode. Bottom (b) baled biomass collection mode.

Lignocellulosic biomass especially agricultural residues is known as the most potential feedstock, which has matured production technologies and abundant availability competitively. This thesis will primarily focus on the supply chain optimisation of lignocellulosic biomass, specifically agricultural residues.

1.2 Previous researchers research on biomass supply chain model optimisation field

The research area of previous work can be summarized in a word cloud shown in Figure 1- 4.

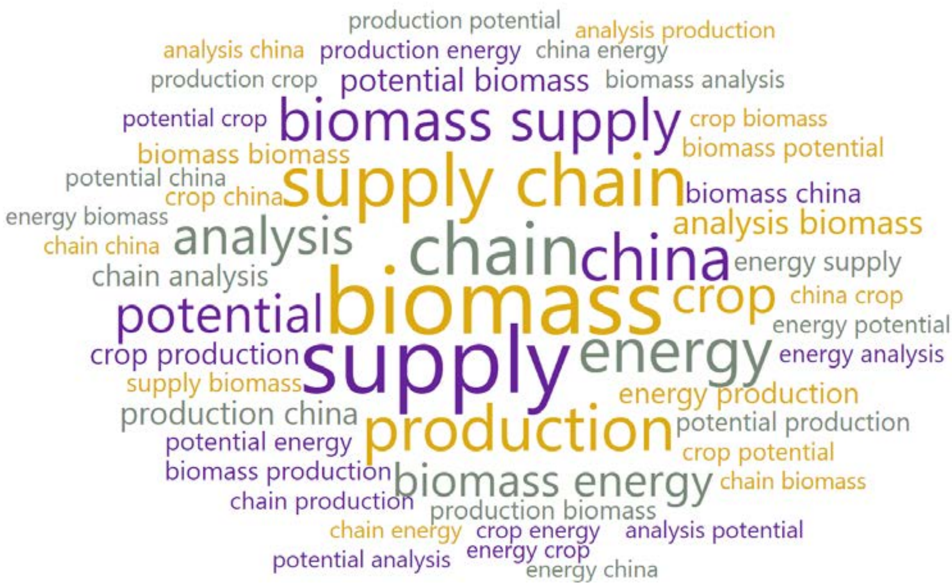

Figure 1- 4: word cloud of biomass supply chain research field.

In order to enhance the elasticity of lignocellulosic biomass supply chain under uncertainty, a robust biomass supply chain model is required. In the past decades, supply chain model has been developed into a complex and efficient system that integrates feedstock production, collection, transportation, storage, pre-treatment and final products conversion technology [25]. Research subjects can be summarised as follows:

- Factors influencing the cost of a biomass supply chain;
- The optimal solution for biomass feedstock production, collection, pre-treatment, storage, and transportation to achieve a balance between the minimal cost and environmental impact (such as number of storage depots, choice of pre-treatment technologies and biomass collection strategy);
- Location allocation issues in storage facilities;
- Transportation mode decision;
- The trade-off between supply chain costs, environmental impact and social benefits
- Impact of uncertainties on a biomass supply chain

1.3 Research scope and objectives

Biomass-based bioproducts are alternative and sustainable resources, which are beneficial to society. However, the high production cost, especially the high cost of the biomass supply chain, restricts its wider deployment. The challenging issues that need to be addressed are listed as follows:

i. In the preliminary planning stage of a biorefinery plant, the biomass potential of the target regions needs to be assessed.
ii. The research on biomass pre-treatment technology has achieved great progress, while there is a lack of systematic evaluation methods that combine biomass pre-treatment technologies with logistics.
iii. Previous research tends to mostly take greenhouse gas emissions into account as an environmentally sustainable standard, while ignoring the importance of soil protection.
iv. Studies on the optimisation of biomass supply chain mostly focus on one single attribute or duo attributes; nevertheless, there are contradictions between optimal solutions under multiple attributes.
v. The pursuit of biorefinery conversion efficiency and lack of innovative conversion process have become a steppingstone for the competitiveness of bioproducts.

As analysed above, in terms of cost control and environmental protection, there is a lack of systematic methods to evaluate, synthesise and optimise the biomass supply chain system. Therefore, this thesis aims to assess the biorefinery supply chain from long-, medium- and short-term strategies; and to comprehensively develop a sustainable biomass supply chain from the perspective of chemical engineering. This thesis aims to achieve the following objectives:

i. To determine biomass sustainable potential using integrated multi-criteria assessment, considering the impact on the environment, such as soil erosion and loss of soil organic matter.
ii. To experimentally investigate the effect of most common pre-treatment technologies of agricultural residues on the logistics system.
iii. To determine the optimum transportation network and infrastructure configuration of the biomass logistic system.
iv. To design a conceptual biorefinery processing network to achieve zero waste discharge and high added value of bioproducts.

1.4 Contribution of the Research

This thesis aims to make the following scientific contributions to the optimisation of biomass supply chain:

i. Incorporating both soil erosion and soil organic matters into biomass sustainable potential assessment improves the reliability of research results and provides detailed information for biorefinery plant planning.

ii. Integrating logistics model, pre-treatment technologies and geographic information system (GIS) as an interaction decision-making system for the optimisation of biomass logistics.
iii. Introducing the concept of zero waste discharge in biorefinery process design to make the refinery process environmentally friendly and improve the competitiveness of bioproducts by extracting high value-added by-products.

1.5 Thesis Structure

This thesis is organised as follows. Chapter 2 reviews existing literature related to the research, in which review previous studies on the optimisation methods of biomass supply chain from three strategic aspects (i.e., long-, medium- and short-term strategies). The research gaps will be therefore identified. To address the identified research gaps, three steps of decision-making strategies methodologies are proposed in Chapter 3: firstly, long-term decision making (at the strategic level) is considered to provide an overview of biomass supply chain, which involves methodologies of biomass potential evaluation and biomass characteristics under various pre-treatment technologies; moreover, the methodologies of logistic system are the key that link to promote the optimisation of medium-term decision making. The biomass residues potential data, characteristics and logistic model are integrated into an interactive systematic decision-making support system so as to achieve optimisation at strategic and tactical levels. Given the features of biomass, a methodology of conceptual biorefinery process network design is proposed to reduce production cost and emissions through refining traditional biorefinery waste into high value-added bioproducts. The Chapter 4 summarises the results of long-term decision-making strategy, with a case study of agricultural residues potential assessment in China. Chapter 5 assesses the characteristics of selected agricultural residues with/without pre-treatment (i.e., torrefaction). Then, Chapter 6 provides a comprehensive optimisation of a biomass logistic system, which contain biomass supply chain strategic and tactical level interaction. A conceptual zero-waste biorefinery process network design is presented in Chapter 7. Finally, the conclusion and future research orientation are discussed in Chapter 8 in the perspective of methods improvement in biomass supply chain system. The thesis structure is illustrated in Figure 1-5.

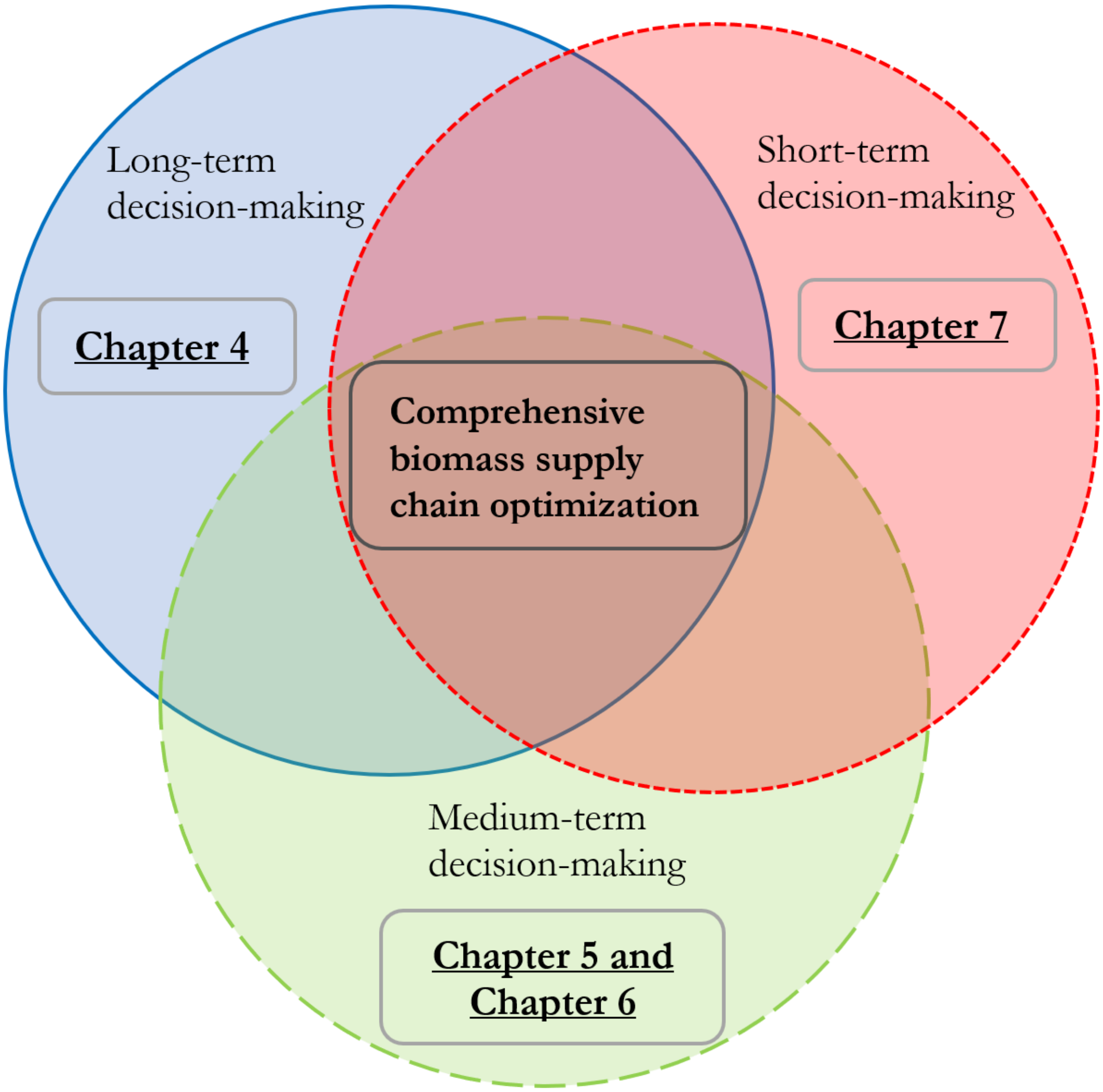

Figure 1- 5: Thesis structure

(Chapter 4: Agricultural residues potential assessment; Chapter 5: Experimental analysis of Agricultural residues; Chapter 6: Logistic model optimization and Chapter 7: Conceptual design of Zero Waste Biorefinery process)

CHAPTER 2:
LITERATURE REVIEW

There is a long history of converting sugar or starch from crops like corn and sugarcane into useful biofuels. Due to continuous improvement over the past few decades, conversion technologies are relatively mature and cost-effective. However, these supply feedstocks are expensive as they are good sources of food. There are some cheap feedstocks such as lignocellulosic biomass, while current conversion processes of which are relatively complex and the conversion technologies are still not economically viable [11]. Thus, there is a need to strike a balance between the cost of feedstock supply chain and the conversion technologies [26]. As discussed in Chapter 1, to optimise biomass supply chain and maximise profit, supply chain optimisation should improve the aspect in long-, medium- and short-term strategy, representing in local biomass resources potential assessment before project establishment; analysing pre-treatment feedstocks characteristics and improving logistic system efficiency; and effective use of co-products simultaneously. Therefore, following sections will introduce the importance of these strategies on biomass supply chain optimisation and review previous research works.

2.1 Availability and economic potential of agricultural residues

Agricultural residues have ascendancy over other types of biomass materials in terms of cost and environmental protection, whose performance currently has alternative usage such as pulping and bedding. However, agricultural residues are seldom used as alternatives, leads to the large amount of residues surplus. Waste agricultural residue either burns or decays in the fields, resulting in a significant waste of resources. Converting agricultural biomass into energy not only enhances the diversity of energy supply, but also helps protect the environment. To allow deploying and constructing biorefinery plants based on agricultural residues, it is essential to assess its availability potential relatively accurately.

The assessment of agricultural residues potential can be roughly divided into three categories: theoretical potential, technical potential and sustainable potential [27, 28]. Theoretical potential refers to the maximum annual quantity of biomass produced within a geographical boundary, with the assumption that there are no restrictions related to harvest, economic or environmental constraints [29, 30]. Technical potential, a subset of theoretical potential, represents the amount of biomass that is technically and economically feasible to be collected, depending on the type of residue and the efficiency of harvesting equipment [28, 31]. Sustainable potential refers to the removal of residues from the field subject to environmental regulations and prevention of any adverse impacts on the land, such as soil erosion or depletion of soil organic matter [4]. The relationship of these three agricultural residue potentials is illustrated in Figure 2- 1.

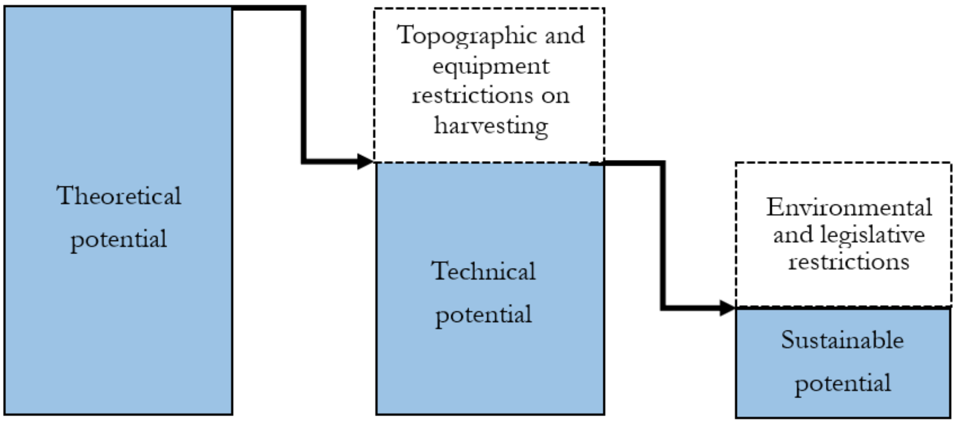

Figure 2- 1. Relation among theoretical, technical and sustainable potentials.

Theoretical potential

The estimate of residue potential depends on an assumption of the relationship between a crop and its residues. Various methodological approaches have been adopted to estimate crop yields worldwide. However, data on crop yield are often insufficient, leading to large gaps in crop yield estimates [32]. One of the most commonly used methods for estimating residues is the residue to product ratio (RPR), which refers to the residue weight relative to crop weight [33]. Another residue estimator is the harvest index (HI), which represents the ratio of crop yield to total aboveground crop production (including straw) [4, 34]. It is generally accepted that RPR is better than HI [35-37] when being used to estimate yield since actual agricultural production may vary greatly between regions. If the study area is large enough, such as at the national or continental scale, the estimation of residue yield based on national average crop production may produce many uncertainties. Therefore, a RPR method at a local geographical scale is needed to allocate reliable theoretical potential.

Technical potential

The amount of harvestable residues could be significantly affected by the working capacity of the harvesting equipment. Previous studies have shown that 15-25% of the total residue is likely to be lost during the harvesting process due to the limitations of harvesting equipment [38, 39]. For example, Weiser et al. [40] estimated the potential agricultural residue in Germany and found that the technical potential was about 50% of the theoretical potential.

Sustainable potential

According to the studies by Monforti et al. [41] and Thorenz et al. [27], extensive collection of residues from the land might have consequences for the depletion of soil organic matter (SOM) and nutrients (i.e., carbon, phosphorus and nitrogen) and soil erosion (SE), affecting soil fertility and environmental sustainability. Returning residues to the field becomes essential with multiple benefits, such as reducing soil evaporation, improving water infiltration, enhancing soil fertility, as well as developing rainfall capture capacity and soil porosity [42-44]. If agricultural residues are to be collected and utilised in a sustainable manner, it is economically feasible to remove the residues without compromising soil heath and water volume [45, 46]. Therefore, an appropriate collection rate of agricultural residues, that accounts for different geographical areas according to their characteristics, should be identified to meet the essential prerequisites of economic viability and environment protection. SOM maintenance and SE control are two primary targets of residue retention, the latter of which depends on soil properties, rainfall, topographic characteristics and agricultural practices [47]. In order to accurately determine the amount of agricultural residues that should be retained in the field to provide sufficient organic matter for subsequent crops, it is of vital importance to take the local soil quality (including both SE and SOM) into account when calculating removal rates. Allmaras and Dowdy [48] claimed that 30% of residues was enough to prevent 80% of soil erosion. Andrews [49] also argued that in order to prevent soil erosion, the maximum removal rate shall not exceed 30% of the total theoretical potential. However, using such a suggested constant value to evaluate soil health is likely to result in widely inaccurate estimates of the sustainable potential of agricultural residues, as the amount of retained residues to ensure soil health depends largely on specific regional soil conditions.

In European countries, residues are usually left in the field as a major source of SOM. After estimating agricultural residues of major crops in 36 European countries, Scarlat et al. [4] assessed the potential of different amount of residues, which took the impact of residue removal rates on SOM into account. However, in regions with intensive agricultural activities such as China, the residues are often not returned but mostly burned in the fields to quickly clear the fields for further land preparation and planting [49, 50]. Liang et al. [51] investigated SOM concentration in China and developed a SOM model based on environmental factors such as soil formation factors, local climate and vegetation. Due to local differences, an improved residue removal model is required to include additional parameters such as soil erosion, soil condition, weather conditions, as well as residue losses and moisture content [52]. Apparently, there is a gap in the existing studies on the methods involving both local SE and SOM when evaluating the potential of sustainable agricultural residues at a higher level of geographical granularity.

To solve these problem, geographic information system (GIS) introduce in biomass potential assessment. GIS is a platform that stores, manages and analyses spatial reference data, which can be used to distinguish the relationships among different data layers and create new spatial layers based on the analysis results [53]. In essence, GIS is a decision support system analysing spatial reference data to solve problems, which has been employed as a strategic tool in the agricultural biomass supply chain [54, 55]. Therefore, GIS plays a critical role in assessing the potential of agricultural residues.

At the macro level, investigating the potential of agricultural residues in a target region not only helps to figure out local resources' potential, but also provides a basis for further formulation of renewable energy policies. Most importantly, as a link of long- and medium-term strategies, residues potential assessment is a cornerstone of building a cost-effective biomass supply chain based on agricultural residues.

2.2 Evaluation of agricultural residue pre-treatment technologies in the biomass supply chain

Most biomass conversion technologies used to produce bioenergy and biochemicals involve pre-treatment process, which plays a crucial role in enhancing the efficiency of biomass conversion, reducing supply chain cost, and improving its efficiency. Lignocellulosic biomass, mainly composed of lignin, cellulose and hemicellulose, the heterogeneous multi-scale structure of its cell wall restricts biomass recalcitrance to decomposition for further valorisation. The application of pre-treatment technologies helps overcome recalcitrance of lignocellulosic biomass and promote its decomposition into individual components. Therefore, this section reviews the latest most-commonly used pre-treatment technologies. Generally, pre-treatment technologies can be divided into physical, chemical and thermochemical technologies (Figure 2- 2). Physical pre-treatment, including grinding, densification, and milling, is mainly used to reduce particle size or surface area by mechanical comminution, which is a necessary step for subsequent chemical or biochemical processing in order to improve future yields [56], while its main disadvantage is high energy consumption. Chemical pre-treatment is a method of biomass degradation through chemical reagents or solvents, which shows highly efficient deconstruction capability. However, toxic materials and carbohydrate loss in the process cannot be ignored. Acid, alkali and ammonia fibre explosion (AFEX) pre-treatment contributes to chemical pre-treatment technologies.

Thermochemical conversion involves the degradation of biomass structure under oxygenic or anoxygenic atmosphere at high temperature, which includes torrefaction and pyrolysis [57].

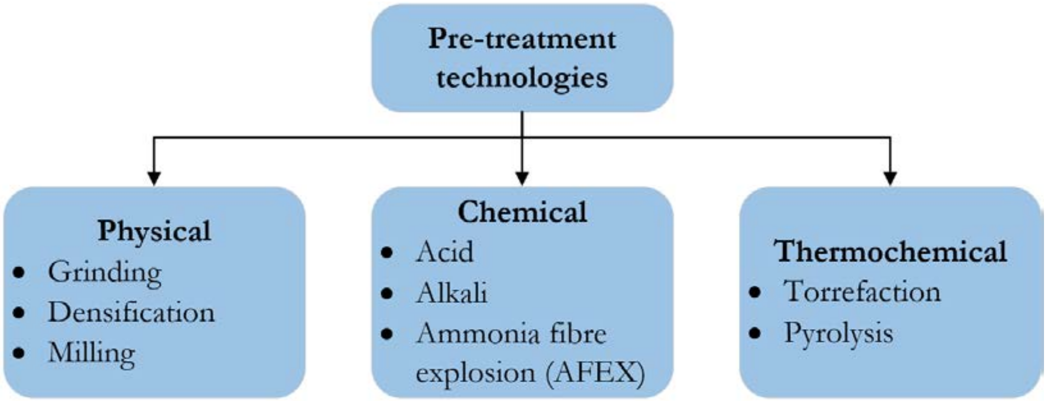

Figure 2- 2: Classification of lignocellulosic biomass pre-treatment technologies.

2.2.1 Physical pre-treatment technologies

Grinding and milling are commonly used in pre-treatment to reduce biomass size, which depends on the type of method and the choice of sieve. Grinding and milling are applied in biomass combustion and bio-oil production so that pre-treated particles improve heat flow and available surface as well as reduce cellulose crystallinity [58, 59]. According to Zakaria et al. [60], the milled particles produce higher glucose/xylose yields after enzymatic production, reaching 67.5% and 80.1% of yields respectively, much higher when being compared with 15.9% and 5.4% for unpretreated samples. Despite that milling and griding improve biorefinery efficiency, it is necessary to address the issue of high energy consumption, which was reported to account for approximately one third of energy demand in the whole process.

Densification is applied to the production of biofuels based on biomass feedstock, mainly to solve problems related to low density in terms of storage and transportation. Major advantages of densification are (1) increasing bulk density, (2) reducing moisture content and (3) improving durability and energy content. The energy consumption of densification depends on the characteristics of biomass such as particle size, composition and moisture content.

2.2.2 Chemical pre-treatment technologies

Acid pre-treatment is employed to improve the efficiency of enzymatic degradation of hemicellulose hydrolysis. Strong acids in diluted form (such as sulphuric acid, acetic acid, phosphoric acid [61]) can be used to treat lignocellulosic biomass. Martin et al. [62] observed that over 70% of cellulose was degraded by acid pre-treatment. It has been found that the glucose yield of biomass pre-treated with dilute acid is higher, reaching 76%, while that of untreated biomass is only 20% [63]. However, the corrosion and fermentation inhibitors are likely to damage reaction vessels and reaction efficiency.

Like acid pre-treatment, alkali pre-treatment (such as potassium permanganate and NaOH) is beneficial to improve the biomass structure in lignin extraction and enhance cellulose degradation efficiency. It is reported that the lignin content of corn stover after alkali pre-treatment has been reduced by 9.7% [64]. However, there are some disadvantages of alkali pre-treatment, such as high cost and limited feedstock types (high lignin biomass inability).

Ammonia fibre explosion (AFEX) is one of the effective lignocellulosic biomass pre-treatment techniques, which treats biomass under moderate reaction temperature (60 to 170 °C) and high pressure (15–30 bar) [65]. It is found that the glucan enzymatic digestibility of corn stalk increases by 87.78% after AFEX pre-treatment [66]. However, the high cost of ammonia and the difficulty in ammonia recycling technology restrict its commercialisation [61].

2.2.3 Thermochemical pre-treatment technologies

Thermochemical pre-treatment technologies with characteristics of higher temperature and conversion rates [72], which is suited for lower moisture feedstock. Depending on pre-treatment reaction temperature and pressure, thermochemical pre-treatment technologies mainly includes biomass torrefaction and pyrolysis.

Torrefaction is a thermochemical process which is carried out in a relatively low temperature range (200-300°C) in the absence of oxygen [67]. Within this temperature range, several chemical reactions occur, including devolatilization, depolymerisation, and carbonisation of cellulose, hemicellulose and lignin; the biomass loses moisture contents and rigid fibre structure, thereby increasing the energy content [68]. The torrefaction process generates a brown to black uniform solid product, as well as condensable (such as water, organics and lipids) and non-condensable gases (CO_2, CO, and CH_4) [67]. Generally, during such a process, approximately 70% of the biomass mass is retained as a solid product, which contains 90% of the original energy content. Normally, the torrefaction process is performed to increase the bulk density of biomass materials, as well as to improve the physical properties of biomass like grindability, particle shape, size, granulation, and calorific value [69]. As a result, the energy per unit volume of torrefied biomass materials is significantly increased, up to 20-23 MJ/kg [70]. Furthermore, torrefaction is seen as very promising technology, which has high process efficiency comparing with pyrolysis[71].

Pyrolysis is a thermal decomposition process that occurs in the absence of oxygen, converting biomass materials into solid charcoal, liquid (bio-oil), and gases at high temperatures, which is regarded as an industrially realised process for biomass conversion [72-74]. Temperatures employed in pyrolysis are between 400 to 800 °C [75] , which is higher than that in torrefaction. The final product contents (the proportion of solid charcoal, liquid, and gases) relays on pyrolysis method, the characteristics of the biomass and the reaction parameters. Therefore, depending on transportation requirement and storage performance, pyrolysis parameters may vary. Apart from pyrolyzed biomass has higher bulk density, ranging between 8 and 12 times that of raw biomass [76]. It was observed additional advantage in enhancing handling and storing efficiency and reducing cost in biomass supply chain. According to Siew and Sadhukhan [77], the storage facility required land area for a 50 MW plant with pyrolyzed biomass as feedstock significantly reduced from 3.9 ha to 1.8 ha. Despite benefit above, the absence of advanced technology in reducing process energy consumption restricts its commercialization.

2.2.4 Summary

To summarise, this section briefly introduces the most used pre-treatment methods for lignocellulosic biomass. The purpose of pre-treatment is to improve hemicellulose degradation and lignin extraction, thereby making biomass conversion more efficient. It has been found in existing studies that pre-treatment methods may vary depending largely on final conversion products and cost control. Since the choice of pre-treatment technologies affects the cost of the whole biomass supply chain, it is necessary to investigate the role and effect of pre-treatment in the supply chain.

2.3 Biomass logistics model

As the most important constituent part of biomass supply chain, logistic system, at the macro level, link that integrates all sub-components in the supply chain, which transportation and storage connect all sub-components. At the micro level, biomass logistics cost account for nearly 90% of total biomass supply chain cost. Thereby, to reduce biomass supply chain cost and increase its efficiency, most importantly optimized logistic system by improving each process in logistic system. The following section will introduce the contribution of biomass logistic system and methods of logistic system optimization.

2.3.1 Biomass logistics processes

The activities involved in transferring feedstocks from fields to biorefinery plants are described by [14] as follows: (a) biomass harvesting and collection, (b) biomass transportation, (c) pre-treatment, (d) storage, and (e) handling.

Biomass harvesting and collection

In general, it seems that biomass harvesting and collection are constantly moving towards a highly mechanised process with high input and yield [78]. In terms of biomass harvesting, the machine collection rate should be considered to estimate the amount of biomass. It is suggested that 10-20% of biomass residue loss is expected in mechanical harvesting [79]. Thus, in biorefinery plant planning, it is significant to consider biomass loss when estimating biomass potential needs during harvesting.

Biomass transportation

Biomass transportation is an important part of the biomass supply chain, energy use and carbon dioxide emissions. Simulating the lignocellulosic biomass supply chain process, Bussemaker et al. [80] found that the transportation cost occupied up to 20% of the entire supply chain cost. Various transportation modes (such as rail or truck) can be adopted according to the source of feedstocks, transportation distance and local conditions (such as infrastructure construction and terrain restrictions). For financial reasons, truck has often been chosen as the primary transportation mode as biorefinery operators often set a 50-mile biomass collection radius in the US [81, 82]. While in China, the government encourages companies to establish a biomass collection radius of no more than 50 km in order to reduce purchase prices and disorderly competition [83]. It is observed that when the number of warehouses increases from three to five, the transportation costs drop by 36.8% due to the reduction in distance. Careful planning and coordination are keys to reducing overall production cost and improving supply chain efficiency [84]. Moreover, greenhouse emission for biomass transportation should be considered in biomass supply chain. Zahraee et al. [85] developed a biomass dynamic simulation model to analyse the effect of transportation model on delivery cost and greenhouse gas emissions. Results showed that truck has lowest greenhouse gas emissions but highest delivery cost comparing with train.

Pre-treatment

The form of pre-treatment varies in line with the type of biomass and its application. For instance, in biomass power generation, it is necessary to increase the bulk density of biomass while reducing its moisture in order to reduce transportation costs and increase supply chain efficiency [81]. Pre-treatment mainly aims to process low density and unstable biomass so that it can be transported and utilised [86]. A variety of pre-treatment methods are available for deification such as pelletizing, briquetting, or cubing. In general, increasing higher bulk density requires higher energy consumption and more complicated operating procedures. Reasonable density helps to save not only the costs of energy consumption and transportation, but also storage space.

Storage

Biomass storage is an essential part of the biomass supply chain. Due to seasonal changes, biomass needs to be stored in a biorefinery plant that operates throughout the year. Therefore, priority is given to maintaining high quality and low daily matter losses in terms of biomass storage. According to Iakovou et al. [23], significant biomass dry matter losses have been observed in various types of storage structure, recorded between 10% and 13%. Furthermore, Rentizelas et al. [13] stated that high moisture is a key factor in maintaining biomass quality. They pointed out that the moisture content of biomass during collection should be kept between 40% and 50%, while the moisture content during safe storage should be maintained between 15% and 20%. Higher moisture content is likely to result in quality degradation and microbial hazards threatening human health. Therefore, an additional drying process is needed to reduce risks related to biomass storage and human health.

Handling

Biomass handling occurs in the loading and uploading process when biomass is transferred from farms to vehicles, then to biorefinery plants or warehouses, which calls for highly intensive labour and loading equipment.

Generally, harvesting and collection methods severely affect the quality of biomass feedstocks directly, which further influence the overall logistic system performance and schedule. Transportation model refers to capacity and type of transportation, depending on feedstocks resources, storage and pre-treatment related infrastructure system. Therefore, as the most critical sub-component, transportation links rest of sub-component in logistic system. The highly efficient transportation schedule and network play a key role in logistic transportation by delivering feedstocks to biorefinery plant on time. In the aspect of inventory planning, biomass storage planning is a complex task due to uncertainty of biomass quality and quantity [45]. The location and capacity of storage infrastructure depend on not only the characteristic of biomass but also transportation type and pre-treatment method. To address these problems, logistic system integration and optimisation methods will be reviewed in the next section. Figure 2- 3 shows the challenges to be solved and scope of the logistic system.

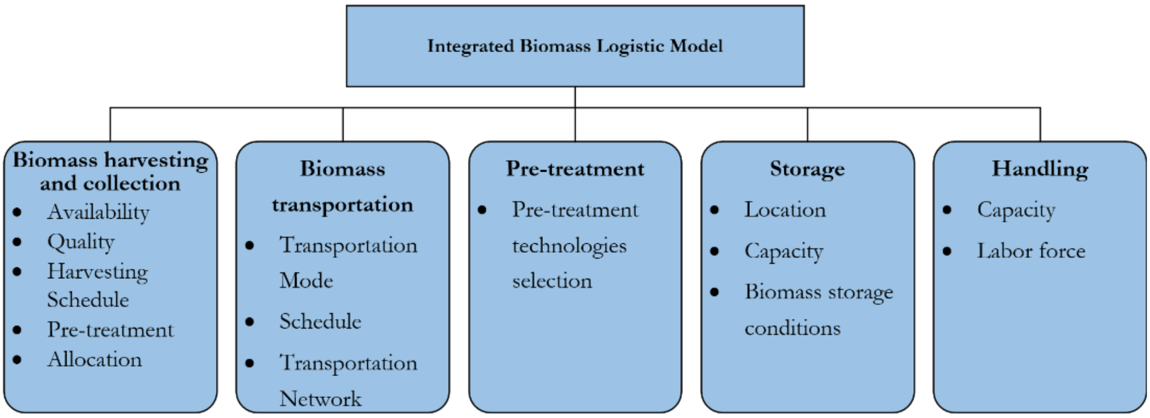

Figure 2- 3: Challenges and scopes along biomass logistics model.

2.3.2 Optimisation of biomass logistics model

The main goal of logistic system optimisation is to design a cost-effective and sustainable logistics system. The research fields of classical biomass logistics model optimisation can be summarised as network design optimisation (applied to transportation process), scheduling optimisation (applied to harvest and collection, storage, and transportation), infrastructure configuration optimisation (applied to pre-treatment and storage), transportation route planning optimisation (applied to harvest and collection, transportation) as well as technology selection optimisation (applied to pre-treatment process). Due to the symbiosis between each sub-process in logistics, for instance, transportation optimisation planning and designing strategies can be extended to fields similar to storage location and biomass collection strategies [87]. Therefore, how to balance the optimal results and objective functions in each supply chain process is one of the top priorities in the optimisation of the biomass logistic system.

To optimise the biomass logistics model, four elements are included in logistics improvement, namely, optimisation object (i.e., facility or biomass feedstocks), objective function (i.e., single-objective or multi-objective), modelling method (i.e., mathematical, heuristic or IT-driven method) and optimisation purpose (i.e., economic, environmental or social purposes), as shown in Figure 2- 4.

From objective function perspective, the single-objective optimisation problem is to find the best solution for one specific criterion or metric, such as maximum profits, energy consumption and greenhouse gas emissions. While a multi-objective optimisation problem is to figure out a comprehensive solution that combines two or more criteria or metrics [88]. It is generally acknowledged that the multi-objective optimisation is more likely to strike a balance between objectives in comparation to the single-objective optimisation [89, 90].

In the logistic model optimisation, researchers focus on the model economic performance as primary objective function. For example, Kim et al. [91] designed logistics network under uncertain parameters to figure parameters range that cause the most change in the profit. With growing awareness of biomass logistic model, objective function is not only limited to economic performance but also environmental and social benefit performance. Roni et al. [92] proposed a multi-objective biofuel logistic model, which considered CO_2 emission during transportation related activities and social impact of biofuels. Malladi et al. [93] optimised forest biomass logistic model by improving transportation network, to reduce logistic cost and CO_2 emission.

In general, optimisation models can be divided into deterministic models and stochastic models [94], depending on the characterisation of input data. Various studies optimise the biomass logistic model from different perspectives of operational, tactical and strategic fields, which can be divided into mathematical optimisation method, heuristic method, and IT-driven method [95]. Among that mathematical programming dominates the improvement of the logistic model [25]. Research fields and methods of logistics optimisation models are to be reviewed and analysed as follows.

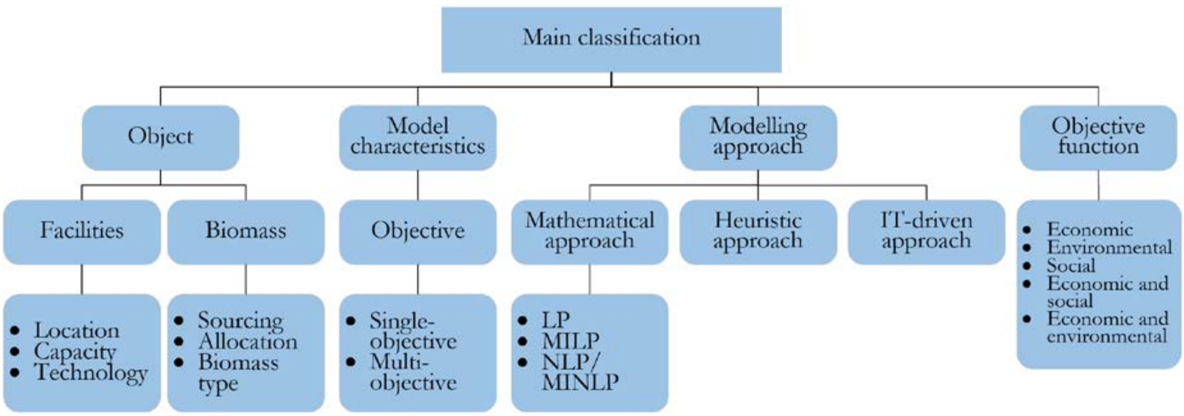

Figure 2- 4: Main categories of biomass supply chain network design models.

2.3.2.1 Mathematical optimisation method

Mathematical programming is the most common optimisation method adopted in transportation planning, including linear programming (LP), mixed-integer linear programming (MILP), mixed integer non-linear programming (MINLP) and non-linear programming (NLP). According to the objective functions, supply chain optimisation aims to achieve economic objectives (maximising profits and net present value while minimising costs), environmental objectives (minimising carbon dioxide emissions and energy consumption) and social objectives (creating more job opportunities and generating positive social impacts) [96].

LP is defined as an objective function and constraints are all under linear conditions. Ren et al. [97] designed bioethanol supply chain model under uncertainties, mainly aiming at the full life cycle profit. It should be noted that in the research of linear programming optimisation, the optimisation function is a single-objective method, which restricts the further sustainability of the supply chain model. Awudu and Zhang [98] pointed out that the major challenge of supply chain model optimisation is to deal with uncertainties. Due to the complexity in actual supply chain management, linear programming may not reflect real problems. Despite its drawbacks, the robustness of linear programming makes it the main method of supply chain management optimisation. Thus, it is recommended to explore both reliable optimisation method and actual conditions in future research.

Similar to LP, MILP has a linear objective function and its limitations. The difference is that 'all or at least one number of decision variables are integers' in the MILP method [25]. Due to the discrete phenomenon in the biomass supply chain, the characteristics of MILP (presence of integer variables) is beneficial to handle multiple processes in biomass supply chain optimisation. Therefore, MILP is the most commonly used method for site selection of biomass supply chain infrastructure [99], which can be applied to supply chain strategy [100, 101], transportation and storage optimisation [102-104] and biorefinery infrastructure location-allocation [105]. Furthermore, the MILP method has a comprehensive assessment system. For example, Budzinski et al. [106] developed a feedstock supply system based on a multi-objective MILP model which incorporates economic and environmental factors into model evaluation. Liu et al. [107] suggested that energy, environmental impact and economic benefits were seen as "3E" criteria to evaluate MILP models.

However, NLP and MINLP methods have nonlinear limitations and/ or objective functions [25]. Due to the complexity of the biomass supply chain, it is hardly possible to simulate all situations through linear programming. Therefore, researchers turned to seek solutions from NLP. Bai et al. [108] optimised bioethanol infrastructure location model with the help of NLP. They evaluated the reliability of the supply chain model under uncertainties. The results showed that NLP had the potential to improve optimality. Most researchers only regarded economic impact as an objective function, while only few researchers, such as Vazifeh et al. [109], considered economic, social and environmental impacts as objective functions to design a biomass feedstock network. Gong et al. [110] developed an algae processing network based on multi-objective

MINLP. They proposed two standard solutions with a view to economic and environmental protection. Despite MINLP and NLP perform well, computational deficiencies are to be exposed if too many restrictions are added.

2.3.2.2 Heuristic method

In general, the mathematical optimisation of the biomass supply chain can gain an accurate optimal solution according to the objective function. However, as the complexity of model algorithms increases, the calculation time increases exponentially [96]. For example, in order to simulate the biomass supply chain as realistically as possibly, it is necessary to add optimisation model restrictions as much as possible, leading to a complicated model and a long calculation time period. Thus, a balanced method is proposed to ensure a better solution and a shorter calculation time. Methods based on heuristic algorithm are used to work out complex problems close to optimal results in a short time. Gunnarsson et al. [103] developed a logistics system based on the forest biomass supply and procurement, which optimised transportation strategies, storage location and harvest area. The robustness of the supply chain model was evaluated for 6 scenarios through the heuristic method and MILP, which showed that MILP can generate high quality solutions, while the heuristic method responds quickly. Singh et al. [111] applied the heuristic method to calculate storage capacity and location in order to reduce computational efforts in the MILP solver. Ayoub et al. [112] designed a biomass energy decision system, including a public database, a simulation mode and a biomass conversion database. To cooperate with complex databases, the system uses heuristic methods to determine the best conversion technology and storage capacity so as to minimise transportation cost and CO_2 emissions.

2.3.2.3 IT-driven method

Due to the restrictions of local conditions, mathematical methods applied to traditional algorithm optimisation cannot generate actual solutions in decision making such as in terms of transportation. The IT-driven method is to integrate various data and supporting applications to coordinate processes in supply chain management [11, 113], which significantly increases the visibility throughout the supply chain. IT-driven methods represented by Geographical information system (GIS) have been widely employed in road networks and biorefinery infrastructure location, improving the reliability of supply chain models and visibility of local conditions including road network, water flows, and administrative boundary. Latterini et al. [114] incorporated terrain slopes into the estimation of biomass supply chains through GIS, thereby determining the optimal biorefinery plant location and transportation route, in which only economic performance was seen as an objective function. Zhang et al. [115] optimised the bioethanol supply chain model by analysing multi-objective functions, which integrated GIS and mathematical model (MILP) in decision making. However, to reduce the complexity of the model, this thesis tends to use the average value of land slopes and land area so that results may be different. Jeong et al. [116] and Kim et al. [117] introduced GIS into the MILP model to determine the best biodiesel refinery plant location. Brownell, and Liu [118] applied GIS into the heuristic method to calculate the number and size of storage location. The optimal configuration was obtained based on supply area, location and biorefinery plant size. Roni et al. [119] optimized biomass logistic model assisting by GIS, which enhance 177.4% supply volume without increase feedstock delivery cost. Salleh et al. [120] improved biomass logistic model by GIS, which optimised biomass supply point, biomass processing facility and biomass demand centre.

2.3.2.4 Summary

As a rich renewable source, biomass is beneficial to promoting local economy and environmental protection. An effective supply chain system plays a vital role in maintaining the competitiveness of biomass-related bioenergy and biofuel. Therefore, the biomass supply chain is optimised to reduce costs and greenhouse gas emissions by improving transportation, pre-treatment, storage, harvest and collection in the biomass supply chain. Simultaneously, as functional requirements change, progress has been made in the optimisation methods of biomass supply chain improvement. At present, major optimisation methods include mathematical, heuristic and IT-driven ones. A more detailed comparison among these three methods is shown in Table 2- 1.

Table 2- 1: Comparison of major optimisation methods.

		Pros	Cons
Mathematical approach	LP	Provides optimum solutions	Sigle objective function; Integer valued solutions cannot guarantee
	MILP	Integer valued solutions	nonlinear effects not considered
	NLP & MINLP	Nonlinear limitations	Computational limitation
Heuristic approach		Quick response; Competitive accurate results	Detailed solutions might incorrect
IT-driven approach		Increase supply chain overall visibility	Complexity calculation; Coordinate with algorithm model

In the mathematical optimisation of the biomass supply chain, LP methods have been applied in optimisation for a long period due to the higher quality of solutions. Through integer valued solutions, MILP replaces LP as the major method to optimise the biomass supply chain. In the past decade, due to the shortcomings of LP and MILP (without considering nonlinear effects), NLP and MINLP are commonly used in model optimisation. However, due to the complexity of modelling restrictions and objective functions, it is difficult to calculate in NLP and MINLP methods. A heuristic method is employed to strike a balance, which obtain accuracy from mathematical methods and computational constraints. An IT-driven method is another major optimisation approach being developed in the past decades, which increases the visibility of supply chain models and reliability of solutions. Nevertheless, in order to obtain accurate results, massive information and complicated modelling increase computational pressure.

A majority of previous studies on logistics model optimisation regard biomass economic performance as an objective function. To design a sustainable biomass supply chain, it is necessary to take multiple objectives into consideration. As is analysed above, despite each biomass supply chain process has been studied in detail [85, 119, 120], research on the integration of interconnected processes into a generic framework is rare. The best solution in one process may not be the optimal choice in another one, which, instead, is likely to exert negative impact on other processes. Hence, it is important to improve the efficiency of the biomass supply chain by treating the process as a whole optimisation system.

According to World Bioenergy Association [121] and Aghbashlo et al. [122], global bioenergy consumption has increased from 42 EJ reach to 55EJ from 2000 to 2018, among which solid biomass thermal power generation accounts for approximately 57% of the total bioenergy. With the increase in demand for bioenergy, the research on biomass-related supply chain has made great progress. Rentizelas et al. [123] and Mana et al. [124] analysed supply chain model of biomass thermal power conversion, and examined the feasibility in economic and technical aspects. However, few researchers have focused on optimising supply chain models based on a specific end-use bioenergy.

Moreover, after reviewing research papers related to biomass supply chain management, Gold, and Seuring [12] found that most studies focused on European countries, the US and Canada, while studies on Asia and Latin America were rare. However, Asian countries, such as China, India and Japan, rank among the biggest emitters of carbon dioxide [125]. Therefore, in order to reduce carbon dioxide emissions, it is urgent for these countries to develop biomass supply chains.

Undeniably, logistics costs occupy the largest part of bioenergy costs. An outstanding bioenergy project not only creates more profits by reducing costs, but also increases revenue by increasing the added value of products. Hence, building a cost-effective biomass supply chain relies on both medium-term and short-term strategies for optimising production processes.

2.4 Value-added by-products optimisation towards zero waste

Bioethanol has been identified as the most widely used lignocellulosic biomass biofuel [126]. It is estimated that bioethanol production accounts for approximately 9% of the world's energy consumption in 2019 [127], significantly reducing pollution and alleviating dependence on fossil fuels. The world has been more and more interested in the use of bioethanol in the past few decades. According to data from Renewable Fuel Association (RFA) [128], global bioethanol production in 2021 is approximately 26 billion gallons, of which US and Brazil contribute more than 80%.

Various methods have been studied to boost bioethanol production. Azhar et al. [126] compared key factors affecting ethanol production, including the efficiency of yeast strains, reaction temperature, PH value, sugar concentration and time, and summarised the optimal fermentation reaction based on various yeast strains. López-Linares et al. [129] and Nascimento et al. [130] examined main variables in acid and alkaline pre-treatment processes to obtain the maximum enzymatic hydrolysis yield, thereby increasing sugar content. Nakanishi et al. [131] attempted to optimise bioethanol refining processes and reaction temperature in alkaline pre-treatment, which increased approximately 14.6% of ethanol production compared with steam explosion used as the pre-treatment method.

However, the production of biofuels may lead to serious environmental consequences [132]. For instance, the production of ethanol from lignocellulose often uses external strong corrosive solvents (such as sulfuric acid and slaked lime) to enhance hydrolysis reaction efficiency, where improper wastewater treatment tends to cause potential secondary pollution. Thus, lignocellulosic biomass refinery is committed to developing high-value by-products with zero waste emissions and low production costs in order to reduce environmental pollution and increase the competitiveness of fossil fuel in the future. Research has already been carried out to optimise the biorefinery process to reduce pollution by improving the efficiency of by-products utilisation, thereby minimising waste. Humbird et al. [133] designed an ethanol conversion process using corn stover as the feedstock, in which waste by-products were burnt to provide heat and energy to support the operation of the entire system. After simple treatment, wastewater is discharged, where pollutants cannot be completely reused (49.5% soluble solids in the wastewater). Large amounts of wastewater pollutants may cause environmental hazards. Bbosa et al. [134] attempted to develop high-value by-products in bioethanol production using hydrothermal liquefaction. More efforts have been made to use microorganisms known as consolidated bioprocessing (CBP) in the pre-treatment of lignocellulose, by replacing contaminated catalysts in the first stage of lignocellulosic refinery. Carrillo-Nieves et al. [135] applied white-rot fungi to decompose lignin in order to enhance lignocellulosic feedstocks fermentation, thereby potentially avoiding pollutants and achieving zero waste. Although CBP has great potential in achieving zero waste, low technology maturity and poor economic performance limit the possibility of its commercial scale at present.

Therefore, using relatively mature technologies to optimise biorefinery processes has become a practical method for minimising negative impacts on the environment and increasing profits of refinery plants. In order to improve the efficiency of biorefinery products and reduce pollution, this thesis attempts to propose a zero-waste sustainable bioethanol refinery process for large commercial biorefinery by adopting mature fractionation technology to extract value-added by-products from ethanol distillation waste. This section aims to improve financial feasibility by maximising the yield of value-added by-products extracted from waste residues, meanwhile reducing carbon dioxide emissions and other pollutants in bioethanol refinery. Finally, the proposed zero-waste bioethanol refinery is to be compared with traditional bioethanol refinery in terms of financial contribution and pollutant emissions.

2.5 Summary and Research gap

According to the above literature review, it can conclude that the study on biomass supply chain optimisation has been conducted thoroughly. To improve biomass supply chain efficiency, researchers enhance its performance from long-term strategies at the strategic decision-making level, medium-term strategies at the tactical decision-making level, and short-term strategies at the operational decision-making level.

For the long-term strategy optimisation, to ensure biorefinery plant has sufficient feedstock to support plant operation, comprehensive biomass potential assessment in a certain region is necessary. To ensure biomass potential has accurate result for decision making, various research investigated biomass potential with massive restrictions in order to minimise the effect of external factors on biomass supply chain. Therefore, depending on restrictions, biomass potential can be divided into theoretical, technical and sustainable potential. From biomass supply chain medium-term strategies optimisation respective, logistics system as the most crucial component of biomass supply chain connects long-term strategy and short-term strategy. At the same time, logistics cost accounts the largest part of total biomass supply chain cost. Thereby, optimising biomass logistics has a significant effect on biomass supply chain cost reduction. Algorithm modelling optimisation is widely applied method, which can be classified as mathematical, heuristic and IT-driven optimisation. Above that, mathematical optimisation is the most common optimisation method. With the growing awareness of logistics optimisation, researchers attempt to improve logistic system by combining mathematical and IT-driven methods performance, in order to reflect realistic external uncertainties.

Improving biomass supply chain not only optimise external environment but also internal environment. In other words, reduce expenditure at the same time increase income. One of the most effective methods for increasing income is by-products valorisation. With consideration of environment production and by-products valorisation, researchers proposed the concept of zero waste biorefinery production.

Despite remarkable improvement in biomass supply chain optimisation, a variety of defects can be addressed and enhanced in these three strategies. In terms of biomass potential assessment (long-term strategy), the methodologies and definition of biomass potential assessment have been conducted thoroughly. However, the methodology of biomass sustainable potential assessment is not clear. Moreover, the rigorous research data of biomass potential assessment in developing countries are missing, such as China. Thus, for long-term strategy, biomass potential assessment, especially sustainable potential assessment criteria need to be identified. Agricultural residues potential assessment in China will as a case study evaluate in the thesis, by adopting a new GIS-based approach, integrated with GIS as a decision support system, for estimating the sustainable potential of agricultural residues at a high geographical granularity level, with a view to both SE and SOM environmental restrictions in the process. The proposed approach is suitable for cases in China without the assessment of sustainable potential, which can be used to comprehensively assess the potential of sustainable agricultural residues.

The sub-component of biomass logistic system is highly synthesised system, which optimising one component performance may drag other sub-components and overall performance. This thesis, thereby, will optimise logistic system comprehensively to explore the optimal configuration. Meanwhile, the biomass characteristics in the most common pre-treatment technologies will assess experimentally to investigate the effect of pre-treatment method on logistic model. In the end, a concept of zero waste biorefinery process network design is proposed in order to increase biorefinery plant income and reduce pollution exhaust.

Part of the contribution of this thesis is related to the agricultural residues potential assessment in China (Chapter 4), the other part is related to the investigation of logistic system optimisation (Chapters 5 and 6), and the last part is related to the zero waste biorefinery process conceptual network design (Chapter 7). In the next chapter (Chapter 3), the mathematical and experimental procedures and tools are explained and related to the corresponding results chapters.

Chapter 3:
METHODOLOGY

This chapter explains the experimental and numerical methods used in this thesis, following the order of the results chapters 4-7. In total, there are four main methodology sections, the first section explains the agricultural residues potential estimation equations, which serves as preparation for Chapter 4. The second section explains the experimental procedure related to Chapter 5, the following section explains the mathematical model used in Chapters 6, along with a dimensional analysis and validation and the last section explains the conceptual process network design applied in Chapter 7.

3.1 Agricultural residues potential assessment

As summarised in Chapter 2, there are three levels of availability potentials of agricultural residues, namely theoretical potential, technical potential and sustainable potential. A stepwise approach has been applied to evaluate agricultural residue potentials. The theoretical potential of agricultural residues was estimated based on the regional annual crop production (CP) and the RPR. To estimate the technical potential of agricultural residues, a spatial technical potential layer was created by splitting the arable land layer from the land cover layer based on GIS data (ArcMap 10.7, provided by Esri) integrated with restrictions on residue collection (the topographic layer from the landform type layer) according to mechanistic capability. This identified the technical potential area. By comparing the technical potential area with the original arable land, the proportion of technical potential was determined. The technical potential of agricultural residues is estimated by multiplying the theoretical agricultural residue by the proportion of technical potential.

The sustainable potential was calculated based on the proportion of the theoretical potential layer in the sustainable potential layer. Arable land from the technical potential spatial layer that did not comply with legislative regulations was not included in the sustainable potential spatial layer. The amount of agricultural residue in the sustainable potential spatial layer can be calculated by multiplying the proportion of the sustainable potential layer by the theoretical potential. The arable land distribution and area under various soil erosion and soil organic matter classifications in the technical potential spatial layer were identified and calculated. The retention rate of residues for individual soil erosion and soil organic matter classifications was guided by a literature review. The total amount of retained residues within the sustainable potential layer was then calculated using the various retention rates and their areas. The sustainable potential was calculated based on the total residue in the sustainable potential spatial layer and the amount of residue retained. Figure 3-1 illustrates the methodological approach adopted in this section and the relationships among theoretical, technical and sustainable potentials.

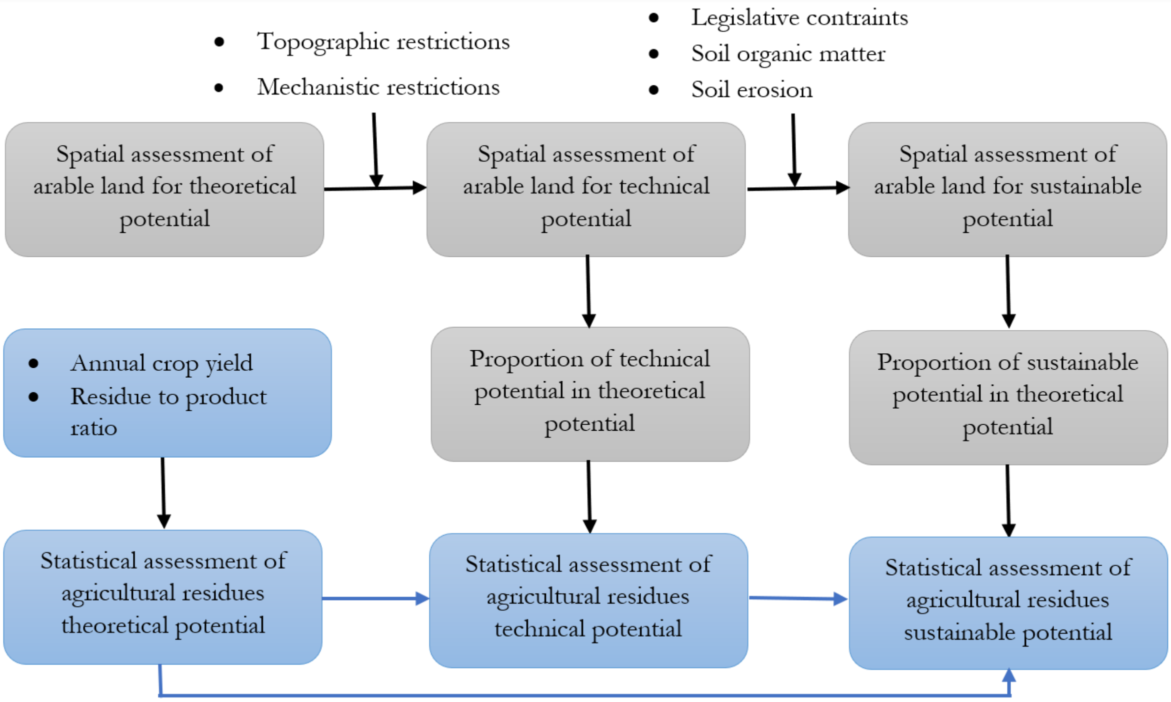

Figure 3- 1: Process of agricultural residue assessment.

3.1.1 Arable land area determination

The framework of the integrated GIS-based modelling approach is presented in Figure 3- 2. The ArcMap 10.6 (an Esri software package) module builder and built-in tools were employed to perform the GIS analysis. The framework for the spatial assessment of arable land included three main approaches. The first step was land cover transformation, classification and mapping. A land use map layer was converted from a raster file to a polygon file to calculate the area of land use. The arable land spatial layer was created by splitting out the corresponding land class from the land use spatial layer. Next, the spatial tool in ArcGIS was used to analyse the resulting arable land layer area; this was compared with statistical data to evaluate its accuracy. Finally, the arable land distribution spatial layer and provincial administrative boundary spatial layer were overlain to generate the arable land distribution by region.

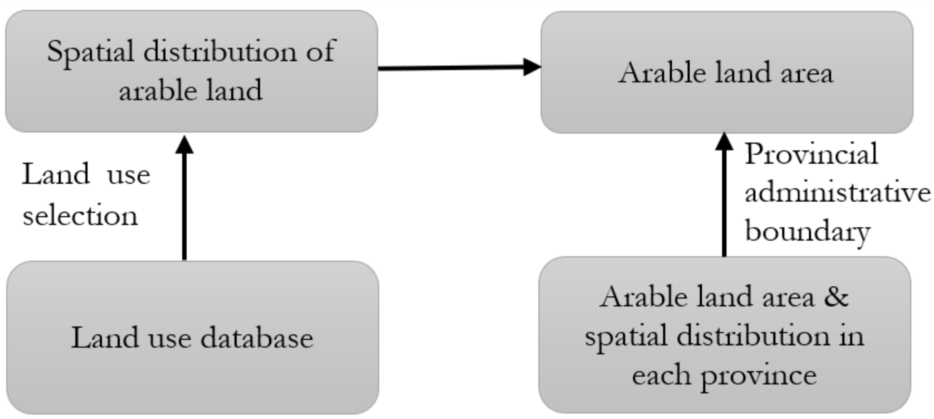

Figure 3- 2: The process of determining residue potential.

3.1.2 Theoretical potential assessment method

The theoretical potential of agricultural residues can be estimated from the regional annual crop production of each crop species *i* and the local residue-to-production ratio *RPR (i, j)* using the following equation:

$$RP = \sum_{i=1}^{m} \sum_{j=1}^{n} CP(i,j) * RPR(i,j) \qquad \text{(Eq. 3.1-1)}$$

where $CP(i,j)$ is the annual production of crop species i in province j and $RPR(i,j)$ is the residue-to-production ratio of crop species i in province j.

3.1.3 Technical potential assessment method

The technical potential of agricultural biomass was estimated based on topographic restrictions, the working capability of the harvesting machinery and the statistics for theoretical potential. A detailed flow chart is presented in Figure 3- 3.

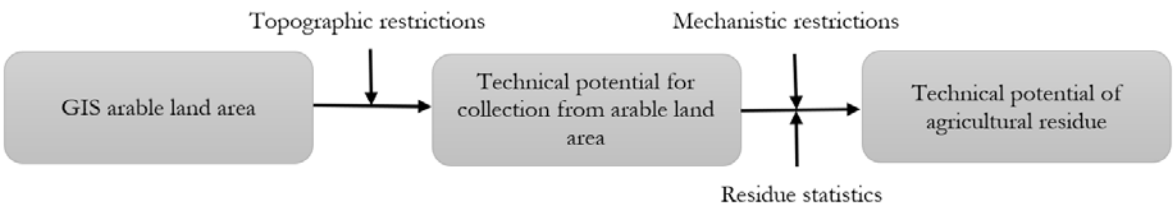

Figure 3- 3: Process of residues technical potential for power generation.

The assessment of technical potential can be divided into two stages: (1) the establishment of the technical potential arable land spatial layer and (2) the area calculation. The arable land area in the technical potential spatial layer was established based on an area-weighting method, which combined arable land and topographic restrictions. First, the spatial topographic layer was collected in a raster format and converted to a polygon format to calculate the area of arable land. Second, the topographic layer was selected and created. Areas with a steep slope (> 15°) were separated from the technical potential topographic layer because of severe soil erosion and the difficulty of harvesting. The arable land spatial layer was then overlain with the topographic layer. Once the arable land spatial layer was established, the arable land distribution and the area with gentle slopes (≤ 15° for mechanised harvesting), representing the technical potential, were calculated.

Once the area of arable land meeting technical potential requirements was calculated, the proportion of the theoretical potential that had technical potential will be estimated accordingly. Due to limits on the operation of the collection machinery, a collection rate of 80% was applied based on the average values suggested in available literatures [4, 38]. The quantity of residue with technical potential can thus be calculated according to the proportion of technical potential arable area, the theoretical potential and the collection rate.

3.1.4 Sustainable potential assessment method

The sustainable potential has been estimated as the amount of residue that can be collected without causing soil erosion, loss of fertility and violation of legislative regulations. To obtain the amount of residue in its sustainable potential, it was first ensured that the arable land was not subject to legislative restrictions. Legislative regulations require a protected area with a radius of 500 m around a water body. Within this area, work activities in any type are prohibited [136]. Therefore, the arable land spatial layer with technical potential was overlain with a 500 m area around water bodies to create an arable land spatial layer that included legislative regulations. Secondly, to address soil erosion control, soil erosion data were collected from the Resource and Environment Data Cloud Platform of China. The classifications and GIS codes for soil erosion are shown in Table 3- 1 and Table 3- 2, respectively.

Table 3- 1: Soil erosion classification.

Soil erosion classification	Average erosion ($t/km^2/year$)			Soil loss thickness (mm/year)
	Water erosion	Wind erosion	Freeze-thaw erosion	
Weak	<200	<500	<1000	<0.15, 0.37, 0.74
Mild	200	500	1000	0.15, 0.37, 0.74
Moderate	2500-5000			1.9-3.7
Intense	5000-8000			3.7-5.9
Strong	8000-15000			5.9-11.1
Severe	>15000			>11.1

Table 3- 2: GIS code for soil erosion.

	Soil erosion classification					
	Weak	Mild	Moderate	Intense	Strong	Severe
Water erosion	11	12	13	14	15	16
Wind erosion	21	22	23	24	25	26
Freeze-thaw erosion	31	32	33	34	-	-

The soil erosion is classified as 'weak' 'mild' 'moderate' 'intense' 'strong' and 'severe' in most Countries, regarding to its assessment system. Based on regulations regarding water and soil conservation[137], areas under 'intense', 'strong' and 'severe' soil erosion are not recommended for farming activities. Thus, to obtain reliable data, the erosion classifications of 'weak', 'mild' and 'moderate' were included in this section, and the classifications of 'intense', 'strong' and 'severe' as restriction criteria were not included. To determine the arable land area under the individual erosion types (weak, mild and moderate SE) and its spatial distribution, the arable land area of each class of soil erosion was overlain with arable land from the technical potential layer with legislative restrictions. The amount of residue cover required for soil erosion control was dependent on the erosion grade. Researchers have agreed that 90% soil loss control can be considered adequate erosion control [43, 49, 138]. The amount of residue cover applied in the GIS model is displayed in Table 3- 3.

Table 3- 3: Residue retention standards for different soil erosion classes [49, 138, 139].

Soil erosion classification	**Amount of mulch ($t/km^2/year$)**
Weak	200
Mild	200
Moderate	300

Thirdly, the area of SOM classifications and its retention rate were assessed. SOM plays a crucial role in maintaining soil fertility for sustainable agriculture. Various studies have suggested that the sustainable removal rate of residues ranges from 20% to 40%. Moreover, 2% SOM has been recommended by various researchers as a reasonable criterion for maintaining the SOM balance in agriculture [43, 140, 141]. There is no doubt that not all arable land can achieve a SOM content of 2%. Thus, the residue retention rate (RRR) was calculated using Eq. 3.1-2 and Eq. 3.1-3[42] to tailor this value to local conditions.

If the SOM content in the topsoil (20 cm) is lower than 2%,

$$RRR_{SOM} = 80\% \text{ of residue production} \quad \text{(Eq. 3.1-2)}$$

and if the SOM content in the topsoil (20 cm) is higher than 2%,

$$RRR_{SOM} = 60\% \text{ of residue production} \quad \text{(Eq. 3.1-3)}$$

To acquire reliable data, the regional distribution of SOM concentration was analysed and data were introduced from Liu [142]. Thus, the amount of sustainable removal residue can be calculated.

SE and SOM are two criteria for soil health and soil fertility. To estimate the sustainable potential of agricultural residues, it is necessary for the retained residue to meet the maximum requirements of amount of residue retained both for SE and SOM. The total residue retained for SE and SOM were calculated and compared and the maximum retained amount was selecting as the sustainable residue retention. The difference between technical potential, legislative regulations and residue retention is the sustainable potential of the agricultural residue.

The total amount of retained residue is dependent on the properties of the land (soil erosion classification and SOM content) and the applied specific residue retention amount (RRA) (using the larger value) was based on Eq. 3.1-4 and Eq. 3.1-5.

If $RRA_{SOM} > RRA_{SE}$:

$$RRA = RRA_{SOM} \quad \text{(Eq. 3.1-4)}$$

If $RRA_{SE} > RRA_{SOM}$:

$$RRA = RRA_{SE} \quad \text{(Eq. 3.1-5)}$$

Thus, the amount of residue with sustainable potential was the difference between the total amount of residue with technical potential under legislative regulations and the amount of residue retained.

3.2 Assessment of agricultural residues characteristics: experimental assessment of torrefaction and raw material

Pre-treatment technologies application significant affect biomass supply chain in the process of transportation and storage. To design an efficiency supply chain network, cost-effective pre-treatment technology is desired. Depending final products, physical, thermal and chemical methods are most common pre-treatment approach in biomass energy conversion. Among that compression widely applied in physical pre-treatment. Due to low energy consumption and high energy density, torrefaction is nowadays an accepted thermal pre-treatment method. Therefore, the most common pre-treatment methods applying in biomass supply chain will be assessed, which includes density, moisture content, energy consumption and heating value assessment. The follow content will introduce biomass properties assessment methodologies.

3.2.1 Determination of moisture contents in biomass feedstock

This experiment will be only tested with corn stalk and rice straw due to limitation of accessible material. The selected rice straw and corn stalk were harvested in north of China. The oven was calibrated to 105 °C with a precision of ±2 °C. All samples will be tested and recorded three times to make sure uniformity, only errors with +2% can be determined as qualified data. Applying the average value of these results, the sample moisture content was determined 3.2.2 Characterisation of torrefied and raw feedstocks

Torrefaction experiment

The schematic of biomass feedstock torrefaction experimental system is demonstrated in Figure 3- 4. The system was consisted of nitrogen cylinder, rotameter (with maximum volume flow of 250 mL min^{-1}), voltmeter, tube furnace, boat crucible (15mm* 75mm) and product gas treatment unit, which are connected by pipes. The nitrogen flow was controlled by rotameter; the voltmeter used to measure energy consumption during torrefaction experiment; the tube furnace is equipped with a quartz tube (with total length 750mm, 650mm effective heating length) and a temperature controller. Experimental samples were carried by a boat crucible, which is replaced in the middle of quartz tube. Three thermocouples were mounted to monitor the temperature changes in the inlet, the middle and outlet of quartz tube. With assistance of a conical flask used as the waste gas treatment unit. Tars and exhaust gas that generated from torrefaction were eliminated and purified.

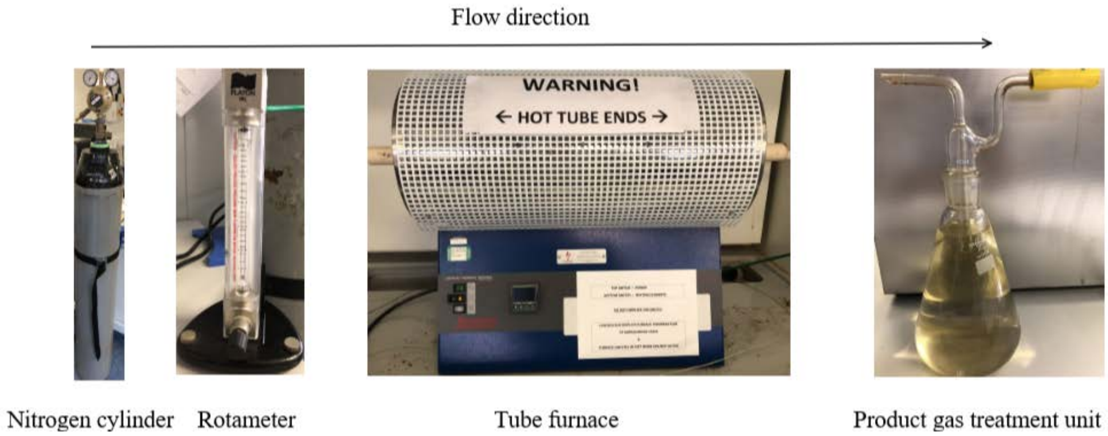

Figure 3- 4: The schematic of experiment system

To secure high results reliability, nitrogen leakage tests were conducted prior to the experiments. Samples undergoing same torrefaction condition were tested twice, and relative error of results between each run was less than 5%, which can approve that the experiment is proceeding rationally.

It was known that final temperature, heating rate and duration time are significant factors in the torrefaction results. Thus, the effect of temperature factor to torrefaction products will be investigated at five distinct levels of torrefaction temperatures: 220°C (light), 240°C, 260°C (mild), 280°C and 300°C (severe) with fixed duration time of 30 mins, heating rate of 20 °C/min, and nitrogen flow rate of 100 mL/min. Each sample was weighed before and again after each experiment to determine the mass loss after torrefaction . The mass yield of residues was obtained from Eq. 3.2-1.

$$Mass\ yield = \left(\frac{m_{torrefaction\ product}}{m_{raw}}\right) \cdot 100\% \qquad \text{(Eq. 3.2-1)}$$

As a common technic, thermogravimetric analysis is widely applied in thermal conversion process, which physical and chemical properties of materials are measured as a function of increasing temperature with constant heating rate, or as a function of time. In this work, Thermogravimetric analyser (TGA) was carried out with a Jupiter STA 449 F3 analyser by NETZSCH (see Figure 3- 5). The combustion profile can be obtained at the heating rate with 20 °C min-^{1}, oxidation atmosphere with a flow rate of 50 mL min^{-1}, and protection gas (nitrogen) flow of 60 mL min^{-1}, where the temperature raises from 25°C to 900°C. Samples were milled and loaded to an Al_2O_3 crucible with 10-20 mg. A Differential thermogravimetry (DTG) curve will indicate the rate of weight loss during temperature increase. The ash content is obtained from TG curve. Among that, samples should collect from various residues to guarantee the uniformity of experiment materials.

Figure 3- 5: Jupiter STA 449 F3 analyser by NETZSCH

Once the content of carbon, hydrogen and nitrogen were measured by carbon hydrogen and nitrogen analyser (CHN analyser), and ash content was obtained from proximate analysis, the oxygen content was calculated by difference [143]. All experiments were run two times and averaged to compensate experimental reproducibility.

Torrefaction energy balance and high heating value (HHV) will be in the experiment. HHV is a vital parameter in determining energy densification of solid product during torrefaction. Energy balance of torrefied product can not only obtain from the difference between energy consumption and HHV, but also from further supply chain such as the effect of torrefied product density on transportation and storage cost in supply chain. Energy balance is a criteria factor that assess the performance of torrefied products.

The higher heating value can be obtained from Eq. 3.2-2 and Eq. 3.2-3.

$$HHV = 0.3491X_C + 1.1783X_H + 0.1005X_S - 0.0151X_N - 0.1034X_O - 0.0211X_{ASH}\ [\frac{MJ}{kg}]$$

(Eq. 3.2-2)

$$LHV = HHV\left(1-\frac{w}{100}\right) - 2.444\frac{w}{100} - 2.444\frac{h}{100}8.936\left(1-\frac{w}{100}\right)\ [\frac{MJ}{kg}] \quad \text{(Eq. 3.2-3)}$$

Where, Xi is the content of carbon (C), hydrogen (H), sulphur (S), nitrogen (N), oxygen (O) and ash in wt%; w is moisture content of the fuel in wt% (w.b.); h is concentration of hydrogen in wt% (d.b.).

The energy yield of torrefaction can display on Eq. 3.2-4

$$Energy\ yield\ (\%) = \frac{Total\ energy\ of\ torrefied\ biomass}{Total\ energy\ of\ raw\ biomass} \times 100\% \qquad \text{(Eq. 3.2-4)}$$

3.3 Logistic model optimization.

The aim of section is to integrate advanced supply chain model elements from previous researchers, designing an advanced supply chain model. A three-step approach contributes present section, which involved the results of pre-treatment characteristics experimental investigation form section 3.2, biomass supply chain model network design and GIS based long-term decision-making supporting system. First, biomass feedstocks (i.e., rice straw and corn stalk) characteristics results will be used for the supply chain model as input variables, followed by the network design of supply chain model, with various advanced network design concept gathers in supply chain model including distribute depot and collection pattern. Depending on statistical data of local conditions and logistic algorithm model, GIS could be used for planning the optimal biorefinery plant and storage depot capacity, location and distance, which enhance logistic model optimization performance. Lastly, a case study of biomass CHP will be analysed. The flow diagram of biomass supply chain model network design is presented in Figure 3- 6.

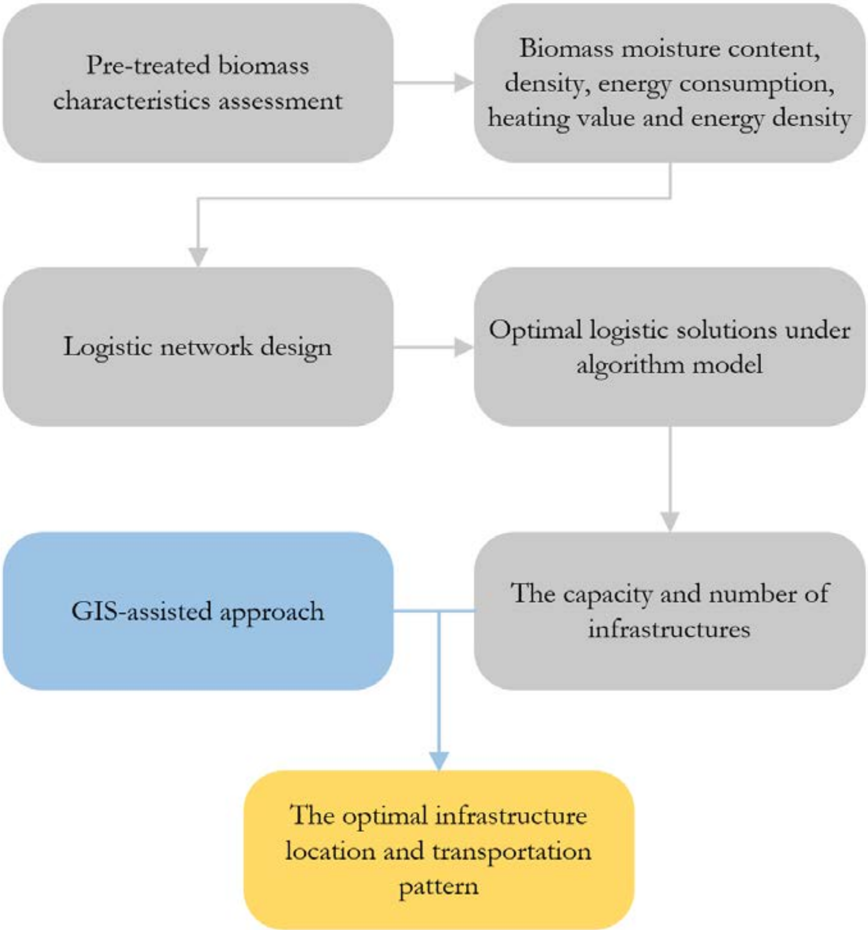

Figure 3- 6: The flow diagram of medium-term decision making.

3.3.1 Biomass logistic network design

As the most important component of biomass supply chain, logistic model plays crucial role in cost control. To do that three step approaches included: First, in biomass supply chain model optimization, a supply chain model (mathematical programming) proposed and the characteristic and effect of pre-treatment methods on supply chain model will access, which investigate the effect of pre-treatment technologies (shredding, compression and torrefaction) on supply chain cost (environmental sustainability and financial cost), cooperating with experimental data and mathematical programming. Biomass CHP will be a case study introduced in supply chain model. Secondly, the long-term decision making will assist by GIS for determining infrastructure location, which transfer supply chain problem from uncertainty to certainty. Lastly, CHP as a case study will launch for building more efficiency and low-cost industry, which connecting long- and medium-term decision makings.

Biomass supply chain model will be developed to maximize profitability index (PI) value during whole supply chain period by maximize revenue and minimize cost, which includes the cost in collection, pre-treatment, transportation, storage and the revenue of profit. PI is applied in capital budgeting to measure the profitability of a project. The PI value can be indicate that how much money will be gained for every dollar invested [144]. Therefore, the PI value above 1 means the project is profitable. Meanwhile, CO_2 emissions along with the pre-treatment, transportation, feed handing and biorefinery processes will be taken account into the supply chain model environmental assessment. Depending on objective function (i.e., financial and environmental consideration), the supply chain model will provide the corresponding solution. By incorporating the input biomass parameters (characteristics and distribution), the number and size of collection facilities and biorefinery plant can be identified.

Two variables contribute decision criteria of present supply chain model, which includes PI value and CO_2 emissions during supply chain processes. To evaluate project financial sustainability, net present value (NPV) and PI value are traditional evaluation factor that direct reflect the profitability of business. The amount of CO_2 emission is evaluated supply chain whether sustainable project.

Supply chain mathematical model

The objective function of supply chain model is maximized profitability index by evaluate NPV and PI value, which shown in Eq. 3.3-1 and Eq. 3.3-2. Where,

$$NPV = (R_p - C_c - C_{mi} - C_{emi} - C_{fuli} - C_t - C_{s1} - C_{s3} - C_{ash} - C_{pm} - C_{ps})D_f - \left(C_{pi} + S_s C_c + \frac{Q}{h\beta_i} C_{ei}\right) \quad \text{(Eq. 3.3-1)}$$

$$PI = \frac{(R_p - C_c - C_{mi} - C_{emi} - C_{fui} - C_t - C_{si} - C_{s3} - C_{ash} - C_{pm} - C_{ps})D_f}{C_{pi} + S_s C_c + \frac{Q}{h\beta} C_{ei}} \quad \text{(Eq. 3.3-2)}$$

Where R_p is power plant revenue; C_c is biomass purchasing cost; C_{mi} is pre-treatment maintain cost; C_{emi} is pre-treatment employee's cost; C_{fuli} is pre-treatment fuel cost; C_t is transportation cost; C_{s1} is storage fixed cost; C_{s3} is storage flexible cost; C_{ash} is ash disposal cost; C_{pm} is power plant maintain cost; C_{ps} is salary and welfare cost; D_f is discounting coefficient; C_{pi} is power plant capital cost; S_s is storage area; C_c is storage construction cost; Q is the total amount of biomass for power generation; h is pre-treatment equipment working time; β_i is pre-treatment equipment working capability; C_{ei} is pre-treatment equipment capital cost.

Constraints

The mass balance must be satisfied at each process in supply chain model, which the total required biomass Q should equal to

$$Q = n\pi r^2 \rho \qquad \text{(Eq. 3.3-3)}$$

Where, r is radius collection radius from field to depot; ρ is biomass distribution density; n is the number of depots.

According to Zhuang *et al* [83] residues collection radius should not 50km thus,

$$R = r + L2 \leq 50km \qquad \text{(Eq. 3.3-4)}$$

Where L2 is distance between depot and power plant.

For biomass availability consideration, the amount of total biomass in the selected area should not less than the amount of biorefinery plant minimal requirement. Therefore, the biomass refinery plant capacity constraints are expressed by

$$\frac{3.6\times10^3 \mathrm{P_n h}}{\eta \mathrm{LHV_i}} \leq \pi \mathrm{R}^2 \rho \, \partial \qquad \text{(Eq. 3.3-5)}$$

Where $\mathrm{P_n}$ is power plant capacity; LHV_i is biomass lower heating value; η is power plant efficiency. ∂ is agriculture residues available collection index.

Biomass demand for operation

$$Q_0 = \frac{3.6\times10^3 P_n h}{\eta LHV} = \pi R^2 \rho \partial \qquad \text{(Eq. 3.3-6)}$$

Due to biomass will loss during transportation and storage, the amount of actual requirement should higher than ideal demand. The total amount of required biomass is

$$Q = Q_0(1+\mu)(1+M) = \pi R^2 \rho \partial \qquad \text{(Eq. 3.3-7)}$$

Where, μ is losses index; M is the moisture content of received residues.

Total cost for power generation

The total cost for power generation was contributed by biomass purchasing cost, pre-treatment cost, transportation cost, storage cost, ash cost and production cost. Shown in Eq. 3.3-8:

$$C_{total} = C_c + C_{pt} + C_t + C_s + C_{ash} + C_p \qquad \text{(Eq. 3.3-8)}$$

Where C_c is biomass purchase cost; C_{pt} is pre-treatment cost; C_t is transportation cost; C_s is storage cost; C_{ash} is ash disposal cost and is power plant operation cosr.

The cost of *pre-treatment* is present in Eq. 3.3-9

$$C_{pti} = C_{di} + C_{mi} + C_{emi} + C_{fuli} \tag{Eq. 3.3-9}$$

Where C_{di} is pre-treatment Equipment cost.

Pre-treatment equipment cost	$C_{di} = \frac{Q}{h_i\beta} C_{ei} \frac{(1 - RV_i)}{n_i}$	(Eq. 3.3-10)
Pre-treatment maintain cost	$C_{mi} = C_{omi} \frac{Q}{h\beta_i} C_{ei} h$	(Eq. 3.3-11)
Pre-treatment employees' cost	$C_{em1} = N_i \frac{Q}{h\beta_i} C_{sal}$	(Eq. 3.3-12)
Pre-treatment fuel cost	$C_{fuli} = O_{coni} \frac{Q}{\beta_i} C_{ful}$	(Eq. 3.3-13)

Transportation cost includes the cost from filed to collection point, the cost from collection point to power station and handing cost.

$$C_t = C_{t1} + C_{t2} + C_{t3} \tag{Eq. 3.3-14}$$

Transportation cost from filed to depot	$C_{t1} = \sum_{i=1}^{n} \iint \frac{\rho \partial f r^2}{\rho_1 V_v} P_t dr d\theta$	(Eq. 3.3-15)
Transportation cost from depot to power station	$C_{t2} = n \frac{\pi r^2 \rho}{\rho_i V_v} f L_2 P_t$	(Eq. 3.3-16)
Loading and unloading cost	$C_{t3} = 4 P_L Q$	(Eq. 3.3-17)

Storage cost involved fixed cost, facility capital cost and variable cost,

$$C_s = C_{s1} + C_{s2} + C_{s3} \tag{Eq. 3.3-18}$$

which shows in the following:

Storage Fixed Cost	$C_{s1} = \frac{Q}{\rho_i H} C_{sm}$	(Eq. 3.3-19)

Storage Facility Capital Cost	$C_{s2} = S_s C_c \frac{(1 - RV_4)}{n_4}$	(Eq. 3.3-20)
Storage Variable Cost	$C_{s3} = P_{os} Q$	(Eq. 3.3-21)

Ash disposal cost present in Eq. 3.3-22. Where,

$$C_{ash} = P_{ash} M_{ash} Q_0 \quad \text{(Eq. 3.3-22)}$$

Power plant operation cost includes investment capital cost, maintain cost, salary and welfare cost. Where,

$$C_p = C_{pai} + C_{pm} + C_{ps} \quad \text{(Eq. 3.3-23)}$$

Power plant capital investment cost	$C_{pai} = C_{pi} \frac{(1 - RV_i)}{n_i}$	(Eq. 3.3-24)
Power plant maintain cost	$C_{pm} = \gamma C_{pai}$	(Eq. 3.3-25)
Salary and welfare cost	$C_{ps} = \lambda C_{pai}$	(Eq. 3.3-26)

Biomass grinding energy consumption is calculated using Eq. 3.3-27:

$$C_{bg} = E_{bg} \frac{1000}{36000} Q_0 C_{ele} \quad \text{(Eq. 3.3-27)}$$

Where, $\mathrm{E_{bg}}$ is electricity consumption for grinding 720 kJ/kg, while $\mathrm{E_{bg-t}}$ torrefied product grinding electricity consumption 36-217 kJ/kg

Power plant revenue

Power plant revenue includes power generation revenue and heating selling cost

$$R_p = R_{pg} + R_h \quad \text{(Eq. 3.3-28)}$$

Power plant power generation revenue	$R_{pg} = 1000\,(P_{ele} + P_s) P_n h$	(Eq. 3.3-29)
Power station heating sealing revenue	$R_h = P_h Q_0 H_{LHV} E_h$	(Eq. 3.3-30)
Power plant net profit	$R_{net} = \left(R_p - C_{total}\right)(1 - income\ tax\ rate)$	(Eq. 3.3-31)

CO_2 emission

CO_2 emission for logistic model includes CO_2 emission during transportation, pre-treatment, and storage. Which,

$$E = E_t + E_{pt} + E_s \quad \text{(Eq. 3.3-32)}$$

Transportation emission from field to depot	$\mathrm{E_{t1}} = \sum_{i=1}^{n} \iint \frac{\rho\, \partial f r^2}{\rho_1 V_v} \mathrm{E_{diesel}} \left(\mathrm{Q_{c_{full}}} + \mathrm{Q_{c_{emp}}}\right) \mathrm{d}r\mathrm{d}\theta$	(Eq. 3.3-33)
Transportation emission from depot to power plant	$E_{t2} = nfL\left(Q_{p_{full}} + Q_{p_{emp}}\right) E_{diesel} Q / \rho_i V_v$	(Eq. 3.3-34)
Transportation emission in loading and unloading	$E_{t3} = \frac{Q}{\beta_i} O_{coni} E_{diesel}$	(Eq. 3.3-35)
Pre-treatment emission	$E_{pt} = E_{ele} O_{coni} \frac{Q}{\beta i}$	(Eq. 3.3-36)
Storage emission	$E_s = \frac{Q}{\beta_i} P_{stack} + \frac{Q}{\beta_i} P_{unstack}$	(Eq. 3.3-37)
Diesel emission	$E_{diesel} = 1 \times 10^{-3} Q_{carbon} \varphi_{carbon} \delta_{carbon} LHV_{carbon}$	(Eq. 3.3-38)

The logistic model variables input values, symbols and references can be found in Appendix I.

3.3.2 GIS-assisted long-term decision-making

A visualized decision supports system could significantly reduce cost in logistic management by identifying potential risk in the aspect of infrastructure planning. In order to further reduce supply chain cost, in the present section, GIS as main technical approaching for supply chain model in terms of agricultural residues potential investigation, transportation route planning, storage location allocation and biorefinery plant location determination. Figure 3- 7. Illustrates the cooperation process between GIS system and logistic model.

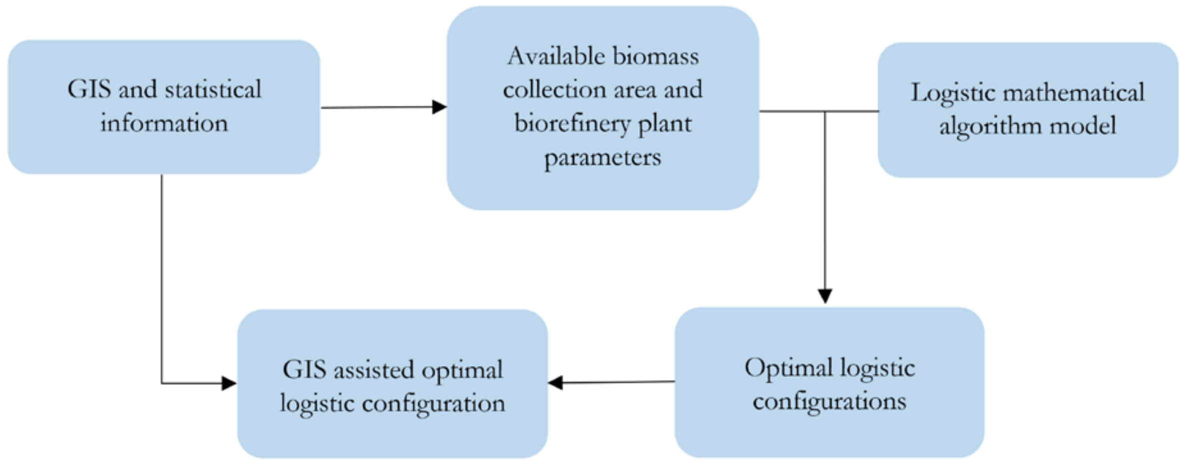

Figure 3- 7: The function of GIS on assisting logistic model for decision making

To operate biofuel refinery plant, long-term decision strategy applied for overview consideration. In previous chapter [145], biomass potential was assessed in order to evaluate biorefinery plant probability in a region. Since a potential region has been determined, biofuel refinery plant location need to be figured. four step approaches are applied in this section. Firstly, cooperating with statistical data (existing biorefinery plants and biomass density), the existed biorefinery plants collection radius and available collection area for new biofuel plant can be analysed by GIS. Once biofuel plant collection area confirmed, GIS could analyse the optimal collection radius, biorefinery plant location and capacity for logistic model for further analysis. Secondly, in logistic model, the optimal pre-treatment method, the number of optimal depots for pre-treatment and storage can be exam. Flowed by, logistical model results will be as input variables in GIS for biomass transportation and collection route calculation. In the end, route information will return to logistical model to output final medium-term decision strategy.

3.4 Conceptual zero waste biorefinery process

3.4.1 Traditional commercial-scale bioethanol production process

A traditional commercial-scale biomass to ethanol biorefinery plant includes the following nine main process steps: (1) feed handling; (2) feedstock pre-treatment; (3) enzyme production; (4) hydrolysis and fermentation; (5) distillation; (6) combined heat and power generation; (7) waste water treatment; (8) storage and (9) utilities management (water system and power system), as represented by National Renewable Energy Laboratory (NREL) [133] as an example shown in Figure 3- 8. Firstly, feedstock is loaded and shredded for downsizing in the ***feed handing process***, followed by the feedstock ***pre-treatment processing*** to decompose lignocellulosic biomass into its components (cellulose, hemicellulose and lignin) for high efficiency hydrolysis.

The sulfuric acid, as a proven competitive low cost and high efficiency pre-treatment solution, has been wildly applied in feedstock pre-treatment. Then, the pre-treated feedstock mixes with enzyme that is produced in the ***enzyme production process*** for ***hydrolysis and fermentation*** under a suitable reaction condition. Finally, the glucose that hydrolysed from cellulose and hemicellulose, catalysed by enzyme converting to ethanol. The ***ethanol distillation process*** will separate ethanol, lignin and stillage. The ethanol and stillage will be further processed for the ***storage*** and the ***wastewater processing*** (the grey flow chart in Figure 3- 9) respectively. The ***storage*** plays a crucial role for elemental sources (i.e., sulfuric acid, protein, ammonia and other inorganic soluble solids) supplying to bioethanol plant. Eutrophic stillage undergoing anaerobic digestion (under ***wastewater treatment processing***) produce treated water and biogas, which as feed transfer to ***feedstocks pre-treatment processing*** and ***combined heat and power (CHP)*** for process water recycling and operation. While the waste water brine discharge to environment. Extracted lignin (from ***ethanol distillation***) and biogas (from ***wastewater treatment***) will be combusted in a ***CHP*** system to produce energy (i.e., heat, power and steam) for biorefinery plant operation and electricity grid in order to increase plant profitability. The ash will be disposed to landfill. The ***utilities*** include on-site recirculation of cooling water and external electricity from grid to support biorefinery plant operation.

From the above description of traditional commercial-scale bioethanol production process, it is clear that various waste streams (such as CO_2, wastewater and eutrophic content) are discarded to the environment, causing secondary pollutants while simultaneously reducing the benefits to a sustainable development, although its original intention was to reuse agricultural waste and protect the environment. For instance, in traditional ethanol refinery process, stillage from ***ethanol distillation*** contains abundant organics (such as furfural, glucose and sugars), which high value contents convert to low value biogas for combustion. Lignin is a huge potential raw material for chemistry industry [146]. While most of lignin in traditional bioethanol refinery will be burnt for power generation, which not only cause source waste but also environmental impact. There is no doubt that the lignocellulose-based bioethanol production cost is much higher than ethanol market value [147]. Thus, optimising processing design and increasing by-products value are key for reducing production costs currently.

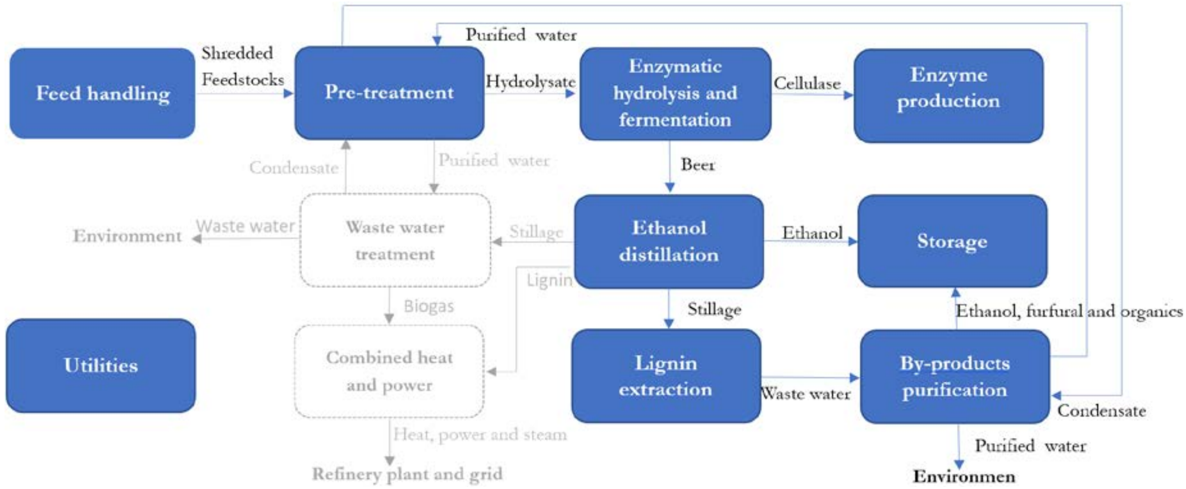

Figure 3- 8: Simplified flowsheet of zero waste and traditional (grey) ethanol biorefinery process.

3.4.2 The concept of zero waste biorefinery process

In comparison to the traditional process, this work aims to maximise the value-added by-products and achieve zero waste emission, and proposed a by-product processing path that extract value-added lignin, furfural and other organics. To realise this, wet stillage (produced from ***ethanol distillation***) will be filtered and dried to separate lignin and wastewater in ***lignin extraction process*** (Figure 3- 8). In this process, the insoluble organics (such as lignin and ash), small amount of water and soluble organics will be removed from stillage. The eutrophic wastewater will be further extracted to generate furfural, ethanol and other organics powder by multistage fractionation in ***by-products purification processing*** and storing in ***storage*** as presented in Figure 3-8. As same with traditional bioethanol production process, purified water will pump to ***feedstock pre-treatment processing*** for water recycling. Except essential usage, the rest purified water will discharge to environment. The organics powder will be returned to soil as fertilizer for soil organic matter protection. Due to no power and heat produced from the refinery process, the plant operation related power and heat needs to be provided from industry electricity grid. The major process updates are summarised as below:

- Multistage wastewater fractionation to extract high value-added materials;
- Lignin extraction replaces CHP production;
- Using latest available Chemical Engineering Plant Cost Index (CEPCI) and Producer Price Index (PPI) for data analysis;
- Recycling water from ***by-products purification processing*** to ***feedstocks pre-treatment processing*** to reduce utilities cost;

▪ energy is supplied from external renewable sources.

3.4.2.1 Lignin extraction process design

Specifically, ***by-products purification process*** and ***lignin extraction process*** towards zero emission were developed. While, the other areas (i.e., feed loading, pre-treatment, enzyme production, hydrolysis and fermentation, distillation, utility, and storage process) are similar to the NREL's process. The stillage which includes insoluble content and wastewater is extracted from ***ethanol distillation process***, venting in tank and filtering wet lignin and waste water in filter (see Figure 3- 9). The wet lignin is then washed in washing tank in order to remove soluble content. After further percolation, the washed water mixes with wastewater transferred for further purification in ***by-products purification***. Coordinating with compressor heater, wet lignin will be dried by hot nitrogen flow, dried lignin and insoluble content will be subsequently collected and stored. The moisture from wet lignin will chill and mix with waste water stream transfer to ***by-products purification.*** The detailed Aspen simulation model for ***lignin extraction process*** will be illustrated in Appendix II.

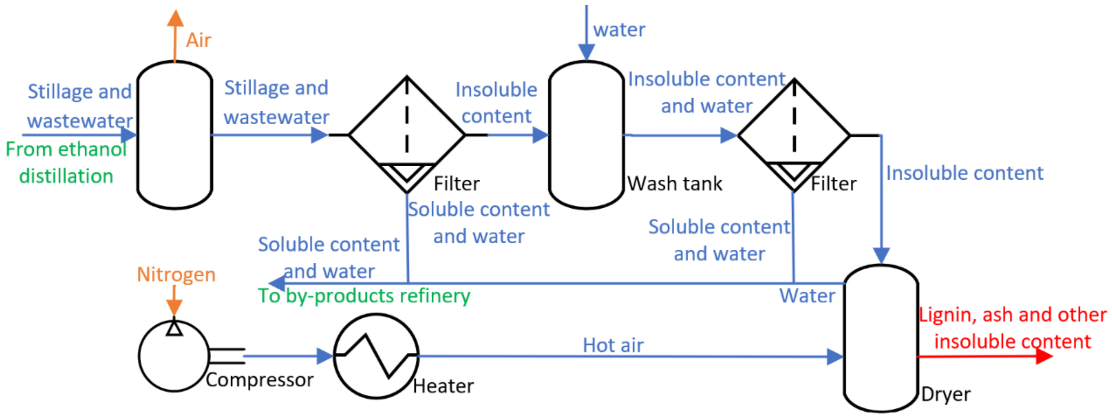

Figure 3- 9: Lignin extraction flowsheet in concept process diagram.

3.4.2.2 By-product purification process design

Due to the fact that different compounds in waste water have different boiling points, (i.e., 161.7°C for furfural [148], 78.4°C for ethanol [149], and 100°C for water [150]) high value-added by-products can be extracted from waste water. Firstly, the wastewater from ***lignin extraction process*** and condensate from ***feedstock pre-treatment process*** will vent and pump to heat exchanger, then transfer to flash tank in order to separate soluble organics (mainly glucose and xylose represented high-boiling components) and other soluble components (see Figure 3- 10). This is followed by the most of water will be extracted after two dehydration process, which will be stored in ***utilities*** for ***feedstock pre-treatment process*** water recycling and discharge to environment respectively. A small part of rest wastewater, which contains water, ethanol and furfural, will remain in ethanol fractionating column for ethanol distillation, ethanol can be separated at a reaction temperature of 80°C in fractionating column. The wastewater will further be dehydrated in tertiary dehydration column, which ensure high concentration furfural could easily extract from mix aqueous solutions in furfural rectification column. In the end, this process will extract high value-added by-products which includes lignin in ***lignin extraction***; ethanol, furfural , purified water and soluble organics powder in ***By-product purification***. The purified water can be reused in ***feedstock pre-treatment*** for operation cost reduction, while dried soluble organics can be returned to soil as fertilizer for environment sustainable purpose. The detailed ***by-products purification*** Aspen simulation model will be illustrated in Appendix III.

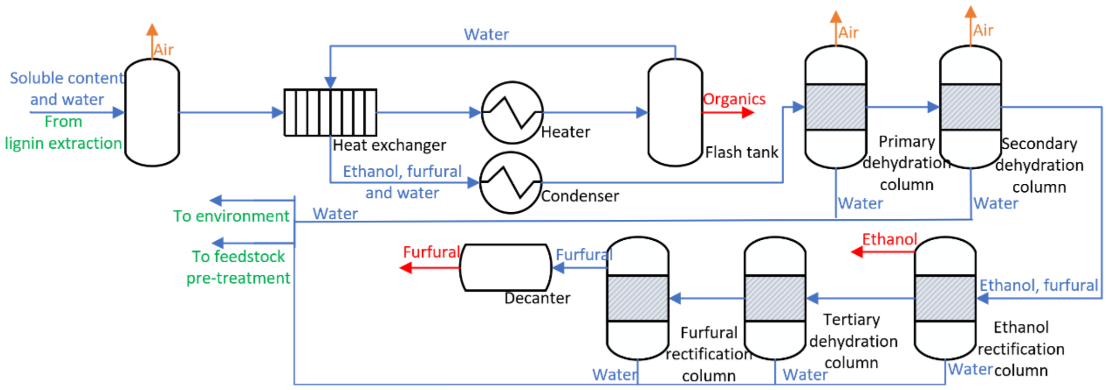

Figure 3- 10: Wastewater multistage purification process in concept process diagram.

The detailed instructions for critical main units used during the process simulations, including washing tank, drying and dehydrating, are listed in Table 3- 4.

Table 3- 4: Description of the unit operation block in Aspen plus simulation.

	Units	Functions	ASPEN blocks
Lignin extraction	Insoluble organics filter	Separate liquid and insoluble components	Filter
	Solid washing	Solid washing	SWash
	Dryer	Solid drying	Flash 2
	Air compressor	nitrogen pressure from 1 bar to 1.2 bar	Compr
By-products purification	Heater	Wastewater heating	HeatX
	Flash tank	high-boiling components separation	Flash 2
	Dehydration column	Wastewater Dehydration	RadFrac
	Dehydration column	Wastewater Dehydration	RadFrac
	Ethanol Separation column	Ethanol extraction	RadFrac
	Dehydration column	Wastewater Dehydration	RadFrac
	Furfural Separation column	Furfural extraction	RadFrac
	Decanter	Furfural refinery	Decanter

3.4.3 Evaluation criteria

In order to comprehensively evaluate and compare the traditional and the zero-waste ethanol biorefinery, financial analysis and environmental impact analysis, in the form of CO_2 emissions, are carried out. The financial analysis is based on year values U.S. dollars at 2020 exchange currency, while the economic assumptions and parameters are similar to the NREL reports [133]. The equipment sizing and related operating and capital costs were determined by the simulation results from Aspen Plus. The operating costs include: (1) variable operating costs associated with feedstocks, raw materials, waste handling, and by-product credits; and (2) fixed operating costs consisting of employees' salaries, labour burden, maintenance, and property insurance. The variable operating costs are calculated based on the Aspen Plus simulation results. The fixed operating costs are estimated following the assumptions of the NREL report [133].

In the aspect of CO_2 emission, zero waste biorefinery was calculated based on electricity consumption related CO_2 emission intensity (g CO_2/kWh) and its energy consumption which was estimated based on results of the energy balance generated by the Aspen Plus simulation, including the thermal energy required in the heat exchangers, re-boilers, as well as the electric energy needs of the pumps, compressors, mills and other equipment.

3.4.4 Material characteristics and process parameters

Feedstock composition

The design of biorefinery process is significant impact by the type and composition of biomass feedstocks. The type of feedstock can affect the important components design and process network design. Such as pre-treatment technologies selection, reactors design and flow rate control. The composition of feedstocks significant influence sugar conversion, which further affect ethanol production. Therefore, a large amount, stable supply and quality steady feedstock is desired. Corn stalk is one of the sustainable potential agricultural residues.

The composition of corn stalk may vary depending on the local weather conditions, soil condition and the type of harvesting and storage. This research evaluated various research paper and averaged composition, showing in Table 3- 5.

Table 3- 5: Summary of corn stalk composition.

Corn stalk (dry wt %)			
Glucan	35.05	Extractives	14.65
Xylan	19.53	Arabinan	2.38
Lignin	15.76	Galactan	1.43
Ash	4.93	Mannan	0.60
Acetate	1.81	Sucrose	0.77
Protein	3.10	Moisture (wt %)	20%

Process design technique parameters

The process network design was proposed based on NREL research. Therefore, the capacity of designed ethanol refinery plant was 2000 MT corn stalks per day with 8410 operation hours, which the feedstock inlet flow was 104167 kg/hr. Depending on conversion efficiency (detailed process conversions rate were shown in [133]), the ethanol yield of refinery plant was 21808 kg/hr (99.38% purity). As by-products of ethanol production, the stillage and wastewater 403607 kg/hr, which will be extracted and purified to high value-added by-products and clean water. For ethanol biorefinery sustainable development and zero waste emission, wastes will move to proposed zero waste process (***lignin extraction process*** and ***by-products purification process***). The detailed, flowrate, simulation model technique configuration and equipment distribution will be list in Appendix IV.

3.5 Summary

In this chapter, the mathematical and experimental methodologies used in this thesis are explained. The biomass potential assessment methods have been introduced for Chapter 4 results, which proposed combining both SE and SOM as assessment criteria for biomass sustainable potential evaluation innovatively. The experimental procedure of biomass torrefaction characteristics using tube furnace has been described because in Chapter 5 the experimental results are discussed, and the same experimental data is also used in combination with a logistic model in Chapters 6. The conceptual simulation of zero waste bioethanol process network design has been introduced in Chapter 7, which is based on advanced bioethanol production experience.

CHAPTER 4:

AGRICULTURAL RESIDUES POTENTIAL AND DISTRIBUTION ASSESSMENT – A CASE OF CHINA

In this Chapter, agricultural residues potentials (includes theoretical, technical and sustainable potentials) and its spatial distribution in China are studied. Firstly, agricultural residues theoretical potential was assessed by RPR and crop production, which crosschecked with Food and Agriculture Organization statistical database (FAOSTAT) for data evaluation. Secondly, the technical potential was estimated with consideration of limitations of topography and mechanical collection. Thirdly, the sustainable potential assessment has innovatively considered both the effect of SOM and SE on soil sustainability development. Lastly, agricultural residues contribution for energy security was proposed

4.1 Data collections

The annual crop production and residue-to-production ratio were two main factors for the estimation of residues theoretical potential. As China is a large agricultural country, the types of crops and their annual productions vary in different regions. To access the latest data, annual crop productions were obtained from each province or municipality subordinate statistics bureau, which are part of the National Bureau of Statistics of China (NBSC). Due to the inaccessibility of the websites of subordinate statistics bureaus (Hubei, Hebei, Yunnan, Tibet, Ningxia and Qinghai provinces), some of the data were collected directly from the NBSC's Statistical Yearbook [151]; the data from 16 provinces or municipalities were acquired for the year 2016, and the remaining regions used the most recent accessible online data (2015).

Region-specific RPR was applied for each crop due to no available overall RPR data to represent the major crops in China. The region-specific RPR data for the major crops are summarised in Table 4- 1, including the most common cereals (wheat, corn, rice, millet and sorghum), root crops (tubers), oil crops (peanuts, sunflower, sesame and rape straw) and fibre plants (cotton and other fibre crops). Table 4- 1 shows the RPRs for 6 major regions in China: Northeast (Liaoning, Jilin and Heilongjiang), North China (Beijing, Tianjin, Hebei, Shanxi, Inner Mongolia, Shandong and Henan), the middle and lower reaches of the Yangtze River (Shanghai, Jiangsu, Zhejiang, Anhui, Jiangxi, Hubei and Hunan), Northwest (Shaanxi, Gansu, Qinghai, Ningxia and Xinjiang), Southwest (Chongqing, Sichuan, Guizhou, Yunnan and Tibet) and South (Fujian, Guangdong, Guangxi, Hainan).

Table 4- 1: RPRs for the major agricultural residues.

	Northeast	North	Middle and lower reaches of Yangtze River	Northwest	Southwest	South	Ref.
Wheat	0.93	1.34	1.38	1.23	1.31	1.38	[152]
Corn	1.86	1.73	2.05	1.52	1.29	1.32	[152, 153]
Sorghum	1.60	1.60	1.60	1.60	1.60	1.60	[154-156]
Rice	0.97	0.93	1.28	1.03	1	1.06	[152, 153]
Millet	1.42	1.45	1.66	1.35	1.72	1.66	[152, 153]
Peanuts	1.50	1.22	1.50	1.33	1.20	1.65	[152, 153]
Rapeseed	-	-	2.05	2.34	2.00	-	[152]
Sunflower	2.74	2.16	2.10	1.92	2.10	2.10	[152]
Tubers	0.71	1.00	1.16	1.07	1.05	1.41	[152]
Beans	1.70	1.57	1.68	1.07	1.05	1.08	[152]
Sesame	3.00	3.00	3.00	3.00	3.00	3.00	[155-157]
Cotton	-	3.99	3.32	3.67	-	-	[152, 153]

Note: The RPR of crop species was calculated on an air-dried basis with 15% moisture [152] .

GIS-related data. A stepwise approach has been clearly illustrated in methodology, the spatial data for GIS modelling is classified as: land cover, administrative boundary, landform type, and soil erosion, as detailed in Table 4- 2.

Table 4- 2: Spatial data for GIS modelling.

Category	Description	File type	Ref.
Land cover	Remote sensing monitoring data on China's land use status	Raster 1 km × 1 km	[158]
Administrative boundary	China Provincial Administrative Boundary Data	Polygon 1 km × 1 km	[159]
Landform type	Spatial distribution data on landform types in China (1:1 million)	Raster 1 km × 1 km	[160]
Soil erosion	Spatial distribution data on soil erosion in China	Raster 1 km × 1 km	[161]

Due to spatial resolution issues related to layer accessibility, the creation of an arable land distribution spatial layer was based on the land use database and Chinese provincial administrative boundary data at a high spatial resolution (1 km × 1 km). These data came from the Resource and Environment Data Cloud Platform of the Institute of Geographic Sciences and Natural Resources Research [158, 159]. The soil erosion data were collected from the Resource and Environment Data Cloud Platform of China [161]. The classifications and GIS codes for soil erosion are presented in Table 4- 3 and Table 4- 4, respectively.

Table 4- 3: Soil erosion classification.

Soil erosion classification	Average erosion ($t/km^2/year$)			Soil loss thickness (mm/year)
	Water erosion	Wind erosion	Freeze-thaw erosion	
Weak	<200	<500	<1000	<0.15, 0.37, 0.74
Mild	200	500	1000	0.15, 0.37, 0.74
Moderate		2500-5000		1.9-3.7
Intense		5000-8000		3.7-5.9
Strong		8000-15000		5.9-11.1
Severe		>15000		>11.1

Table 4- 4: GIS code for soil erosion.

	Soil erosion classification					
	Weak	Mild	Moderate	Intense	Strong	Severe
Water erosion	11	12	13	14	15	16
Wind erosion	21	22	23	24	25	26
Freeze-thaw erosion	31	32	33	34	-	-

4.2 Validation of the arable land spatial layer data source

The statistical data from the National Bureau of Statistics of China (NBSC) on annual crop production and the area of arable land were compared with the Food and Agriculture Organization statistical database (FAOSTAT) [162]. It was found that in China, 1658064 km^2 was defined as arable land in 2015, which closely matches the figure of 1663738 km^2 from the NBSC [163]. However, the statistics on crop production from FAOSTAT and NBSC differed: 623.19 Mt was reported by FAOSTAT [164] versus 660.60 Mt reported by NBSC [151]; this difference of 5.67% indicated that the data were reasonably reliable. This comparison was followed by an evaluation of the spatial data. There are two primary errors in GIS mapping: the classification of land cover and the area of a specific land use. Land cover misclassification typically has a high probability in GIS mapping [30]. For example, grassland is misclassified as arable land. Simultaneously, inadequate spatial resolution might overestimate or underestimate the specific land area. To assess the reliability of the GIS mapping data, a single indicator (arable land) analysis was conducted. The accuracy of the GIS mapping for the area of arable land was evaluated using statistical data from NBSC as a reference. The comparison between the NBSC statistical data and the GIS data are presented in Figure 4- 1.

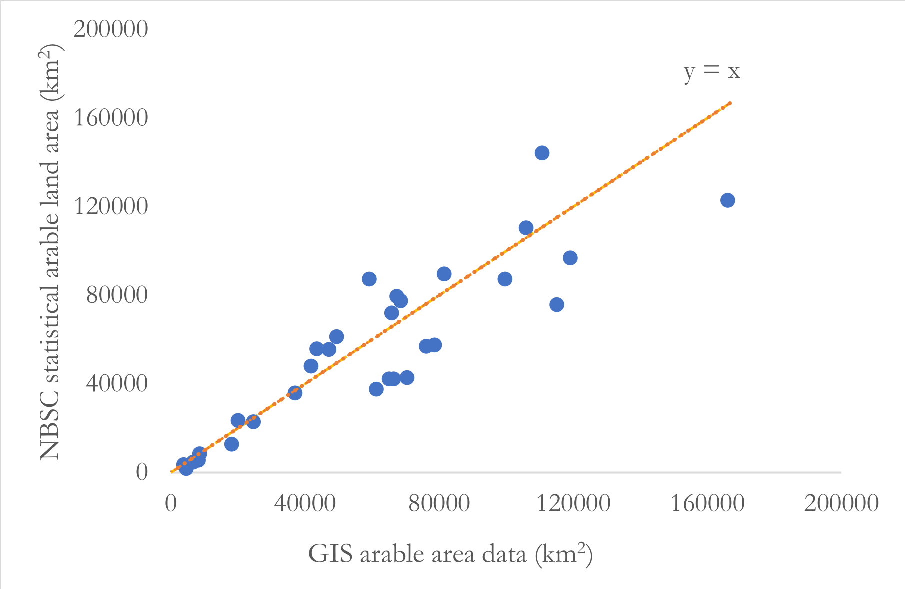

Figure 4- 1: The arable land difference of NBSC statistical and GIS data of 31 provinces in China.

Figure 4- 1 shows that the deviation of GIS data on arable land area in each province from the statistical data ranged from 1.74% to 72.73% (deviation= [statistical data-spatial data]/statistical data). To justify the quality of the overall land cover map, a confusion matrix and Cohen's Kappa index were introduced. The confusion matrix is the most common method used to evaluate the overall accuracy of GIS map classifications [165-167]. The principle of the confusion matrix is that cells selected based on the GIS mapping classification are compared with reference data (the actual classification). The confusion matrix contains the predicted class (plot) and the actual class (reference plot). The predicted plot data were selected and covered the most common land use types (agriculture, forest, water and urban) in the GIS map to acquire an unbiased estimation. The reference plot data were visually assessed and divided into a corresponding classification. The confusion matrix was produced by comparing the predicted plot data from GIS layer and the reference plot data to determine the overall accuracy of the GIS maps.

Cohen's Kappa index can be used to measure the classification accuracy, which is derived from the confusion matrix [30, 168]. The Kappa index compensates for the effect of differences in class sizes in the sampled data and are more reliable than a single indicator analysis. The Kappa index is expressed in Eq. 4.1-1:

$$k = (P_o - P_e)/(1 - P_e) \qquad \text{(Eq. 4.1-1)}$$

where P_o is the total number of correct predictions of classification in the reference plot (total classification accuracy) and P_e is the proportion of the reference plot correctly predicted by chance under the assumption of independence. A higher Kappa index value indicates better spatial classification. The evaluation standard is presented in Table 4- 5 [169].

Table 4- 5: Cohen's Kappa index assessment [169].

Kappa index	Strength of agreement
<0.00	Poor
0.00-0.20	Slight
0.21-0.40	Fair
0.41-0.60	Moderate
0.61-0.80	Substantial
0.81-1.00	Almost perfect

In this section, 323 plots were selected to analyse the accuracy of the GIS assessment against visual observations, including 149 agricultural lands, 99 forest lands, 52 water areas and 23 urban areas. The results are shown in Table 4- 6. The overall accuracy of land use classification for the 323 plots was over 81% and Cohen's Kappa index was 0.73, which indicates that the layer exhibits satisfactory classification and high quality. Despite the high accuracy of land use classification, arable land cover is more difficult to classify, due to the low accuracy of arable land recognition algorithm. Beyond that, two main reasons which could affect arable land accuracy are the large object sample and the land cover GIS data updating manner. The main research object was arable land, which accounts 46% of total samples. From the aspect of statistics, larger sample means higher probability of failure. On the other hand, with the development of urbanization, arable land might occupy by other functions, which increased accuracy of arable land recognition on GIS.

Table 4- 6: Assessment of the GIS land use layer.

Land type	Total plots assessed by GIS	Actual plots checked by visual observation				Accuracy* (%)	Cohen's Kappa index
		Agriculture	Forest	Water	Urban		
Agriculture	149	98	28	2	21	65.77	0.73
Forest	99	3	93	3	0	93.94	
Water	52	2	0	49	1	94.23	
Urban	23	1	0	0	22	95.65	

*Accuracy = the number of plots with agreement between GIS and visual inspection/total number of assessed plots.

4.3 Theoretical potential of agricultural residues in China

4.3.1 Agricultural residue production and characterization

It was estimated that 1001.47 Mt of residue (air-dried, 15% moisture) were produced in 2017, which is slightly higher than the value of 901 Mt determined by Liu and Li [153] in 2010 and

819.7 Mt determined by Jia et al. [154] in 2014 (Figure 4- 2). From 2010 to 2017, crop production rose from 559.1 Mt/year to 661.6 Mt/year, which represents an increase of 18.3% [170]. The total amount of residue rose from 901 Mt in 2010 to 1001.47 Mt in 2017, which represents an increase of 11.2%. Thus, the residue result is in consistent with other sources. The agricultural residue decreased in 2014 because the researchers applied an outdated RPR value. In regard to the distribution of crop residue, cereal residues (corn, rice, wheat, sorghum and millet) showed the highest potential with approximately 864.13 Mt of residue (86.27% of the total). The most promising crop residue was corn stalks, which contributed the majority of the agricultural residue with 440.64 Mt, representing 44% of the total (Table 4- 7). The second and third largest residues were rice straw and wheat straw, which represented 24.11% and 17.62% of the total residue, respectively. Cereal residues were followed by oil crop residues, which accounted for 5.55% of the total agricultural residue in China. The detailed data and references are presented in Appendix V.

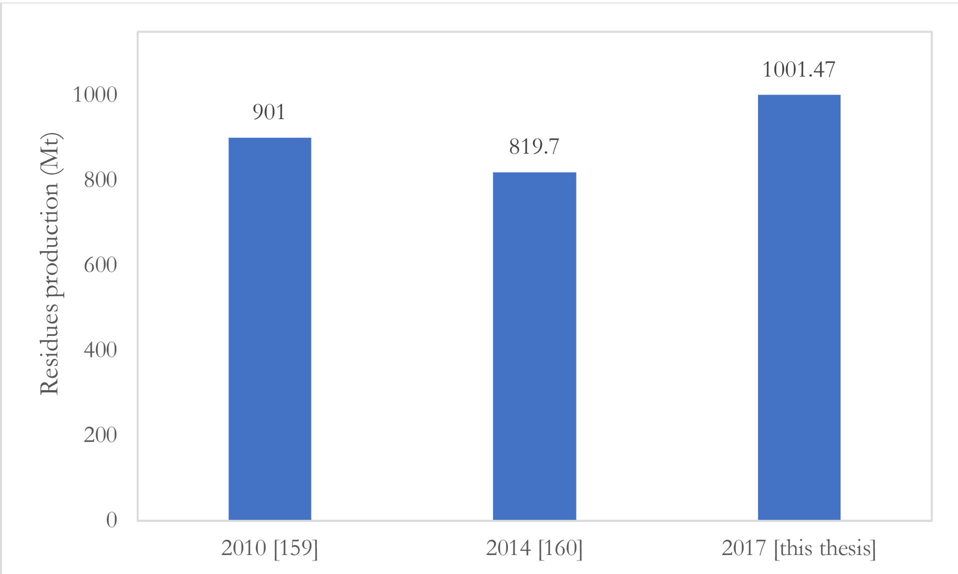

Figure 4- 2: Theoretical potentials of agricultural residues in China.

Table 4- 7: Distribution of theoretical potential of crop residues.

	Residues (Mt/year)	**(%)**		**Residues (Mt/year)**	**(%)**
Corn	440.64	44.00	Cotton	23.15	2.31
Rice	241.45	24.11	Peanuts	21.71	2.17
Wheat	176.46	17.62	Sunflower	4.62	0.46
Tubers	30.47	3.04	Sorghum	3.22	0.32
Beans	28.13	2.81	Millet	2.36	0.24
Rapeseed	27.05	2.70	Sesame	2.19	0.22
Total	1001.47	100			

4.3.2 Spatial distribution of agricultural residue potential in China

There were significant regional differences in agricultural residue potential (Figure 4- 3). These differences were influenced by local environment, economic development, topography and agricultural production. The agricultural residue resources were primarily located in the North, the middle and lower reaches of the Yangtze River and north-eastern China. Those three districts accounted for over 79% of the residue resource. Among these, North China was the most promising district, producing 329.83 Mt of agricultural residue per year (33% of total). South China produced the smallest fraction of the residue.

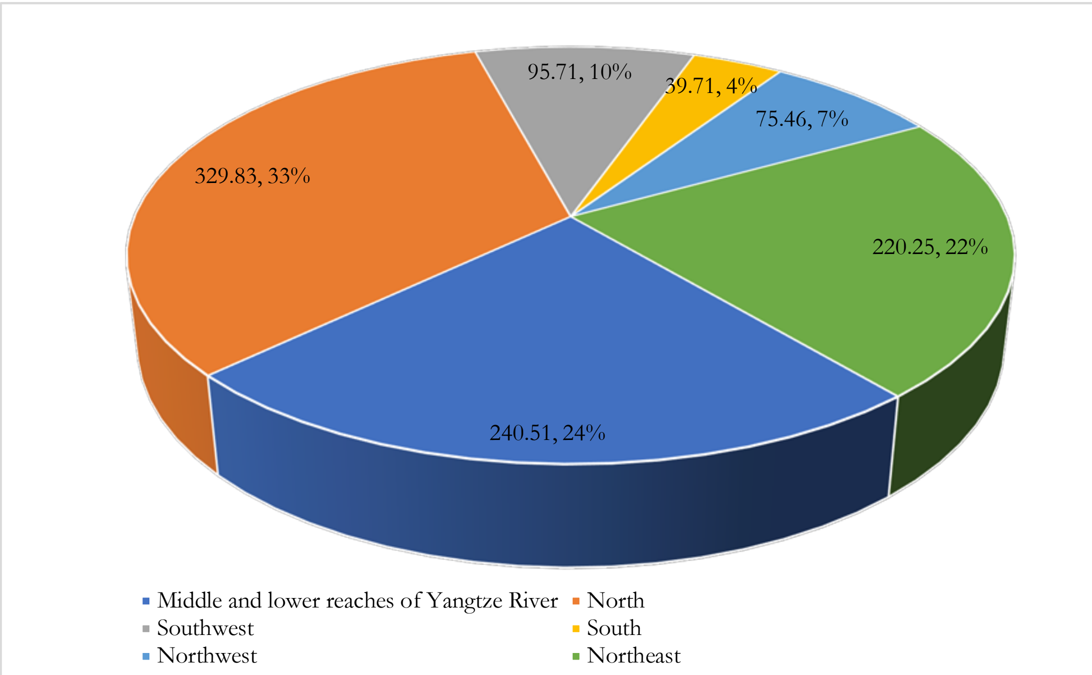

Figure 4- 3: Spatial distribution of theoretical potential of agricultural residues.

From Figure 4- 4 and Table 4- 8, it can be seen that the agricultural residue is primarily found in the North of China, particularly in Heilongjiang, Henan and Shandong Provinces, which accounted for 110.04, 100.65 and 86.48 Mt, respectively. The main reason for the high amount of residue in these areas is the widespread cultivation of corn. As a C4 photosynthetic species, corn stalks have a higher residue yield [38], which is almost twice the weight of the grain.

The production of corn stalks is concentrated in the northern China, particularly in the Northeast, which includes Heilongjiang, Jilin and Shandong Provinces and accounts for 39.8% of the total amount of corn stalks (Figure 4- 4). Rice requires large amounts of water to supply its growth; southern China has abundant rain, which creates an appropriate growth environment for rice. Thus, rice straw is concentrated in southern China, particularly in the Southwest in areas such as

Hunan, Jiangxi and Hubei (which accounted for 36.0% of the total rice straw residue). The climate contributes to abundant water resources and high-quality soil resources in Heilongjiang, which make it a satisfactory source of rice straw (27.35 Mt per year, 11.3%). Wheat is a traditional food source in northern China. Thus, the wheat straw residues are higher in northern China than in other regions. The wheat straw resources were high in Henan, Shandong and Hebei (28.1%, 18.9% and 11.4%, respectively).

Table 4- 8: Theoretical potential of agricultural residues in the top 10 provinces.

Province	Theoretical potential (Mt/year)	(%)
Heilongjiang	110.04	10.99
Henan	100.65	10.05
Shandong	86.48	8.64
Jilin	70.25	7.01
Hebei	59.72	5.96
Inner Mongolia	56.58	5.65
Anhui	54.10	5.40
Jiangsu	50.13	5.01
Hubei	46.86	4.68
Hunan	45.71	4.56

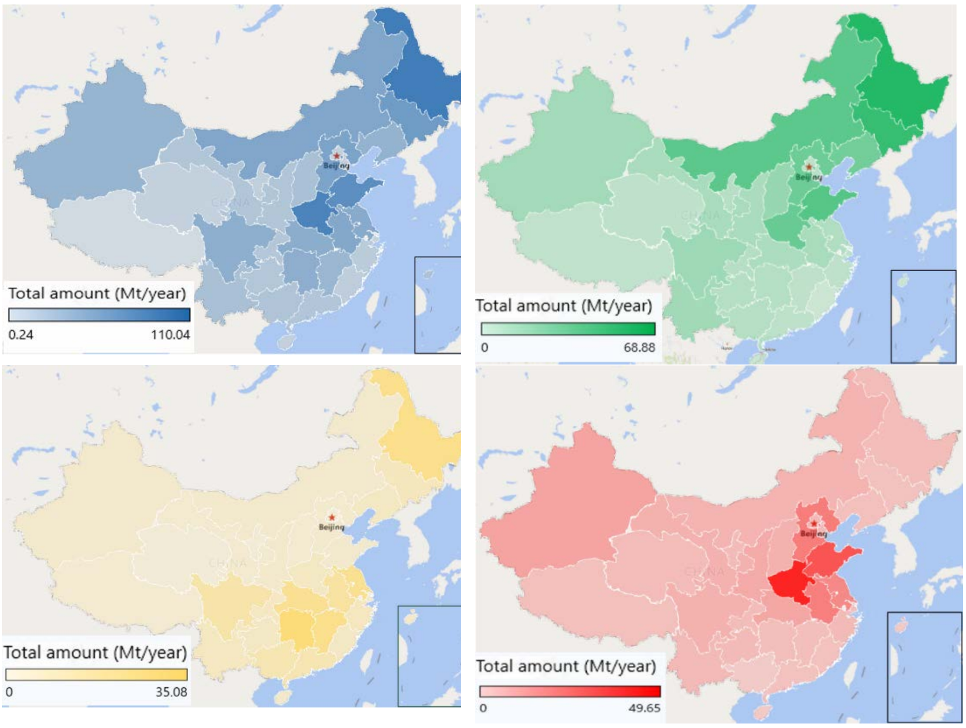

Figure 4- 4: Top left, (a) distribution of total agricultural residue potential; top right, (b) corn stalk distribution; bottom left, (c) rice straw distribution; bottom right, (d) wheat straw distribution.

4.4 Technical potential of agricultural residues in China

The assessment of the technical potential of agricultural residues was performed in 2 steps. First, the collectable technical potential in the arable land spatial layer was evaluated based on the slope of the land using GIS data. This was followed by the introduction of statistical data on economically available arable land to determine the technical potential of the residue.

The green area in Figure 4- 5 (a) shows the arable area in China. Due to the influence of local climate and precipitation centred in the east, the arable land was concentrated in eastern China. However, topography was another constraint on the distribution of arable land. Mechanised harvesting can occur on gentle slopes; in Figure 4- 5 (b), the major of the gently sloping land is located in North and Northeast China, which results in a higher level of crop production and residue potential. The available collecting area was generated by considering both the distribution of arable land and the topographic distribution, which is illustrated in Figure 4- 5 (c).

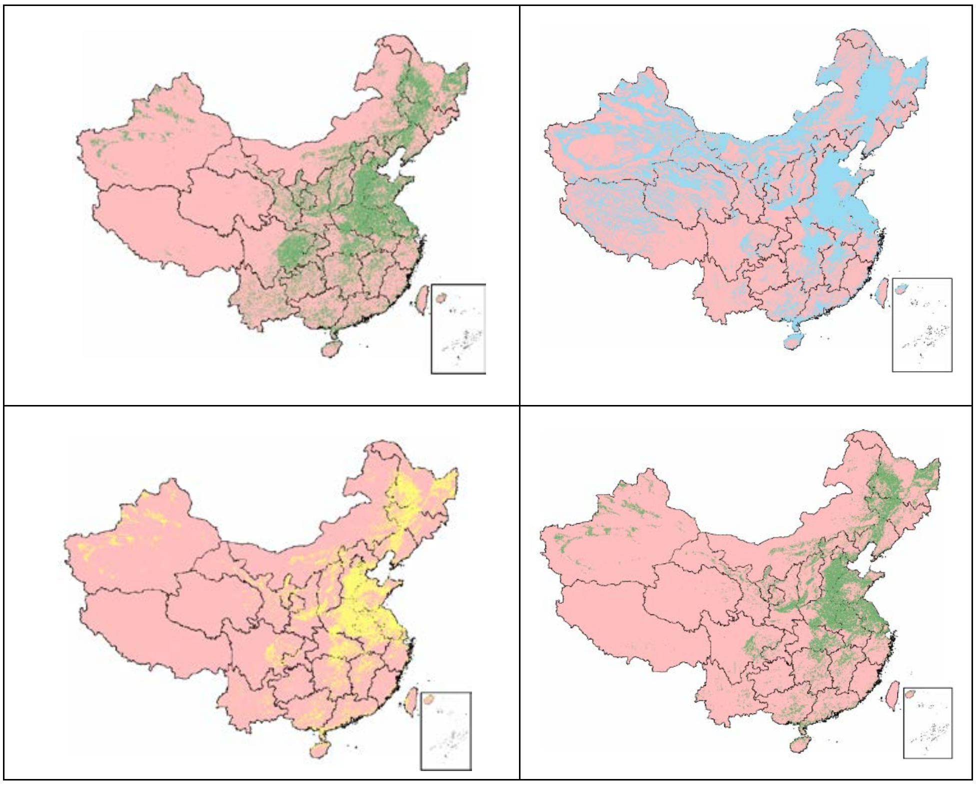

Figure 4- 5: Top left, (a) distribution of arable land in China; top right, (b) distribution of gentle slopes; bottom left, (c) available arable land under topographic restrictions; bottom right, (d) distribution of arable land under legislative regulations.

Of the total arable land, 64% (1070020 km^2) was identified as having technical potential (Table 4- 9). The remaining 36% of arable land was not considered in this section due to the steep slope and the resulting difficulty in collecting residues. Due to the heterogeneity in topography, the distribution of arable land in each province may differ. Thus, the amount of residue depends on the economically available arable land area. The technical potential of residues under available arable land was 707.28 Mt per year, which accounts for 70.62% of the total residue. The detailed arable land availability and its residue potential for each province is presented in Appendix VI. As previously mentioned, the collection capability was set at 80% of residue that can be collected from the field, which results in 565.82 Mt of residue that can be collected on an annual basis. The remaining 20% is left in the field as fertilizer.

Table 4- 9: The technical potential of agricultural residue in China.

	Arable land size (km^2)	Residues potential (Mt/year)
Total arable land (theoretical potential)	1663738	1001.47
Arable land under technical potential restrictions	1070019	707.28
Residue technical potential (80%)	-	565.82

4.5 Sustainable potential of agricultural residues in China

In this section, the arable land that also meets the environmental restrictions is calculated. Because soil erosion and SOM were introduced as restrictions via GIS, the sustainable potential of the residue was lower than the technical potential.

4.5.1 Arable land with legislative regulations (water protection areas)

Figure 4- 5 (d) shows the distribution of available arable land under legislative regulations, which requires harvesting activity to be at least 500 m away from any water body. To satisfy this regulation, the arable land was further reduced from 1070020 km^2 to 1060092 km^2, and the amount of residue decreased by approximately 0.83% from 565.82 Mt to 561.15 Mt per year (Table 4- 10). The arable land in the individual provinces is presented in Appendix VII.

Table 4- 10: Residues with sustainable potential under legal regulations.

	Arable land size (km^2)	**Residues potential (Mt/year)**
Technical potential	1070020	565.82
Under regulation	1060092	561.15

4.5.2 Arable land with soil erosion

Figure 4- 6: Left, (a) arable land under weak soil erosion conditions; middle, (b) arable land under mild soil erosion conditions; right, (c) arable land under moderate soil erosion conditions.

The spatial distribution of soil erosion and the statistics on arable land soil erosion were determined and are shown in Figure 4- 6 and Table 4- 11. Over 97.7% of the arable land under legislative regulation was considered environmentally friendly, which represents approximately 1035844 km^2. Of this area, 887140 km^2 of arable land was located in areas with weak soil erosion and produced 465.51 Mt of residues annually, and 93566 km^2 was located in areas with mild soil erosion and produced 53.24 Mt of residues per year; 30.62 Mt of residue was produced annually on 55139 km^2 of arable land with moderate erosion.

Table 4- 11: Soil erosion for arable land and corresponding residue potential.

	Arable land size (km^2)	Residues potential (Mt/year)
Weak soil erosion	887140	465.51
Mild soil erosion	93566	53.24
Moderate soil erosion	55139	30.62
Total	1035844	549.37
Under legislative regulation	1060092	561.15

To prevent soil erosion, mulch is applied to arable land. For land that is defined as having weak or mild soil erosion, 200 t of residue needs to be returned to the field per square kilometre. For moderate soil erosion, the quantity of residue is 300 t. A total of 20% of residue is returned to the field as a result of the operation of the harvesting machinery; the additional amount of residue that needs to be returned is presented in Table 4- 12. To prevent soil erosion, 212.68 Mt of residue is required each year, of which 177.43 Mt is baseline mulching to prevent weak soil erosion. For mild and moderate soil erosion, the total amount of residue was less than that for weak soil erosion because of smaller area of arable land in these erosion classes (18.71 and 16.54 Mt, respectively). Therefore, the total available residue potential under soil erosion conditions was 336.69 Mt annually.

Table 4- 12: Residue potential and requirements under soil erosion.

	Arable land area (km^2)	Residues potential (Mt/year)	Residues left in field (Mt/year)	Total residues required for mulching (Mt/year)	Deficits (Mt/year)	Available residues (Mt/year)
Weak soil erosion	887140	465.51	116.38	177.43	61.05	288.08
Mild soil erosion	93566	53.24	13.31	18.71	5.40	34.53
Moderate soil erosion	55139	30.62	7.66	16.54	8.89	14.08
Total	1035844	549.37	137.35	212.68	75.34	336.69

4.5.3 Arable land with adequate soil organic matter (SOM)

To maintain soil fertility and SOM balance, residues must be returned to the soil. As mentioned previously, an accepted value for SOM ranges between 1% and 3% as a sustainable standard, and the 2% SOM selected in this section is within this range. Approximately 84.6% of the arable land available for collection was assessed a SOM value of less than 2%, which represents 406.26 Mt of residue per year; therefore, 143.2 of the 561.15 Mt of residue is available for another use, as shown in Table 4- 13.

Table 4- 13: Residues potential and requirements for SOM.

	Arable land area (km^2)	Residues returned to field (Mt/year)	Residue availability (Mt/year)
SOM ≥ 2%	162913	92.93	61.95
SOM < 2%	897179	325.01	81.25
Total	1060092	417.94	143.2

SOM and SE are two critical factors for soil fertility. Sustainable residue removal should meet both SOM and SE requirements. Because the amount of residue retained for SOM is higher than that for SE, the residue availability under SOM requirements can be considered the sustainable potential of the agricultural residue. Thus, the agricultural residue with sustainable potential in China was 143.2 Mt annually, which is 14.3% of the theoretical potential and 25.3% of the technical potential.

4.6 Hypothesis: The sustainable potential of agricultural residue for green power

This thesis assessed the potential of agricultural residue in China, which includes the theoretical potential, technical potential and sustainable potential. In 2017, the theoretical potential was 10001.47 Mt agricultural residue, and the technical potential was 565.82 Mt, which is approximately 56.5% of the theoretical potential. To ensure environmental sustainability, the sustainable potential was downsized to 143.20 Mt, as shown in Figure 4- 7.

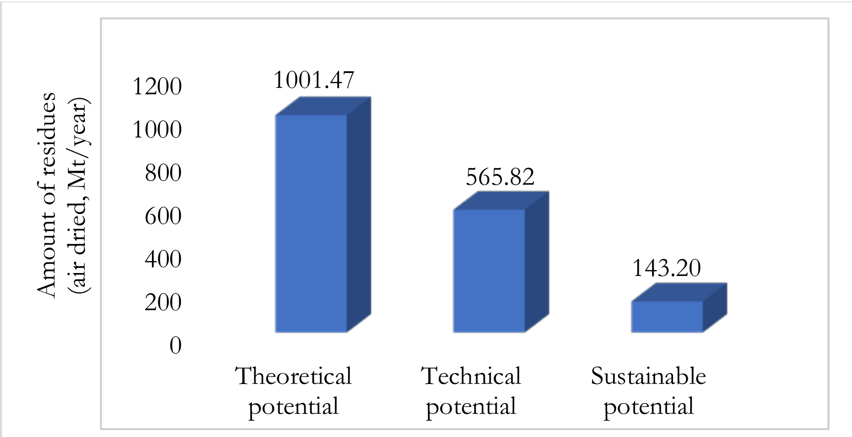

Figure 4- 7: Theoretical, technical and sustainable agricultural residue potential in China.

The agricultural residue was estimated on the basis of air-dried RPR with a moisture content of approximately 15%. The theoretical, technical and sustainable potential residues available for green power generation were 851.25, 480.95 and 121.72 Mt/year, on dry basis, respectively.

The heating value is an important criterion for the evaluation of power generation. The heating value is defined as the heat released during combustion [171]. The heating value can be classified as a lower heating value (LHV) or a higher heating value (HHV). The difference between the LHV and the HHV relates to whether the energy in the water vapour is considered as part of the unit output during energy generation [172]. In power generation, the energy in water vapour is not considered. Thus, the LHV is applied in power generation calculations. The average LHV value of crop residues reported in the literature is shown in Table 4- 14.

The theoretical, technical and sustainable potentials translate to 1.39×104 PJ, 7.81×103 PJ and 1.99×103 PJ of energy per year, respectively. In general, the efficiency of power generation ranges from 20-25% [123, 173, 174]. Thus, the 7.81×103 PJ of residue (technical potential) that can be collected represents between 1.56×103 PJ and 1.95×103 PJ of power annually, which can produce at least 433.3TWh to 541.7 TWh per year (assuming 3.6 MJ = 1KWh). To ensure environmental sustainability, agricultural residues converted to power should remain within the range of 111.1 TWh and 138.9 TWh (0.40 ×103 PJ to 0.50×103 PJ) per year.

Table 4- 14: The lower heating value of major crop residues in China.

	LHV (db, MJ/kg)	Reference		LHV (db, MJ/kg)	Reference
Corn	13.54	[175-178]	Sesame	14.55	[179]
Rice	15.14	[180, 181]	Sunflower	14.41	[182]
Cotton	13.39	[176, 177]	Millet	16.09	[182]
Wheat	14.39	[176-178]	Tubers	14.24	[183]
Sorghum	15.99	[184-186]	Beans	15.96	[187]
Peanut	13.72	[188, 189]	Rapeseed	15.59	[179]

Because agricultural residues are utilized not only for power generation but also have uses in other industries (such as for forage, industrial materials and bioenergy), unutilized residues are limited. According to the press office of the Ministry of Agriculture, 20% of collected residues are abandoned [190]. Thus, 20% of the technical potential calculated for power generation in the thesis is actually available. Between 86.67 and 108.34 TWh of power could be produced annually if the abandoned residues were recycled for power generation. This represents 1.58% of the national energy consumption in 2018 (6844.9 TWh) [191]. A conservative estimate is that the available sustainable agricultural residue potential could be converted to between 22.2 and 27.8 TWh per annum.

4.7 Summary of chapter

A three-step GIS-based approach involving the evaluation of theoretical, technical and sustainable potentials for agricultural residues has been proposed in this work, with the novel characteristic of considering simultaneously regional annual crop yields, topographic and legislative restrictions, as well as SE and SOM environmental restrictions at a regional level. The proposed approach was applied to assess the sustainable potential of agricultural residues available for potential power generation in China. This approach provides a detailed assessment of residue potential and its provincial distribution using the latest crop production statistics and high-resolution GIS digital spatial data. It was found that 1001.47 Mt of residue is produced annually, including corn stalks (440.64 Mt), rice straw (241.45 Mt) and wheat straw (176.46 Mt). The retention of residues plays a crucial role in reducing soil erosion and increasing soil organic matter and nutrient (such as carbon, nitrogen and phosphorous) sequestration to maintain soil quality. Due to the long-term indiscriminate removal of residues, the density of soil organic matter is far below the standard level in much of China, which leaves only 143.20 Mt of residue that can be considered as sustainable potential of agricultural residues, which could produce from 22.2 to 27.8 TWh each year. This result demonstrates the benefits from adopting the proposed approach for a more realistic sustainable potential assessment. This thesis indicates that, among China's 31 provincial regions, Heilongjiang holds the greatest potential for the establishment of an agricultural residue-based economy by virtue of its resource availability.

This work contributes to academia by proposing the sustainable potential assessment approach that can be applied to any geographical context. The work contributes also to practice and policy making, since the application of the approach in the case of China highlights the large difference between the theoretical, technical and sustainable potential, that fully accounts for the regional differences in annual crop yields, the local topographic, legislative and environmental restrictions. The outputs can be used by practitioners engaged in the bioenergy value chain to identify areas where there is sufficient sustainable potential to exploit, and by policy makers to ensure that any incentives are focusing on areas where exploitation of the agricultural residues will not lead to environmental degradation, in terms of soil erosion and soil organic matter loss. To maximise the value of these sustainably available agricultural residues, further work will continue to assess its potential for the production of high value-added chemicals or materials.

Chapter 5:

BIOMASS PRE-TREATMENT AND ITS IMPACT ON BIOMASS LOGISTICS

Pre-treatment has significant impact on performance and cost control of biomass supply chain, especially on logistics. Pre-treatment technologies can convert biomass at modest scales into dense energy carriers that ease transportation and handling. Various research has clarified the important of biomass densification on logistics cost saving and efficiency improvement in Chapter 2. Subsequently, pre-treatment is a key step in the total supply chain. As mentioned, torrefaction is a very promising pre-treatment technology, thus, in this chapter, the experimental work on torrefaction of corn stalk and rice straw is presented. The objective of this experimental work is to find out the optimal torrefaction reaction temperature, which contains the maximum heating value and minimum energy losses relatively. The torrefaction results are presented by the physical and chemical analysis, demonstrating appearance and chemical properties related characteristics (element analysis, energy density heating value and energy consumption) respectively. Later, the heating value increase of torrefied corn stalk and rice straw are compared with energy losing rate results.

5.1 Physical characteristics

The experiment result shows that the moisture of received rice straw and corn stalk are 3.45% and 20% respectively. From torrefaction experiment, it can be seen a significant physical appearance difference in both rice straw and corn stalk, which straws turn to dark with increase torrefaction temperature. Furthermore, material hydrophobic and fragility was significantly improved. Sample of corn stalk and rice straw was observed fragile at higher temperatures in comparison with the raw material. Therefore, torrefied material grindability has improved. The physical appearance of raw and torrefied residues was displayed in Table 5- 1.

Table 5- 1: Physical appearance of corn stalk and rice straw and torrefied product at different temperatures.

	Raw	220°C	240°C	260°C	280°C	300°C
Corn stalk					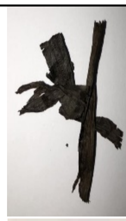	
Rice straw						

5.2 Chemical characteristics

The changes in the element component of material under various torrefaction conditions are present in Table 5- 2. samples under higher torrefaction conditions witnessed significant mass reduction, which is due to hemicellulose decomposition and the start of cellulose decomposition. As volatile matter (includes carbon dioxide, carbon monoxide, large amount of acetic acid and other heavier products of organic molecules [192]) released in decomposition process, which encouraged oxygenated and hydrogenated compounds to escape and torrefied products concentrate in fixed carbon. Therefore, it can be seen that the carbon ratio in biomass component increases along with higher torrefaction temperature. On the contrary, oxygen and hydrogen content were corresponding decrease, which results in nitrogen has relative increase.

Table 5- 2: Properties of raw, torrefied corn stalk, and rice straw.

	Ultimate analysis (wt%, db)				Ash	Energy	HHV	Energy consumption
	C	H	O	N	(%)	density	(MJ/kg)	(MJ/kg)
Rice straw								
raw	38.78	5.76	45.47	0.69	9.30	1.00	15.42	-
220°C	41.05	5.39	39.70	0.84	13.02	1.06	16.29	15.80
240°C	43.03	5.22	37.76	0.64	13.35	1.10	16.98	15.32
260°C	46.78	5.09	33.53	0.66	13.45	1.20	18.52	15.86
280°C	48.53	4.95	30.63	0.94	14.95	1.25	19.28	18.61
300°C	54.71	4.39	17.87	1.10	21.94	1.42	21.95	20.05
Corn stalk								
raw	42.51	6.00	43.92	0.33	7.24	1.00	17.21	-
220°C	45.50	5.79	43.43	0.53	4.75	1.05	18.11	14.85
240°C	45.95	5.75	38.97	0.69	8.64	1.08	18.56	15.32
260°C	48.52	5.59	36.21	0.51	9.17	1.14	19.58	15.86
280°C	51.03	5.37	32.95	0.49	10.16	1.19	20.51	17.79
300°C	60.87	4.70	18.14	0.78	15.51	1.43	24.57	20.05

In the change of heating value and energy density for each sample under various torrefaction conditions, as ratio of carbon content increase in the sample, the HHV and energy density have corresponding improve. On the other hand, torrefied biomass is more competitive than raw biomass in logistic transportation, due to higher energy density means higher energy to carry. The higher torrefaction temperature results in volatile matter decomposition, which affect mass yield and energy yield decrease in samples.

Figure 5- 1 illustrate samples HHV under various torrefaction temperature. The heating value of corn stalk higher than that of rice straw, that because of higher carbon content in corn stalk. The HHV in both corn stalk and rice straw was observed increase with higher temperature. HHV of raw residues sits at the range of 15.42 to 17.21 MJ/kg. When undergoing torrefaction, its HHV boosted to the maximum range of 21.94 to 24.57 MJ/kg. The HHV of torrefied corn stalk has increased 5.23% at 220°C, 7.62% at 240°C, 12.75% at 260°C, 16.85% at 280°C and 35.88% at 300°C. It can be seen that corn stalk undergoing 300°C has rapid increasing rate of HHV, which raise to 19.79% than torrefied product at 280°C. For rice straw, the highest increasing rate was obtained in 300°C (13.84% higher than that at 280°C). It can be seen that rice straw is more sensitive than that of corn stalk in lower and middle torrefaction temperature.

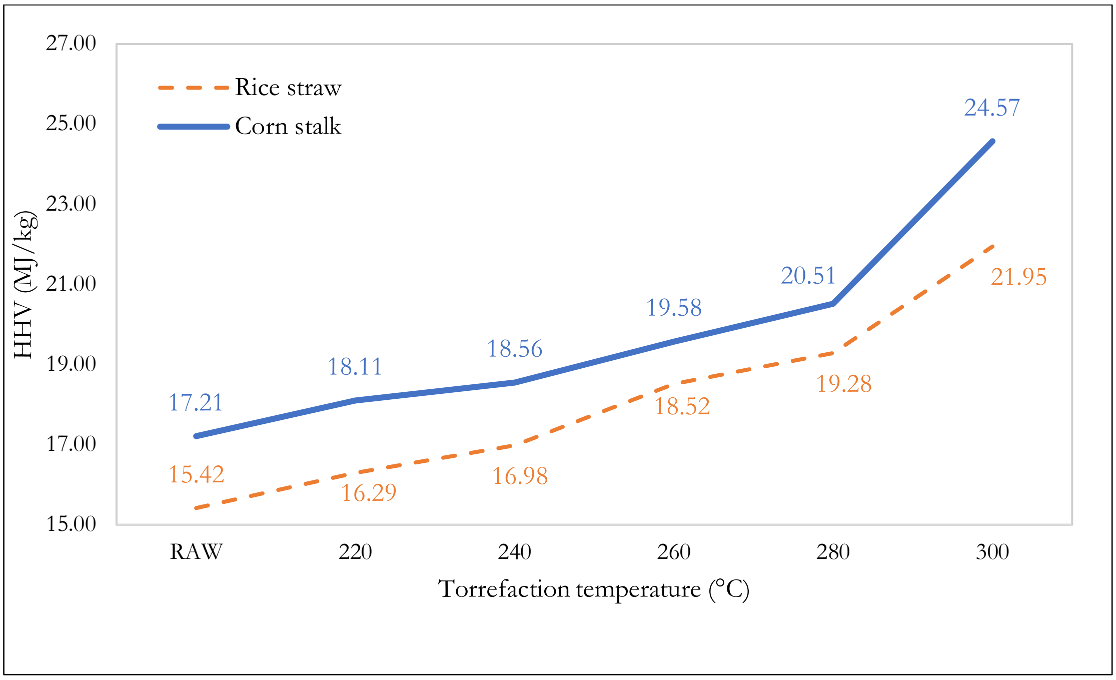

Figure 5- 1: Torrefaction material HHV.

As expected, mass yield decreased with rising temperature, especially for residues under severe temperature (over 280°C) due to hemicellulose and cellulose decomposition, which results in large increased mass loss (Figure 5- 2). In other words, thermal decomposition plays a dominating role in high temperature. The mass yield of rice straw decreased dramatically from 86.99% at 220 to 49.85% at 300°C. As well as corn stalk, from 85.36% at 220°C to 47.77% at 300°C on corn stalk. Similar trends can be observed in energy yield. It can be seen that the rice energy yield dropped from 91.91% at 220°C to 70.96% at 300°C. While, pointing to corn stalk, the energy yield decreased from 89.80% at 220°C to 68.20%, where 21.6% energy escaped to torrefied product.

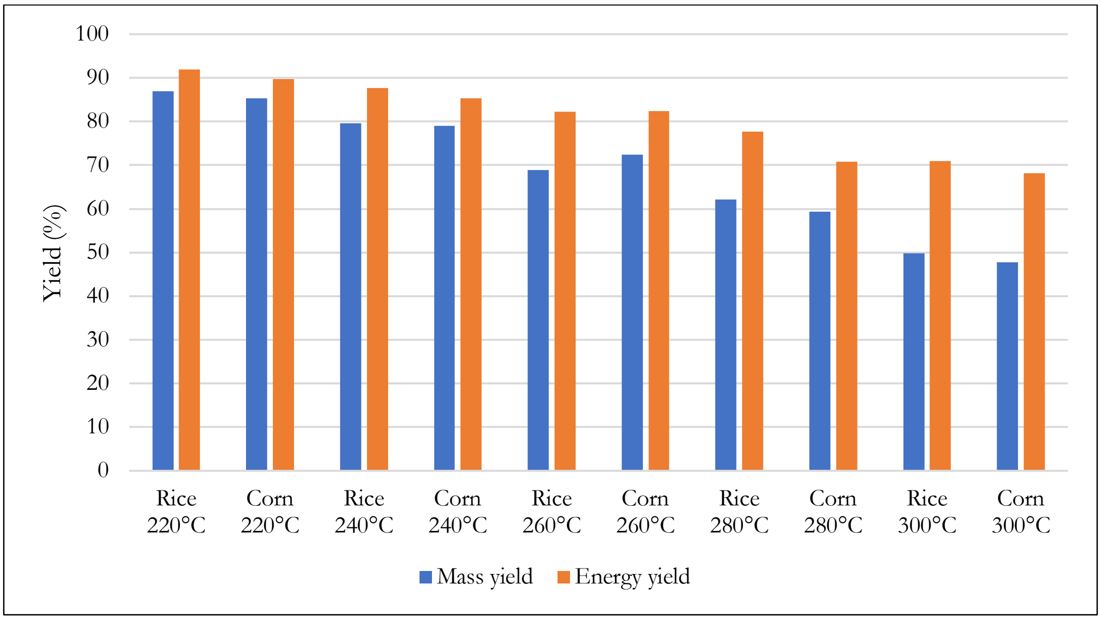

Figure 5- 2: Mass yield and energy yield of rice straw and corn stalk at different torrefaction temperature.

Figure 5- 3 and 5- 4 presented rice straw and corn stalk heating value increase rate and energy losing rate under various torrefaction conditions. Biomass material has a higher unit heating value after torrefaction treatment, due to the evaporation of its moisture and decomposition of its low molecular volatiles. Energy loss rate and HHV increase rate could indicate the optimal torrefaction conditions, which increase torrefied biomass feedstocks heating value without causing energy waste at the same time. In terms of rice straw, HHV increase rate higher than that in energy losing rate before 280 °C. The optimal temperature of rice straw is in the range of blow 280 °C. Because of minimal energy lose in that temperature range. Figure 5- 4 shows corn stalk under 260 °C to 280 °C has a significant mass loss. Therefore, torrefaction of corn stalk over 260 °C is inefficient. A temperature of 260 °C was chosen as optimum for corn stalk, since less energy is wasted compared with other temperatures.

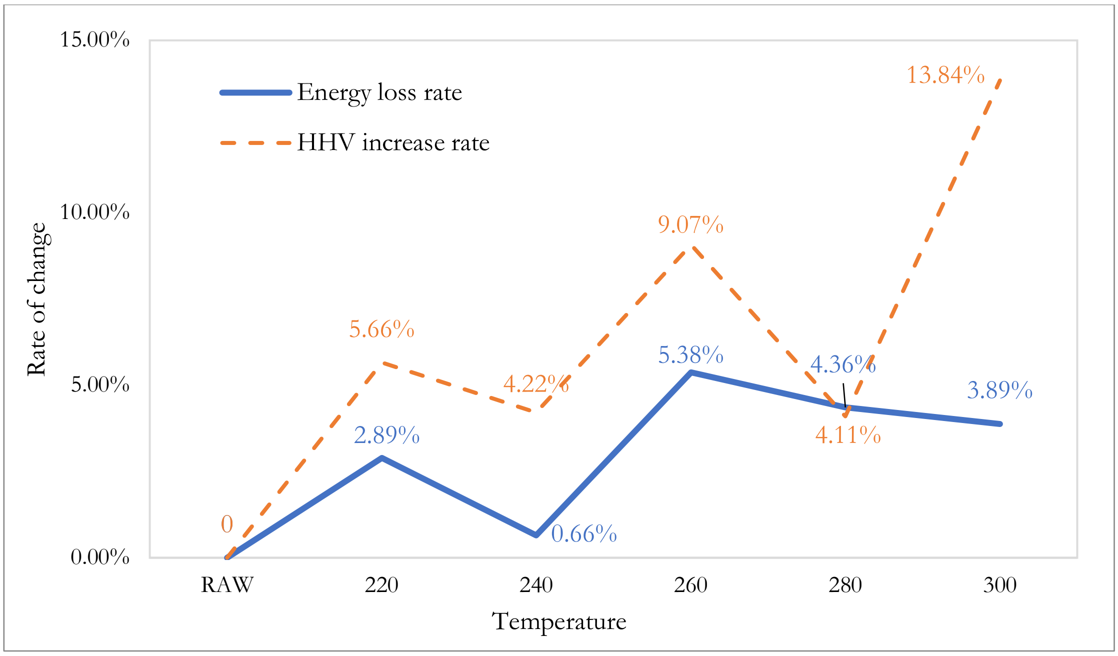

Figure 5- 3: Rice straw HHV increase rate and energy losing rate under various torrefaction temperature.

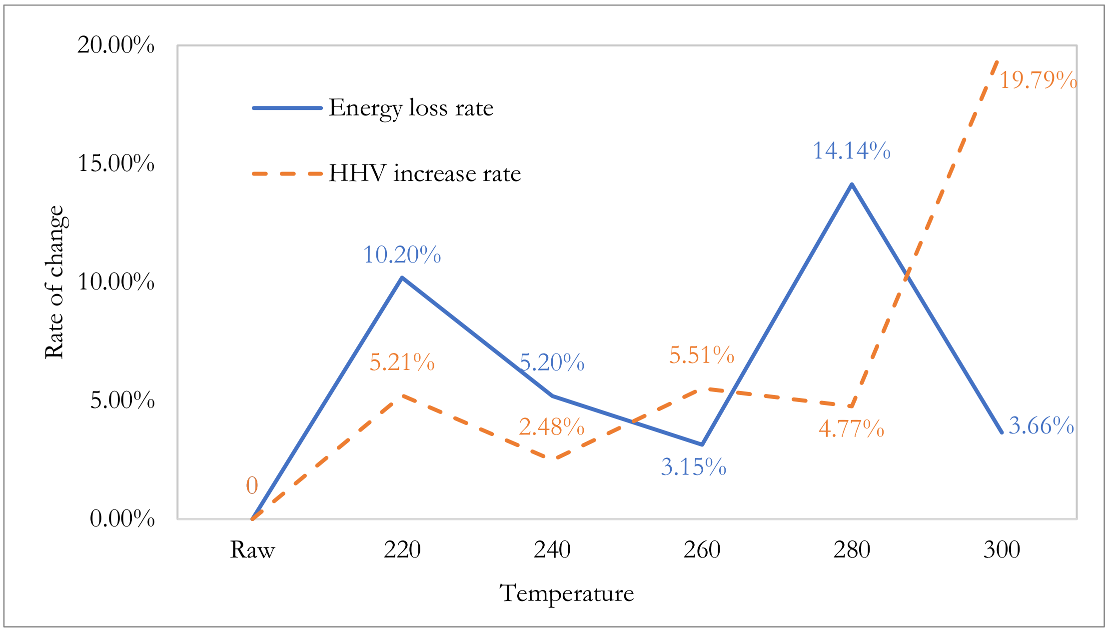

Figure 5- 4: Corn stalk HHV increase rate and energy losing rate under various torrefaction temperature.

5.3 Summary of chapter

Pre-treatment technologies play crucial role on biomass supply chain cost control and efficiency improvement, especially on logistics. This chapter investigated agricultural residues (corn stalk and rice straw) characteristics under torrefaction from physical and chemical aspects. This section determined moisture content of received rice straw and corn stalk, which tested contain 3.45% and 20% respectively. From agricultural residues torrefaction chemical characteristics assessment, it was found that the heating value for both rice straw and corn stalk increase with torrefaction temperature. Due to biomass component decomposition, energy yield and mass yield decrease with torrefaction temperature increasing. The mass loss in rice straw was observed higher than that in corn stalk. To balance high energy density and low mass yield, the optimal torrefaction temperature of corn stalk and rice straw was assessed in the last of this chapter. The optimal torrefaction temperature was experimentally determined, which considered by energy losing rate and HHV increase rate. Based on experimental results, optimal torrefaction temperature for rice straw and corn stalk is at the range of 220 °C to 280 °C and 260 °C respectively.

As reviewed in Chapter 2, biomass has the characteristics of low bulk density, which biomass pre-treatment is necessary for biomass logistic efficiency improvement. on the other hand, the research for the impact of biomass pre-treatment on biomass logistic model is rare, thus, experimental results as input variable will introduce into further logistic algorithm model analysis.

Chapter 6:

BIOMASS LOGISTIC OPTIMIZATION

Biomass logistics as a medium-term strategy links long-term strategy and short-term decision. For the most realistic simulation of biomass logistic system, in this chapter, the logistic model combines results from Chapter 4 and Chapter 5 as case study to evaluate the effect of pre-treatment methods on logistic model. Furthermore, to improve logistic model efficiency and reduce logistics cost, logistic model optimised by GIS assistance. A sensitivity analysis of optimized biomass logistic model will be drawn at the end of this chapter.

6.1 Biomass logistic model based on long-term decision-making strategy assessment: a case study of CHP plant in Heilongjiang

This section displays results of pre-treatment method on biomass logistics performance, which from three aspects to explore logistic model. Firstly, determine CHP production technical and pre-treatment parameters. Secondly, identify the candidate research area based on assessment criteria. Lastly, an economic and environmental analysis of logistic model were drawn.

6.1.1 Agricultural residues conditions and assessment design

As results in previous work [145], Heilongjiang province has the largest agricultural residues potential in China. While the number of biorefinery plant and capacity are not match its position. Therefore, it has potential for building more biofuel plant.

Heilongjiang province was estimated over 110 million-ton agricultural residues produced a year under 122940.3 km^2 arable land. For agricultural sustainable consideration, it was expected the residues density 57.48 ton/km^2 (based on agricultural residues sustainable potential analysis on [145]). For agricultural residues characteristics experiment analysis, collected agricultural residues has 15% moisture and 0.087 ton/m^3 bulk density. According [123] research, CHP system has approximate 31.85% electricity efficiency and 49.95% heat efficiency. 30 constructed biomass related biorefinery plants data in Heilongjiang were collected from governmental report and industrial report, which includes plant capacity, biomass consumption and GIS location. The existed biorefinery plant information was summarised in Appendix VIII.

The start point of this study was to identify the location of agricultural residues-based CHP plant, resources available area and infrastructure's locations for establishing a cost-effective sustainable logistic model. The effect of pre-treatment method on logistic model was investigated in this section, which includes 5 main scenarios assessment. All scenarios were modelled for collecting demanded agricultural residues and delivering them to final CHP plant for power and heating production. All scenarios are summarized in Table 6- 1.

Table 6- 1: CHP biorefinery plant conditions for five scenarios.

Scenario	Raw material	Torrefied material	Loose Density 0.087t/m^3	Compression	
				Density 0.4t/m^3	Density 0.8t/m^3
1	√		√		
2	√			√	
3	√				√
4		√		√	
5		√			√

6.1.2 Determination of candidate CHP plant location

Based on statistical data, the existing biorefinery plant location can be presented by GIS in Figure 6- 1 (a). Among that rectangle, circle and triangle node present biorefinery plant capacity of 40, 30 and 15MW respectively. It observed that biorefinery plant concentrate in southeast and southwest of Heilongjiang. Depending on local arable land distribution (Figure 6- 1 (b)) and agricultural residues density (results from Chapter 4.: agricultural residues assessment) and annual biomass consumption, the biomass collection area for each biorefinery plant can be calculated and displayed in Figure 6- 2 (a). In order to reduce disorderly competition and biorefinery company biomass purchasing cost, a buffer zone (5km longer) introduce into GIS. Figure 6- 2 (b) presents the buffer zone area under arable land. It can be found that under developing arable land in the southwest and east, which this area can be defined as potential biorefinery plant candidate location.

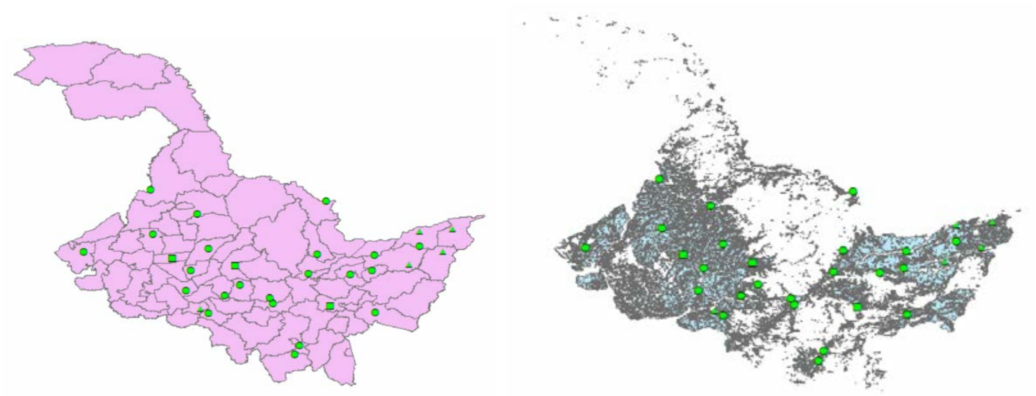

Figure 6- 1: Left (a) Existing biorefinery plant location in Heilongjiang. Right (b) Arable land distribution in Heilongjiang.

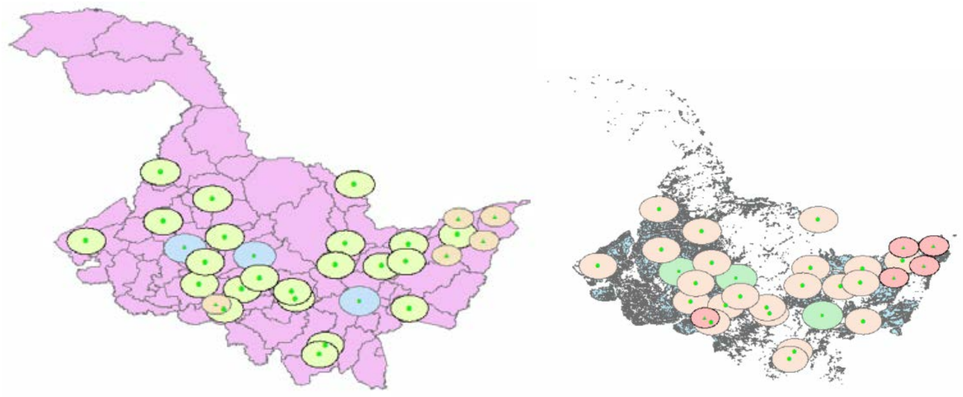

Figure 6- 2: Left (a) Biomass collection area for existing biorefinery plant. Right (b) Buffer zone in collection area.

Based on results of existing biorefinery plant collection area, three candidate area present in Figure 6- 3. Candidate area properties summarized in Table 6- 2. Candidate b has the largest area and arable land, which account 66% of total candidate area and 54% of arable respectively. Biomass potential can be assessed by biomass density, which candidate area A, B and C contain 916691, 2210867 and 949331 tonnes residues. It estimated that the biorefinery plant capacity in area A, B and C are 148, 357 and 153 MW respectively (7600 working hours and 15% moisture applied).

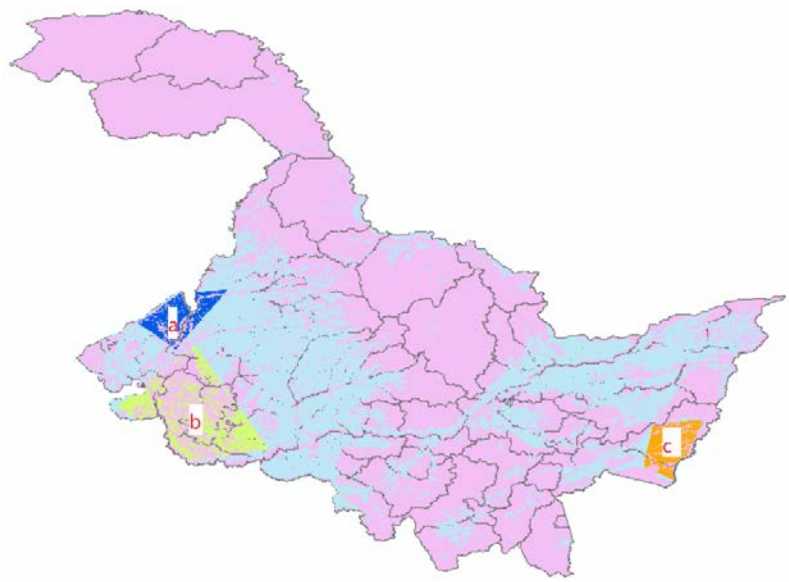

Figure 6- 3: Candidate biorefinery plant area a, b and c under arable land.

Table 6- 2: Candidate area properties.

Candidate area	Area (km^2)	Collection radius (km^2)	Arable land area (km^2)	Biomass density (t/km^2)	Biomass potential (t)
A	4759.37	38.93	3200.50		916691
B	18194.99	76.12	7718.94	286.42	2210867
C	4614.82	38.34	3314.46		949331

The biorefinery capacity in candidate area can be estimated by LHV (16315 and 19050 kJ/kg for raw and torrefied materials), CHP plant operation time and electricity efficiency, which summarized in Table 6- 3.

Table 6- 3: Biorefinery plant capacity in candidate area. (Unit: MW)

Candidate area	Biorefinery plant capacity (raw material)	Biorefinery plant capacity (torrefied material)
A	148	106
B	357	256
C	153	101

This section will analyse candidate area C as a case section of logistic model assessment. Because arable land accounts approximate 71.8% of total area in candidate C, which concentrated arable land could reduce cost in collection processing. Such as transportation cost and energy consumption. Since candidate biorefinery plant location determined, local conditions can be introduced into logistic model. Due to agricultural residues has others application (e.g., cattle feeding and energy), utilizing residues for biorefinery might not fully employment. Thus, the followed result will analysis the effect of residues available utility on biorefinery pre-treatment selection and logistic model profitability.

6.1.3 Biomass logistic model analysis

Financial analysis

Table 6- 4 summarized the PI value of CHP logistic model under five scenarios and agricultural residues availability. It was found that with residues available increase, the minimal refinery plant capacity has corresponding raise. Profitability index is to measure investment attractiveness, which project's PI value above 1 deems a profitable investment. Under a lower availability (20%), the optimal PI value occurs in scenario 2, which indicates compression with bulk density 0.4 t/m^3 is a cost-effective pre-treatment method for CHP refinery. It changed to torrefaction when residues availability and capacity expanded. The detailed breakdown of financial criteria of each availability is presented in the Appendix IX.

Table 6- 4: Logistic model PI value under different available utilities and scenarios.

Availability	Capacity (MW)	Scenario 1	Scenario 2	Scenario 3	Scenario 4	Scenario 5
20%	20	4.00	4.02	3.94	2.85	2.98
40%	40	4.91	4.88	4.79	5.30	5.23
60%	65	5.64	5.65	5.55	6.19	6.12
80%	85	6.10	6.12	6.02	6.74	6.66
100%	110	6.08	6.13	6.02	7.29	7.21

According to Ministry of Agriculture press office [193], the under-utilized agricultural residues account approximate 20% of total residues production. In this case, 20% resides available utilization will be further detailed analysis.

Table 6- 5 summarized financial criteria of CHP plant under five pre-treatment method scenarios. The financial analysis results expose that all pre-treatment method scenarios have positive net present value (NPV), which all projects are profitable. Scenario 1 has the highest NPV value, which pre-treatment cost significantly reduce total expenditure. In pre-treated scenarios, scenario 2 (compression with density 0.4 t/m^3) has the lowest cost and highest income. In spite of scenario 3 (compression with density 0.8 t/m3) has advantage in storage and transportation, the high expense in pre-treatment equipment and truck maximum loading weight increase expenditure and transportation cost. Torrefaction equipment cost and large amount of biomass for torrefaction drag down torrefaction-based CHP plant NPV value.

Table 6- 5: breakdown of financial criteria for CHP scenarios. (Unit: M€)

	Scenario 1	Scenario 2	Scenario 3	Scenario 4	Scenario 5
Biomass purchasing cost	5.29	5.29	5.29	6.34	6.34
Pre-treatment cost	0.00	0.58	0.78	1.32	1.87
Storage cost	1.15	0.96	0.94	1.13	1.12
Transportation cost	1.26	0.97	1.05	1.18	1.18
Ash disposal cost	0.11	0.11	0.11	0.10	0.10
CHP operation cost	1.82	1.82	1.82	1.82	1.82
Total cost	9.63	9.73	9.99	11.86	12.43
Electricity income	16.71	16.71	16.71	16.72	16.72
Heating income	4.21	4.21	4.21	6.27	6.27
Revenue	20.92	20.92	20.92	22.98	22.98
Total income	11.29	11.19	10.93	11.12	10.55
Net present value	120.34	119.23	116.93	114.02	113.35
Profitability index	5.29	5.33	5.26	3.70	3.90

Profitability index (PI) is to measure investment attractiveness, which PI value above 1 deems a profitable investment. Among that scenario 2 has the highest PI value. Torrefaction pre-treatment equipment cost restricts its PI performance. Therefore, under mutually exclusive projects, the project with highest value (scenario 2) should be undertaken.

The biomass unit cost for logistic process can be estimated based on total cost, which scenario 5 has the highest unit cost (133.43 €/ton) for transforming biomass from field to CHP plant. While the lowest unit cost is scenario 1, followed by scenario 2, which estimate 91.05 and 92.52 €/ton respectively. On the other hand, due to torrefied biomass increased grindability and torrefied exhaust gas react into CHP system, which reduce energy consumption in pre-treatment and enhance heating selling income.

In the aspect of logistic cost distribution (Figure 6- 4), biomass purchasing cost account the largest proportion, which shares over 60% of total logistic cost in all scenarios. In the pre-treated scenarios, pre-treated related employee cost and equipment cost account for a considerable proportion. In non-pre-treatment and compression scenarios, storage cost is the second largest cost after biomass purchasing cost. Therefore, keeping biomass in low purchasing cost and dry matter loss could enhance project's profitability significantly.

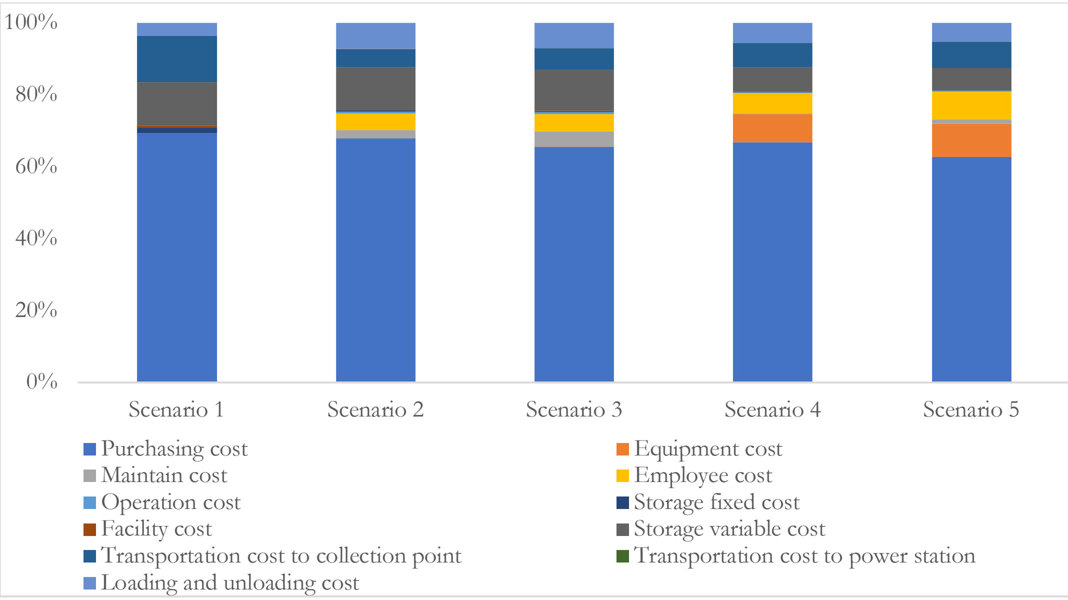

Figure 6- 4: Biomass logistic model total cost distribution for a year operation.

Logistic system emission

Biomass based CHP seen as a carbon free system, therefore, the process of transportation, pre-treatment and storage account in CHP supply chain CO_2 emission. In CHP logistic model, the emission of power relayed equipment was exempt, due to electricity source form CHP generation. Figure 6- 5 summarized CO_2 emission in logistic process, which non-pre-treated biomass has the lowest CO_2 emission (579.80 t). Biomass pre-treatment has advantage in reducing transportation cost. However, repeated loading and unloading biomass enhance CO_2 emission in biomass logistic system, which biomass need to load four times for transportation and storage. Thus, biomass loading emission accounts the largest part in these scenarios. On the other hand, pre-treated biomass increased transportation capability, in which a significant CO_2 emission reduction can be observed in biomass collection.

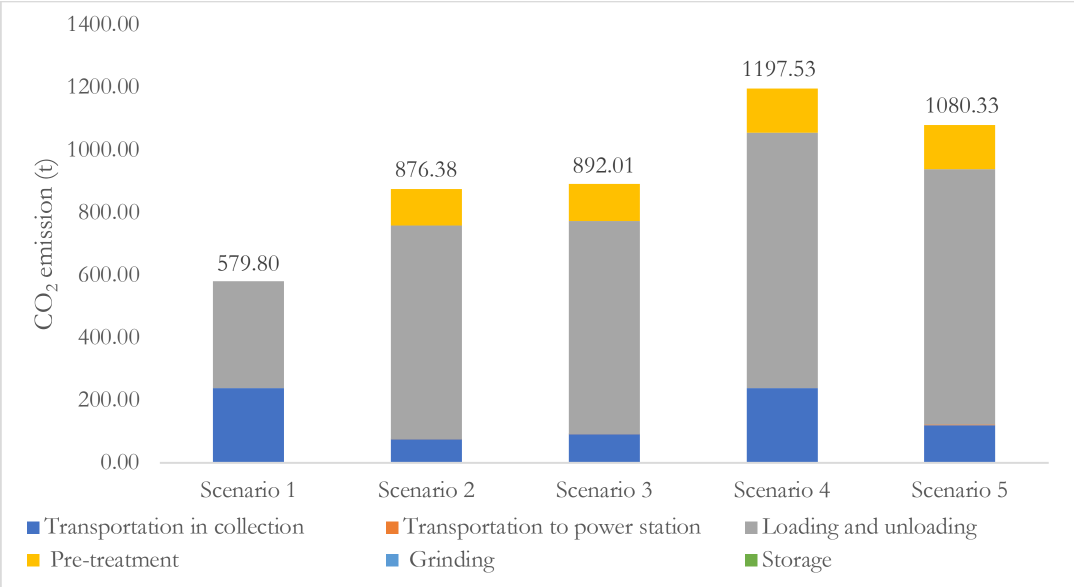

Figure 6- 5: CO2 emission distribution in CHP logistic supply chain.

It can be seen that transportation in collection emission in scenario 4 is higher than scenario 5 under the same conditions. That because of optimal output result difference. In scenario 4, the optimal number of depots under maximum profit as objective function is one, where the depot located in CHP plant. Long collection distance increase CO_2 emission in biomass collection transportation. While logistic model results shows that distributed depot was the optimum solution for maximum profit in scenario 5. Comparing with centralized depot, multiple distributed depots have advantage in increasing collection efficiency, reducing collection radius and collection cost in financial consideration.

Summary

Five different pre-treatment methods were assessed in biomass logistic model, which non-pre-treated biomass has advantage in both annual profit and environmental emission. Followed by compression as pre-treatment method. Due to high expenditure of pre-treatment equipment, torrefaction was not the optimal pre-treatment method for CHP generation. In spite of lower cost in non-pre-treated scenario, with increase transportation distance, the shortage of biomass characteristic (low bulk density) might dramatically increase. Model results reveal that distributed depot has benefit in reduce transportation and CO_2 emission. PI value is an indicator that evaluate project attractiveness, Scenario 2 will be applied in further GIS analysis and supply logistic model optimization since it has the highest PI value.

6.2 GIS transportation route analysis

The optimal depot of Scenario 2 analysed by logistic model was six. Therefore, optimal location of refinery plant and depots determination can be assisted by GIS analysis. Depending on requirements which refinery plant close to city for sufficient labour force and depots close to main road for increasing transportation efficiency, the optimal location for candidate area C illustrated in Figure 6- 6.

Where, the hatch area represents candidate area C, yellow area represents arable land distribution, red line represents main road, green circle represents optimal CHP biorefinery plant location and green triangle represent depots' location.

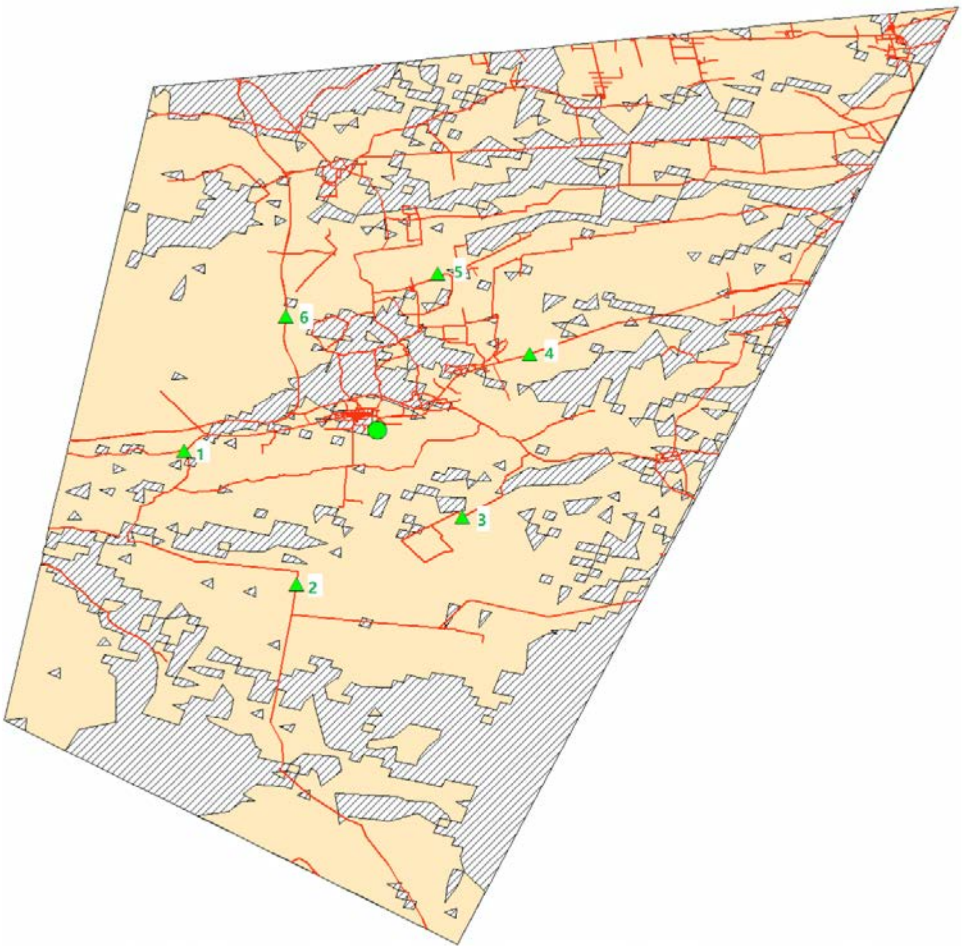

Figure 6- 6: Optimal location of CHP refinery plant and depots determined by GIS.

The detailed distance between refinery plant and each depot is demonstrated in Table 6- 6. GIS results reveal that the average distance between optimal depot and refinery plant is approximate 0.75 km shorter than that in mathematical algorithm logistic model. Mathematical algorithm logistic model can provide a general optimal solution to simulate local conditions that minimize effect of uncertainty on solutions as much as possible. While GIS could provide comprehensive analysis for local conditions. Therefore, to increase logistic model reliability, Logistic model and GIS analysis combination is an optimum solution.

Table 6- 6: Distance between refinery plant and depot.

Depot	Distance (km)
1	18.60
2	24.05
3	25.88
4	18.40
5	23.86
6	21.46
Average distance for GIS analysis	22.04
Average distance for logistic model	22.79

Based on the result of GIS analysed transportation distance by introduce into logistic model, the optimized results observed the transportation cost from €0.9700m reduce to €0.9698m and overall CO2 emission from 876.38t decline to 876.30t per year, which illustrate a 0.02% and 0.01% reduction respectively. With average 15 years investment lifetime of CHP plant, it could save at least €3000 and 1.2t CO2 (Table 6- 7).

Table 6- 7: CO2 emission and financial analysis under logistic mathematical algorithm model and GIS-assisted model.

	Logistic mathematical algorithm model	Logistic with GIS assisted model
CO_2 emission (Unit: t)		
Transportation in collection	74.28	74.26
Transportation to power station	1.88	1.81
Loading and unloading	682.30	682.30
Pre-treatment	117.93	117.93
Grinding	0.00	0.00
Storage	0.00	0.00
Total	876.38	876.30
Financial analysis (Unit: M€)		
Transportation cost	0.9700	0.9698

6.3 Sensitivity analysis of logistic model based on GIS optimization

The financial analysis illustrated in this work was based on various assumptions, such as biomass purchasing price and equipment's cost, which the stability of parameter value is highly affected by external environment (e.g., supply and demand). Moreover, the value of related to investment (e.g., CAPEX cost and construction cost) parameters can be site-specific, which simulated result was based on the certain situation. Once the value of critical parameters is modified, the project profitability might change significantly. For above reason, to minimize the effect of external uncertainty on logistic results stability, it is considered essential to exam sensitivity analysis for logistic model results. Most of parameters adjust in the range of −25% and +25% of their baseline value [123]. The baseline, lower and upper value of parameters for sensitivity analysis are summarized in Table 6- 8. PI value considered as assessment criteria present in Figure 6- 8.

Table 6- 8: Parameters and ranges of sensitivity analysis.

Parameter	Baseline Value	Unit	Sensitivity analysis range			
			Lower Parameter Value	Decrease %	Upper Parameter Value	Increase %
Biomass purchasing price	39.7	€/t	29.8	-25%	49.7	25%
Compression equipment price	1986.8	€	1490.1	-25%	2483.4	25%
Mass loss	0.10	-	0.08	-25%	0.13	25%
Oil price	0.9	€/L	0.6	-25%	1.1	25%
Storage facility construction cost	2.6	€/m^2	1.9	-25%	3.2	25%
Storage operation cost	6.9	€/t	5.2	-25%	8.6	25%
Transport price	2.6	€/tkm	2.0	-25%	3.3	25%
Loading and unloading cost	0.5	€/t	0.4	-25%	0.7	25%
Ash treatment cost	13.2	€/t	9.9	-25%	16.6	25%
Power plant CAPEX Reference investment cost	36365562.9	M€	27274172.2	-25%	45456953.6	25%
Electricity selling	0.10	€/kWh	0.07	-25%	0.12	25%
Heating selling	5.2	€/GJ	3.9	-25%	6.5	25%
Discount rate	8	%	6%	-25%	10%	25%
Employee salary	29541.1	€	22155.8	-25%	36926.3	25%

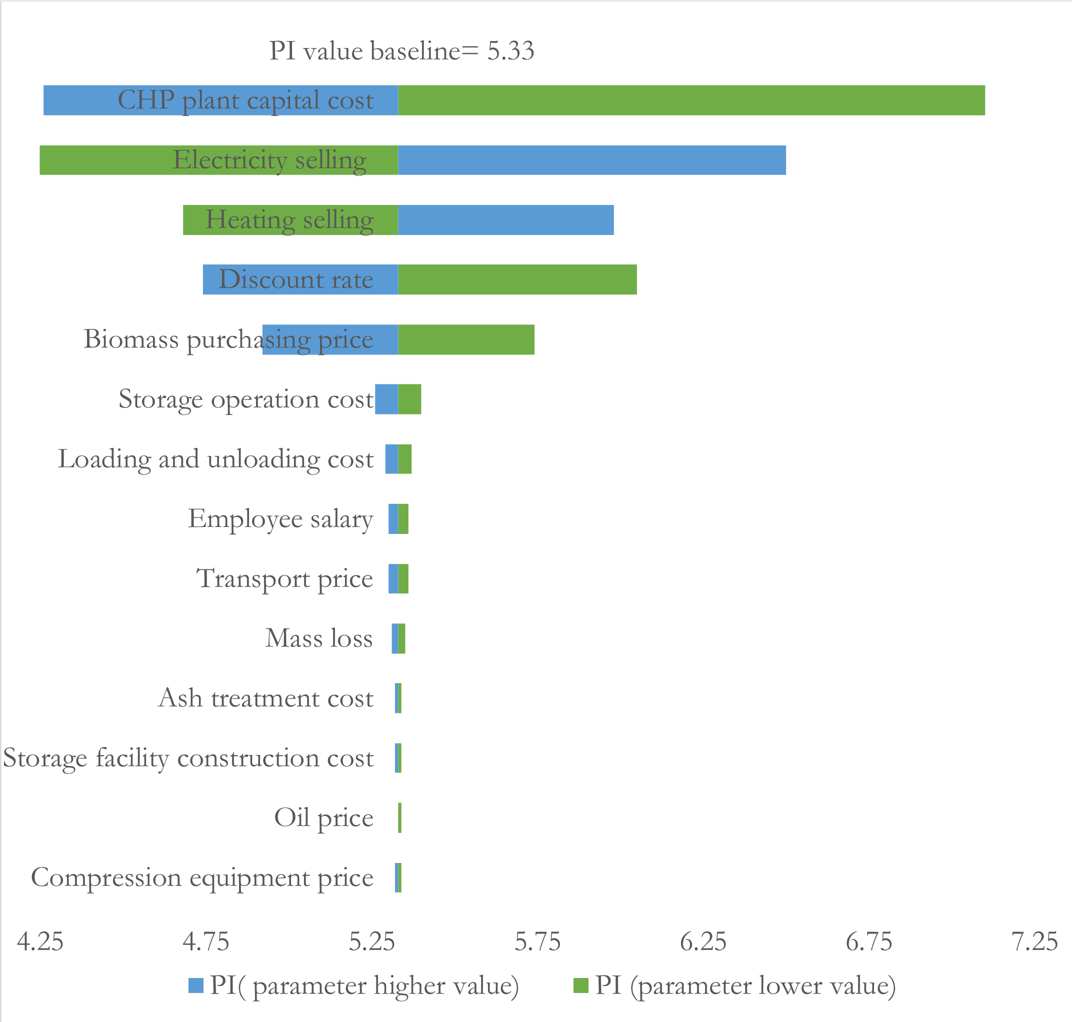

Figure 6- 7: Sensitivity analysis for biomass compression as pre-treatment scenario.

The sensitivity analysis results show that the most influential parameter is CHP plant capital cost. Capital cost with reduce 25%, the PI value raise from 5.33 to 7.1, which increase over 33.2%. This indicates the criticality of enhancing technology development in order to reduce capital cost. Electricity selling price appears the second influential parameter affecting CHP plant profitability. As power plant most important profit, the effect of electricity price fluctuation on power plant stability is more profound. Discount rate is an unignored parameter for CHP plant investment. It inspired the important of low interest rate funding solutions, in order to reduce investment risk. Biomass purchasing price is an influential cost-related parameter. A 25% decrease in biomass purchasing price results in CHP plant profitability increasing 7% to 5.74.

6.4 Summary of chapter

Medium-term decision-making is an important component in connecting others strategy of supply chain, which plays role in increasing supply chain cost-effective. This section investigates agricultural residues characteristics under raw material and torrefaction firstly. It was found that torrefied residues have higher energy density and heating value that that in raw material. Decomposition exists in torrefaction, which mass yield and energy yield decrease with increase torrefaction temperature. Followed by, logistic model was analysed for investigating the effect of pre-treatment method on logistic model. Results indicated that under the same residues demand, non-pre-treated CHP plant has better performance in profit and CO_2 emission. In terms of pre-treated CHP plant, compression express greater advantage than torrefaction. CHP plant-based torrefaction as pre-treatment method has advantage in reduce CHP operation cost and increase total income. Due to high torrefaction equipment expenditure, restricts it overall performance. PI value is indicator that evaluate investment attractiveness. In spite of non-pre-treated CHP plant had better profit performance, CHP plant applying compression as pre-treatment method has the highest PI value. To simulate close to realistic results, various restrictions and parameters applied in logistic model. The more restriction means more logistic model error. Thus, to minimize effect of error on results, combining GIS to provide a better solution. GIS analysed optimal depot and CHP refinery plant location based on the optimal pre-treatment method. Comparing with logistic model, GIS optimized results reduce 0.02% transportation cost and 0.01% CO_2 emission. For the sensitivity analysis, CHP plant capital cost was the most influential parameter for keeping plant profitability stabilization.

Drawbacks and further research

Medium-term decision-making logistic model as a general optimization approach was useful in changing decision environmental without requiring sophisticated reprogramming, which providing comprehensive analysis and precise solutions. However, repeated utilization between multi-approach for supply chain efficiency improvement increase software complexity and using threshold. Using interactive system optimization will be next research field, in order to reducing using threshold and increasing using efficiency.

Chapter 7:

ZERO WASTE BIOREFINERY PROCESS NETWORK DESIGN: A CASE STUDY OF AGRICULTURAL RESIDUES-BASED ETHANOL PRODUCTION PROCESS OPTIMIZATION

This chapter presents the thermodynamic model of zero waste bioethanol production network design, which converts wastes to high value-added by-products. The estimated results in this chapter are presented from the aspect of model material balance, energy consumption, economic and environmental analysis.

7.1 Material balance

Aspen Plus process model simulated the process that stillage discharge from ***ethanol distillation process*** undergoing ***Lignin extraction*** and ***By-product purification***. The obtained high-value added by-products and its purity by **lignin extraction** and ***By-product purification process*** are presented in Table 7- 1.

Table 7- 1: By-products yield from the zero waste biorefinery process simulated by Aspen Plus.

	Yield (kg/hr)	Purity (%)
Raw lignin	26024.1	47.0
Organics	25080.7	-
Raw ethanol	202.0	90.1
Furfural	528.3	98.7
Purified water	349440	99.5

In ***lignin extraction process***, the insoluble contents such as lignin, cellulose and ash were extracted with 12% moisture, which accounts 6.4% of total inlet stillage (26024.1 kg/hr). According to the simulation results, lignin shares approximate 47.0% of extracted insoluble solid that is worth between 300 to 450 US dollar per metric ton based on market value in 2020 [194, 195] ($375/t, assumed for the calculations in this work). While, the soluble content and waste water mix aqueous solutions (375283 kg/hr) will move to ***By-product purification*** for high value content refinery.

In ***by-products purification***, 25080.7 kg solid soluble organics are extracted per hour which account approximately 7% of mix aqueous solutions. 90.1% purity of ethanol (202 kg/hr) and 98.7% purity furfural (528.3 kg/hr) could contribute $1650.95/t [196, 197] and $1600/t [198] for biorefinery plant cash flow respectively. 349440 kg/hr purified water with 99.5% purity was generated in ***By-product purification***, out of which 136508 kg/hr replace utility water for water recycle in ***pre-treatment process***. The rest of 212932kg purified water will discharge to environment per hour. The recycled purified water could save 0.23 million dollars for refinery plant a year. The detailed flowrate of each stream presented in Appendix X.

7.2 Energy consumption

In the aspect of energy consumption, according to Aspen Plus simulation results, the total energy consumption of ***lignin extraction*** and ***by-products purification*** is 399.08 MW (1436677.55 MJ/h) shown in Table 7- 2. Among that ***by-products purification*** shares the largest energy consumption, which account 397.65 MW, in which large amount of water purification consume the most of energy.

Table 7- 2: Energy consumption in zero waste emission biorefinery simulated by Aspen Plus.

Process	Unit name	Function	Energy consumption (MW)
Lignin extraction	Compressor	Compress air	0.13
	Heater	Heating air	0.45
	condenser	Colling steam	0.82
	Pump	Stillage transfer	0.02
	Pump	Wastewater transfer	0.01
	Primary Filter	Solid filtering	0.00
	Washing water Filter	Solid filtering	0.00
	Total Sum		**1.43**
By-product purification	Heat exchanger	Organics extraction	18.74
	Heater	Organics extraction	15.59
	Wastewater condenser	Wastewater colling	220.67
	Furfural condenser	Furfural steam cooling	0.87
	Wastewater pump	Wastewater pumping	0.06
	1st dehydration pump	Wastewater pumping	0.04
	2nd dehydration pump	Wastewater pumping	0.01
	Ethanol pump	Wastewater pumping	0.00
	3rd dehydration pump	Wastewater pumping	0.00
	1st dehydration column	Water extraction	15.88
	2nd dehydration column	Water extraction	3.66
	Ethanol column	Ethanol extraction	119.34
	3rd dehydration column	Water extraction	1.99
	Furfural column	Furfural extraction	0.80
	Total Sum		**397.65**

Table 7- 3 summarised the energy consumption distribution during in ethanol production and energy content of ethanol and by-products. It was shown that the total energy consumption for ethanol production was 566.87 MW. While the produced ethanol only contained 162.70 MW, which account approximate 28.7% of energy consumption. One of a major reason is the energy content of high value-added by-products cannot take account into total energy content. From energy point of review, this ethanol refinery production process is not profitable. The main purpose of research is high value-added products rather than energy balance. In the aspect of sustainable development, the beneficial of material is much valuable than that in the aspect of energy.

Table 7- 3: Energy consumption and production for ethanol refinery.

	Energy (MW)	Market price ($/ton)
Energy consumption for ethanol production	167.79	-
Energy consumption for value-added production	399.08	-
Produced ethanol	162.70	1650.95
Raw lignin	-	375
Organics	-	0
Furfural	-	1600

7.3 Financial analysis

In this work, costs related to equipment, instillation, staff salary and energy are referred in 2020 and adjusted by Chemical Engineering Plant Cost Index (CEPCI), Producer Price Index (PPI), Labour Index and EIA Average Wholesale price of year 2020. The capital cost and operation cost breakdown by process areas and cost components are shown in Figure 7- 1 and Figure 7- 2 respectively. The total capital cost of proposed zero waste refinery plant is 145 million dollars, while the most expensive area is in ***pre-treatment process***, which requires multiple stages to condition pre-treated slurry by over liming. Biorefinery plant operation cost is divided into fixed operation cost and variable cost which includes by-products; energy consumption and capital depreciation. Comparing with traditional bioethanol process, the energy source of zero waste bioethanol process from external electrical grid. There is no doubt that energy consumption occupied the largest operation cost (76.46 M$/year). On the other hand, by-products are refined to high value-added commodities contributing to increased plant revenues (89.39 M$/year). The detailed equipment cost and capacity of ***Lignin extraction*** and ***By-product purification*** are presented in Appendix XI.

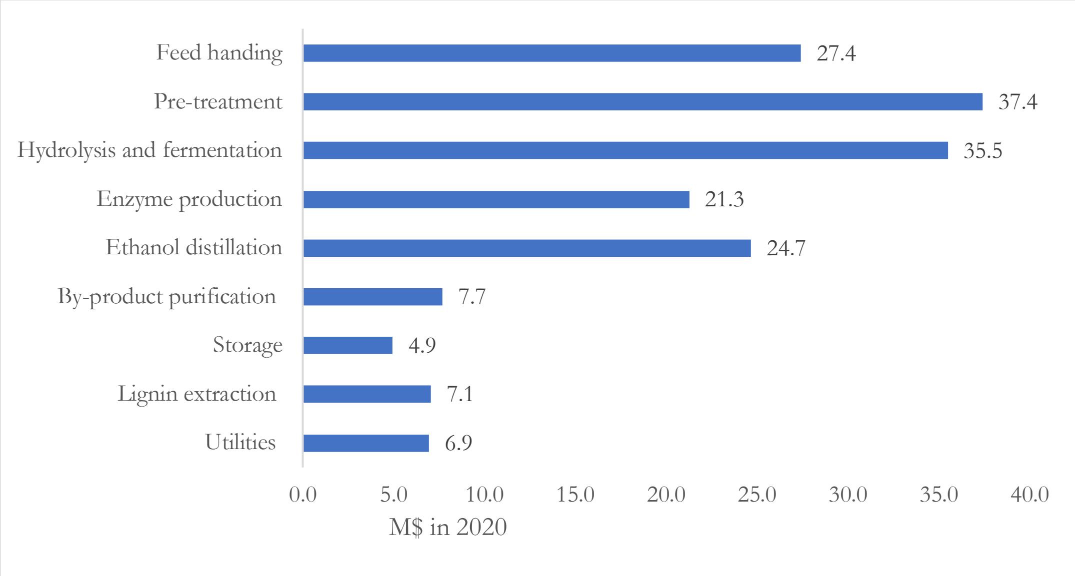

Figure 7- 1: Zero waste biorefinery plant capital cost breakdown by sub-processes.

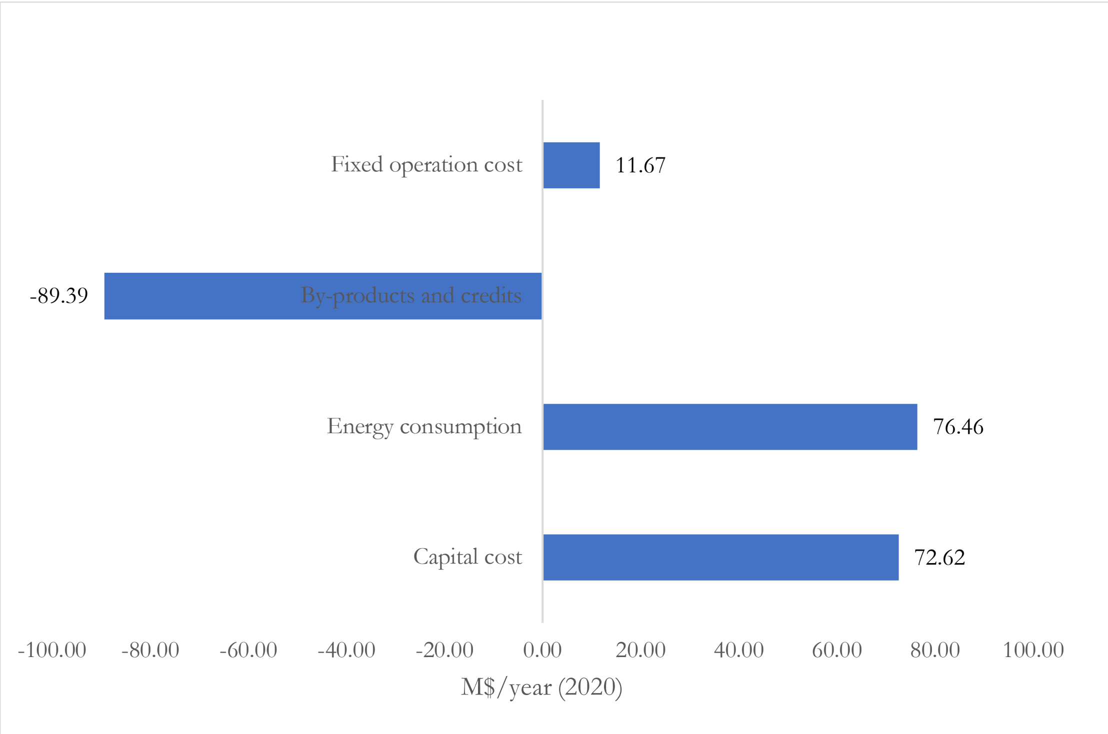

Figure 7- 2: Zero waste biorefinery plant operation cost distribution.

Table 7- 4 compares the minimum ethanol selling price (MESP) between the proposed zero waste and the traditional biorefinery plant. MESP is a parameter indicating the lowest ethanol price that could cover cost and generate 10% internal rate of return (IRR) for the ethanol refinery plant. MESP of zero waste biorefinery plant is 20.5% lower than that of the traditional biorefinery plant ($1.78/gal against $2.24/gal). While that average ethanol market price was $2.04/gal on April of 2021 [199], indicating a considerable profit space in proposed ethanol process. Waste water recycles into refinery plant operation, which results in the raw material cost

drop from 14.1 to 13.6 cents/gal ethanol. In traditional ethanol refinery plant, higher capital cost leads to higher capital depreciation and average return on investment, while the limited by-products restrict its profitability, which could rise up potential cost (minimum ethanol selling price). Thus, zero waste biorefinery plant has great advantage in MESP. On the other hand, large amount of electricity consumes during in ethanol production resulting in significant utility cost increase (the utility cost from 1.5 cents/gal raise to 125.3 cents/gal).

Table 7- 4: Minimum Ethanol Selling Price distribution in zero waste and traditional biorefinery plant (cents/gal ethanol).

Name	Zero waste biorefinery plant	NREL (traditional) biorefinery plant
Feedstock and Handling	74.1	
Sulfuric Acid	2.7	
Ammonia	7.2	
Glucose (enzyme production)	21.4	
Other Raw Materials	13.6	14.1
Utility cost	125.3	1.5
By-product income	-146.5	-10.8
Fixed Costs	19.1	20.1
Capital Depreciation	14.6	22.3
Average Income Tax	8.2	12.7
Average Return on Investment	38.5	59.2
Minimum Ethanol Selling Price	$1.78/gal	$2.24/gal

7.4 Model validation

There are limited data available to perform validation of the proposed zero-waste biorefinery concept, which is ascribed to its novelty. Lynd et al. [200] optimized the NERL process with three types of models in 2017. In the one of process models, the authors proposed a process that extracts lignin only, while the wastewater undergoes anaerobic treatment discharge to environment with external energy from electricity. The total capital cost of Lee et al. was $250 million against $281 million of our proposed process. If remove inflation impact to the year of 2017, our proposed process capital cost will adjust to 269 million. The capital cost contributes by direct investment (equipment expenditure) and indirect investment (fixed rate of direct investment). When split direct investment contribution, it can be found that the equipment cost for lignin extraction is 10 M$ against our proposed 7.1M$. One of hypothesis is equipment cost reduction with technologies improvement. Thus, we think the assumed data is reliable and acceptable. The difference is because of increased expenditure of multistage refinery process in the proposed zero-waste concept ***by-products purification***.

7.5 CO2 emission

In terms of environmental impact, CO_2 emission is a critical criterion for biorefinery environmental assessment. Table 7- 5 summarises CO_2 emissions in both zero waste and NREL biorefinery plants, which includes CO_2 produce from reaction in processes and electricity consumption. The CO_2 emission of electricity is calculated based on the data from Energy Information Administration (EIA) in 2020 in US (0.01 kg of CO_2/kWh for average renewable electricity) [201].The total CO_2 emission of zero waste emission plant accounts approximate 27.6% of that in the traditional bioethanol plant. To extract high concentration by-products from mix aqueous solutions, high volume of water needs to distillate which results in significant electricity consumption in ***By-product purification***. In terms of NREL refinery plant, extracted lignin form stillage convert to heat and power to whole refinery plant operation, leading to high CO_2 emission in ***CHP process***.

To achieve zero waste refinery plant competitiveness in CO_2 emission, 0.11 kg CO_2 emissions per kWh of all kinds of electricity (including renewable and fossil energy) is the maximum requirement. Reducing unit electricity CO_2 emission and developing cleaning energy such as wind power, hydropower and nuclear power are critical for reducing zero waste biorefinery plant CO_2 emissions. Thus, the suggestion is that the zero waste biorefinery plant should be operated in low carbon emission European countries such as Sweden, Norway and Lithuania with 0.008, 0.019 and 0.022kg/kWh respectively in 2019 [202], if the CO_2 emissions need to be lower than the traditional refinery plant.

Table 7- 5: CO_2 emission in zero waste and traditional biorefinery plant.

	Zero waste biorefinery plant			Traditional NREL biorefinery plant		
	Total CO_2 emissions (t/hr)	Stream amount (t/hr)	Unit CO_2 emission	Total CO_2 emissions (t/hr)	Stream amount (t/hr)	Unit CO_2 emission
Feed handing	0.01	104.17	0.00	0.00	104.17	0.00
Pre-treatment	0.06	482.98	0.00	0.00	482.98	0.00
Hydrolysis and fermentation	0.02	471.89	0.00	0.00	471.89	0.00
Enzyme production	2.42	47.22	0.05	2.38	47.22	0.05
Ethanol distillation	20.74	510.83	0.04	20.73	510.83	0.04
By-product purification or waste water pre-treatment	7.59	375.28	0.02	4.00	558.17	0.01
Storage	0.00	78.16	0.00	0.00	26.33	0.00
Lignin extraction or CHP	0.01	457.26	0.00	87.67	768.26	0.11
Utilities	0.06	136.51	0.00	0.00	82.22	0.00
Total	30.9			114.7		

Note: The total process stream between zero waste and traditional ethanol biorefinery plant are vary due to process reaction conditions are differ.

7.6 Sensitivity analysis

A conventional approach to understanding the importance of individual inputs is to perform single-point sensitivity analysis whereby a metric (e.g., MESP) is evaluated at the lower (-25%) and higher (+25%) bounds of each input parameter. Zero waste biorefinery sensitivity analysis has been performed on the impact of the most critical parameters affecting financial feasibility, such as capital cost, by-products income (furfural price, lignin price) and operational expenditure (feedstock price and enzyme price) on MESP (Table 7- 6).

Table 7- 6: The effect of individual input on MESP value.

	By-product sale price		
	+25%	Default value	-25%
Lignin ($/t)	468.75	375.0	281.25
Furfural ($/t)	2000.0	1600.0	1200.0
Electricity ($/kWh)	0.05	0.04	0.03
Feedstock ($/t)	73.13	58.5	43.88
Capital cost (M$)	351.40	281.12	210.84
Enzyme ($/t)	562.50	450.0	337.50

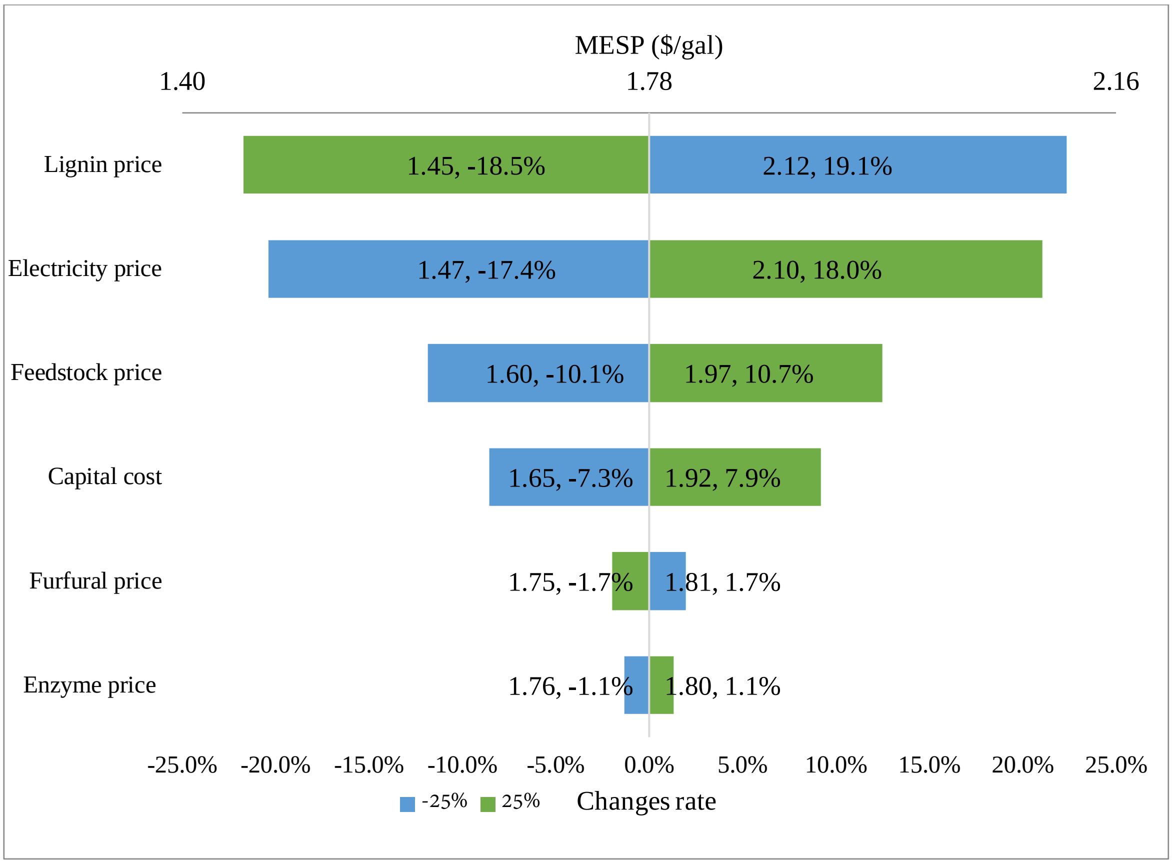

Figure 7- 3: The impact of parameters on MESP sensitivity

Figure 7- 3 illustrates MESP performance under single parameter fluctuation, which shows none of parameter plays domestic role on MESP oscillation (over 25% deviation). It is clear that MESP is highly sensitive to the lignin price, due to the high value and large amount of this particular by-product. When lignin price increased from $375.0/ton (base case scenario) to $468.8/ton, the MESP value dropped by 18.5%. In the meanwhile, electricity price is also a key parameter that affects MESP value with positive relationship (higher electricity price, higher MESP value). Thus, decreasing electricity price could increase bioethanol competitiveness in market, and anyone interested in the zero-waste concept should be focusing on low electricity prices to improve the financial performance of the plant. MESP has a relatively high sensitivity to feedstock price and capital cost, although not as high as in the case of lignin and electricity price. In general, enzyme cost is seen as a bottleneck in bioethanol refineries refinery [203]. However, in this study its impact on MESP is less sensitive compared to other investigated factors.

7.7 Summary of chapter

This chapter proposed bioethanol refinery process design towards zero-waste emissions, with its technical feasibility has been verified and proven by the Aspen plus simulation. zero waste emission process appears to be more competitive than traditional biorefinery plant in terms of profitability in ethanol market, especially if low electricity prices can be achieved. The results show that feedstock ***pre-treatment process*** and ***fermentation process*** are critical areas in capital cost distribution. High value-added by-products income improve the bioethanol plant profitability. MESP is important parameter that evaluates bioethanol plant profitability, which has been employed to evaluate bioethanol plant profitability. Comparing with traditional bioethanol plant, zero waste biorefinery plant has great advantage in control capital cost and by-products income creation. However, a potential drawback of the proposed biorefinery plant is electricity resource related CO_2 emission. If plant operate in high CO_2 intensity of electricity generation. With increasing strict emission standards, zero waste emission biorefinery plant needs to seek upgrading, and ideally to be supplied by green electricity. There is a trade-off identified, in the form of higher electricity consumption, while on the other hand more biomass is transformed into useful products and less waste is generated. High value-added by-products play a crucial role in the proposed bioethanol plant profitability, which leads to MESP sensitivity. The results shows that the by-product (such as lignin) with higher unit price and productivity result in higher MESP fluctuation. Lignin is main by-product of ethanol refinery which has higher unit price ($1600/ton), when lignin peddle price increase 25%, MESP will reduce 18.5%, followed by electricity price and feedstock price. In order to increase zero waste emission ethanol competitiveness, optimizing operation cost will be the primary task, while improving bargaining power and reducing costs (such as feedstock cost and enzyme cost) is an efficiency way.

Chapter 8:

CONCLUSIONS AND FUTURE WORK

8.1 Conclusions

This thesis project has illustrated optimize biomass supply chain from three decision making strategy, which involved long-term, medium-term and short-term strategy. Each strategy has corresponding decision making level, containing strategic, tactical and operational level. Chapter 1 has introduced the basic knowledge of biomass supply chain characteristics and research gap in previous biomass supply chain optimization. Chapter 2 comprehensively reviewed biomass supply chain based on three decision making level, which summarized present academic contributions and identified research gaps. The main research gap are summarised as follows:

i. Location selection is a crucial factor that affect biomass refinery plant profitability. Therefore, comprehensive residues potential assessment is necessary. Most of researcher assess residues potential focus on residues production and collection radius. For sustainable development, soil conditions should be considered.
ii. In the aspect of logistic model optimization, researchers trend to improve logistic model by a single sub-process optimization. Due to logistic model is highly synthesised system, the optimum solution in one process might not the best in another, which drag total logistic model performance.
iii. Various researchers attempt to improve conversion efficiency in order to produce competitive products. The large amount biorefinery waste was rare attention.

Based on research gaps, research methodologies along with research scopes were proposed in Chapter 3. Meanwhile, Chapter 4 illustrates a detailed description of the contribution from this thesis, which are summarised as follows:

i. In order to investigate the maximum collectable residues with cause environmental damage, soil erosion (SE), soil organic matter (SOM) and terrain information are introduced in residues potential assessment. Cooperating with geographic information system (GIS), a sustainable residues potential gained, which providing an overview information for further biomass refinery plant planning.
ii. Experiential analysed multiple agricultural residues characteristics and applying in pre-treatment processing technologies

iii. Analysed the effect of pre-treatment technologies on biomass logistic system, which providing corresponding pre-treatment technologies solutions depends on the type of biomass conversion technology.
iv. Uncertainty is the main challenge in supply chain model, therefore, converting uncertainty problem to a certainty problem was the main approach in logistic model optimization. To comprehensive optimize biomass logistic model, GIS as main analysis tool that plays crucial role in main sub-processes (transportation, pre-treatment and storage) of logistic model optimization. By interaction between GIS and logistic model, refinery plant location, transportation network design, storage depot location and capacity were determined.
v. For biorefinery industry sustainable development and producing competitive products, a conceptual zero waste biorefinery process network design was proposed.

As a whole, this thesis has proposed a novel approach, form three aspects of decision-making level to optimize agricultural residues-based supply chain system, which has filled several research gaps. The framework of supply chain can be adopted as an aiding tool for biorefinery plant planning, including capacity determination, transportation network design, infrastructure's location planning and process network design. To ensure biorefinery industry sustainable development, financial should not be the only considerable criteria, environmental impact need to be accounted, not only atmosphere, but also soil and water protection. Lastly, the possible extension of future work of this thesis is presented.

8.2 Future work

As mentioned, several research gaps have been addressed in this thesis. Some of potential future research can be conducted that improve industry competitive and sustainability, which summarized as follows:

i. The quality of biomass is highly relays on seasonal and weather conditions, which the efficiency of biorefinery production extremely uncertain. Thus, to make sure biomass production stable, continually quality assessment need to be investigated in early stage.
ii. At the present, researchers pay more attention on mainstream biomass (such as agricultural residues, forest residues and refuse-derived fuel). The lack of motivation on new generation biorefinery (e.g., algal conversion) will damage energy innovation. Therefore, it is suggested to develop the next generation technologies, applying

experiences learnt from previous technologies to reduce energy cost and enhance biorefinery industry sustainable development.

iii. The comprehensive analysed supply chain system, which optimise biorefinery supply chain from biomass potential assessment, collection region determination to biomass transportation and infrastructure allocation is rare. Therefore, developing a user-friendly and visualized supply chain platform can be future research work.

iv. In the past decade, material technologies have made great progress, while the research of biorefinery equipment was rarely reported. To ensure bioproducts competitiveness, not only improve conversion technologies but also cost control. Biorefinery is a heavy asset industry, which cost control in capital cost is more significant in it on logistic model. Thus, develop advanced equipment material could significantly improve bioproduct competitive.

The aforementioned future works are expected to (i) bioenergy could expand fuel market reducing fossil fuel dependent. (ii) enhance capital invest in biorefinery industry for sustainable development.

Appendix

Appendix I. Value of input variables and indices in supply chain model.

Symbol	Variables	Value	Unit	Ref.
Q_0	Biomass demand for power generation	tonnes/year	-	
P_n	Power generation capacity	20-30	MW	25 MW applied
h	Operation time	7600	h	[204]
η	Power generation efficiency (%)	36.9	%	[205]
LHV	Lower heating value (kJ/kg)	16315	kJ/kg	Calculated from pervious experiment
ρ	Biomass feedstocks distribution density	818068.1	kg/km^2	Calculated from pervious experiment
R	Collection radius	-	KM	
r	Distance from field to storage depot	-	KM	
$L2$	Distance from storage depot to power plant	-	KM	
∂	Agriculture residues available collection index	0.95		[206]
μ	dry matter loss coefficient	10	%	[207]
M	moisture content of received residues	15	%	Calculated from pervious experiment
C_c	biomass purchasing cost	-	€	
C_{pt}	biomass pre-treatment cost	-	€	
C_t	transportation cost	-	€	
C_s	storage cost	-	€	
C_{ash}	ash disposal cost	-	€	
C_p	power plant cost	-	€	
P_c	purchasing price	39.75	€/t	[208]
C_{d1}	equipment purchasing cost	-	€	
C_{m1}	maintain cost	-	€	
C_{em1}	employees' cost	-	€	
C_{ful1}	operation cost (fuel cost)	-	€	
β	equipment working capability	4	t/hr	[209]
C_{e1}	purchasing price for each equipment	5166	€	[209]
n_1	equipment utilization life	10	Year	Assumed
RV_1	rest value of equipment	5	%	[210]
C_{om1}	fixed percentage 0.2%	0.2	%	[204]
N_1	the number of employees	2		[209]
C_{sal}	the salary of each worker each year.	9843	€/year	[211]
O_{con1}	energy consumption	1	L/hr	[209] 0.4 t/m3 equipment
C_{oil}	oil price	0.86	€/L	[212]

Continued on next page

Symbol	Variables	Value	Unit	Ref.
C_{ele}	Electricity price	-	€	
O_{con2}	energy consumption	3	kWh/hr	[209] 0.8t/m3 equipment
$C_{e2refer}$	Reference size of torrefaction plant	200000	t/year	[213]
RV_2	rest value of equipment	5	%	[210]
F	scale factor	0.7		[214]
n_2	torrefaction equipment utilization life	10	year	Assumed
C_{om2}	fixed percentage	0.2	%	(Qin Zhang *et al.*, 2013)
N_2	the number of employees	3		[209]
C_{t1}	the cost from filed to collection depot	-	€	
C_{t2}	the cost from collection depot to power station	-	€	
C_{t3}	handing cost	-	€	
f	road tortuosity factor	1.4		[215]
P_t	transport price	2.65	€/km/t	[216]
V_v	transportation vehicle volume	100	m3	[204]
ρ_1	biomass loss bulk density from filed to storage depot	0.087	t/m3	Calculated from pervious experiment
n	the number of storage depots	-	-	
P_L	2 times loading and unloading cost	2.5	€/t	[217]
C_{s1}	Storage fixed cost	-	€	
S_s	storage area	-	m^2	
C_{sm}	management cost for storage.	1.2	€/m^2	[218]
H	the height for storage	6	m	[204]
ρ_i	biomass bulk density in storage	-	t/m^2	
C_{s2}	Storage facility cost	-	€	
C_c	storage facility construction cost	-	€	
RV_4	Net salvage value of storage facility	5	%	[210]
n_4	storage depot utilization life	15	Year	Assumed
C_{s3}	storage variable cost	-	€	
P_{os}	operation cost	3.2	€/t/m^2	[210]
M_{ash}	ash content of biomass (%)	7.24	%	Calculated from pervious experiment
P_{ash}	ash disposal cost (£/t)	100	€/t	Assumed
Q_{ash}	Ash quantity	-	-	
C_{pi}	total investment cost for biomass plant	-	€	

Continued on next page

Symbol	Variables	Value	Unit	Ref.
n_5	power plant operation period (year)	15	Year	Assumed
RV_5	Net salvage value of power plant	5	%	[210]
$C_{pi\,refer}$	power plant investment cost under referred size	36365563	€	[213]
γ	maintain cost factor	2.5	%	[204]
λ	salary and welfare factor	2.4	%	[204]
θ	Power plant scale factor	0.7		[204]
C_{bg}	Biomass grinding cost	-	€	
E_{bg}	electricity consumption for grinding	52.56	kJ/kg	[219]
R_{pg}	Power plant power generation revenue	-	€	
P_{ele}	electricity on-grid sealing price	0.75	€/kWh	[220]
P_s	subsidy from government	0.081	€/kWh	[220]
P_h	heating sealing price	5.18	€/GJ	[221]
T_h	heating sealing period	5	Month	[221]
H_{LHV}	lower heating value for heating supply (MJ/kg)	15.59	MJ/kg	Calculated from pervious experiment
E_h	power plant heating efficiency	49.95	%	[205]
E_t	CO_2 emission in transportation	-	t	
E_{CO2}	Total CO_2 emission	-	t	
E_{pt}	CO_2 emission in pre-treatment	-	t	
E_s	CO_2 emission in storage	-	t	
E_{diesel}	CO_2 emission for diesel	-	kg/kg	
Q_{carbon}	Carbon content in diesel	20.2	ton carbon/TJ	[222]
φ_{carbon}	Carbon oxidation rate in diesel	0.98		[222]
δ_{carbon}	carbon and carbon dioxide mass ratio	3.6667		[222]
LHV_{carbon}	diesel lower heating value (kJ/kg)	42.652	kJ/kg	[222]
E_{t1}	CO_2 emission in transportation from field to storage depot	-	t	
E_{t2}	CO_2 emission in transportation from storage depot to power plant	-	t	
E_{t3}	CO_2 emission in transportation handling	-	t	

Continued on next page

Symbol	Variables	Value	Unit	Ref.
$Q_{c_{emp}}$	empty truck diesel consumption in collection	0.08	l/km	[210]
$Q_{c_{full}}$	full loaded truck diesel consumption in collection	0.11	l/km	[210]
$Q_{p_{full}}$	full loaded truck diesel consumption to power station	0.25	l/km	[210]
$Q_{p_{emp}}$	empty truck diesel consumption to power station	0.15	l/km	[210]
β_4	loading and unloading equipment working capacity (t/hr)	30	t/hr	[210]
O_{con4}	diesel consumption (l/hr)	14.86		[210]
E_{ele}	Electricity CO_2 emission (renewable)	0	kWh/t	[223]
O_{con2}	Electricity consumption	3	kWh/hr	[209]
β_5	stacking equipment capacity	30	t/hr	[210]
P_{stack}	stacking equipment power	30	kw	[210]
β_6	unstacking equipment capacity	20	t/hr	[210]
$P_{unstack}$	unstacking equipment power	30	kw	[210]
NPV	net present value	-	-	
PI	profitability index	-	-	

Appendix II. Equipment distribution of lignin extraction process.

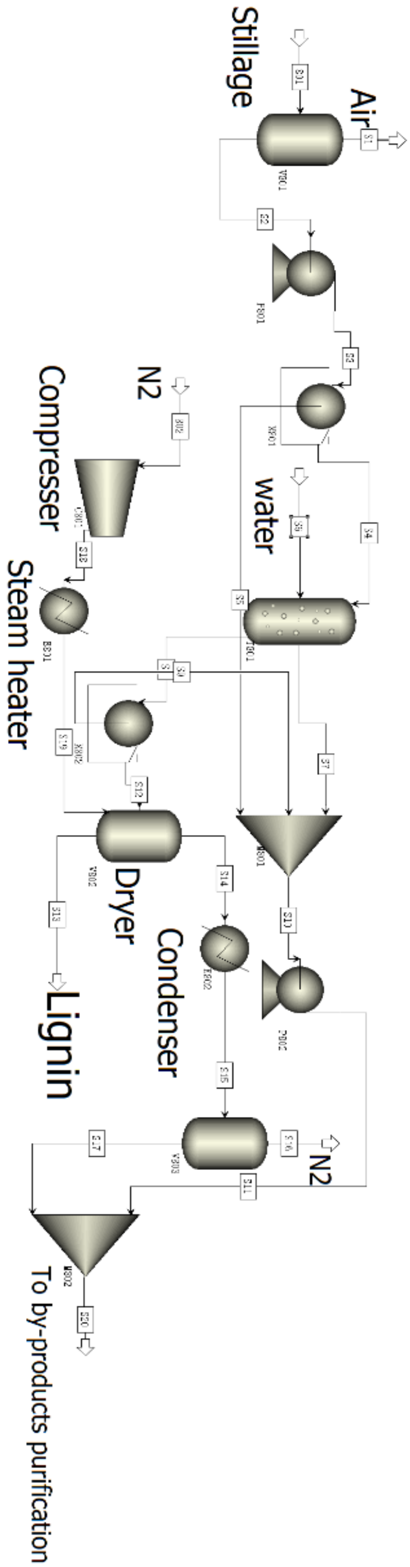

Appendix III. Equipment distribution of by-products purification process.

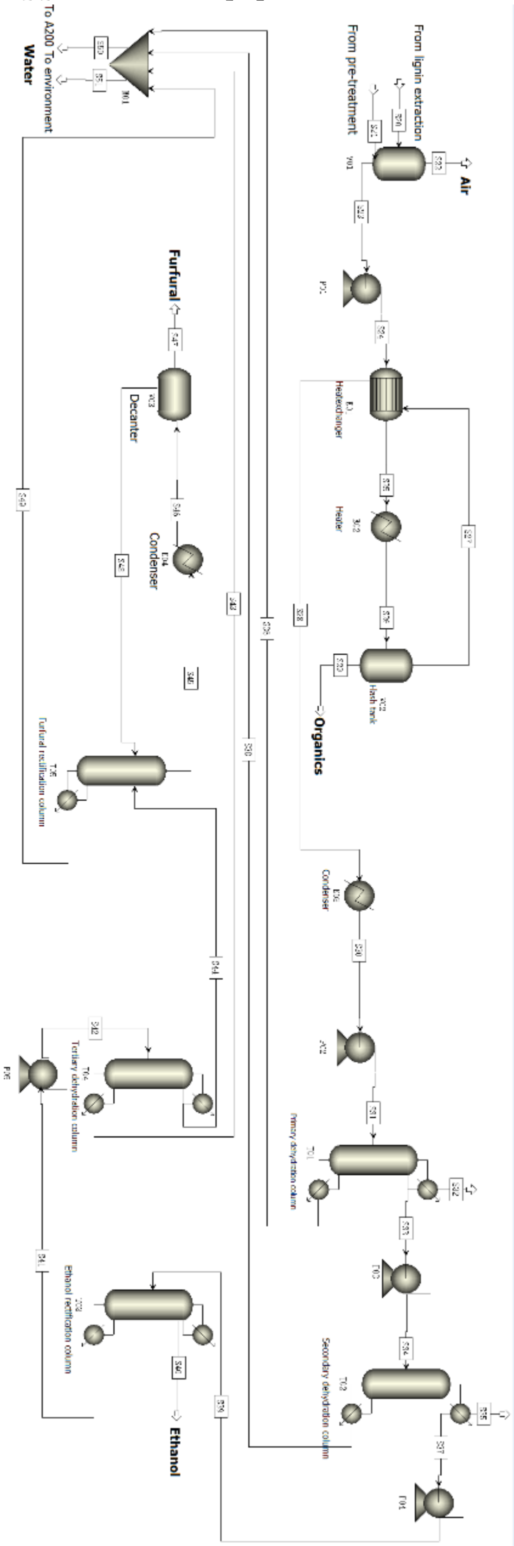

Appendix IV. Aspen simulation equipment name and technique configuration .

Equipment code	Name	Technique configuration
V801	Vent tank	
P801	Pump	Discharge pressure: 3bar
X801	Filter	Fraction of solids to solid outlet: 0.99
		Liquid load of solid outlet: 0.33
T801	Wash tank	Liquid-to-solid mass ratio: 0.3
M801	Mixer	
C801	Compressor	Discharge pressure: 1.2bar
E801	Stream heater	Temperature: 125 °C
X802	Filter	Fraction of solids to solid outlet: 0.99
		Liquid load of solid outlet: 0.2
P802	Pump	Discharge pressure: 2bar
E802	Condenser	
V802	Dryer	Pressure: 0.1bar
V803	Vent tank	
M802	Mixer	
V01	Vent tank	
P01	Pump	Discharge pressure: 5 bar
E01	Heat exchanger	Hot inlet-cold outlet temperature difference: 20°C
E02	Heater	Temperature: 90 °C
V02	Flash tank	Temperature: 125 °C
		Pressure: 0.1 bar
E03	Condenser	
P02	Pump	Discharge pressure: 3 bar
T01	Primary dehydration column	Reflux ratio: 1
		Distillate to feed ratio :0.347
P03	Pump	Discharge pressure: 3 bar
T02	Secondary dehydration column	Reflux ratio: 5.5
		bottoms to feed ratio :0.944
P04	Pump	Discharge pressure: 3 bar
T03	Ethanol rectification column	Boil up ratio: 20
		Distillate to feed ratio :0.03
P05	Pump	Discharge pressure: 3 bar

Continued on next page

Equipment code	Name	Technique configuration
T04	Tertiary dehydration column	Reflux ratio: 1 Distillate to feed ratio :0.2
T05	Furfural rectification column	
E04	Condenser	
V03	Decanter	
M01	Mixer	

Appendix V. Agricultural residues theoretical potential distribution, MT

Province	Total amount	Wheat	Corn	Sorghum	Millet	Rice	Tubers
Anhui	54.10	19.23	9.12	0.00	0.00	18.82	0.33
Beijing	1.42	0.83	0.57	0.00	0.00	0.00	0.01
Chongqing	13.90	0.22	3.41	0.16	0.00	5.10	3.31
Fujian	5.27	0.00	0.00	0.00	0.00	4.17	1.00
Gansu	16.02	3.32	8.77	0.00	0.00	0.03	2.05
Guangdong	14.88	0.00	0.72	0.00	0.00	11.09	1.35
Guangxi	17.53	0.00	3.62	0.00	0.00	11.53	1.06
Guizhou	14.35	0.77	4.04	0.00	0.00	4.24	3.25
Hainan	2.04	0.00	0.00	0.00	0.00	1.49	0.37
Hebei	59.72	20.16	35.21	0.00	0.00	0.47	1.34
Heilongjiang	110.04	0.35	68.88	0.54	0.10	27.35	0.58
Henan	100.65	49.65	37.54	0.05	0.11	4.51	0.88
Hubei	46.86	6.74	7.31	0.03	0.00	24.67	1.06
Hunan	45.71	0.13	4.08	0.04	0.00	35.08	1.00
Inner Mongolia	56.58	2.53	43.21	0.50	1.11	0.79	1.38
Jiangsu	50.13	16.16	5.65	0.00	0.00	24.64	0.33
Jiangxi	34.25	0.04	0.32	0.00	0.00	27.21	0.55
Jilin	70.25	0.00	60.46	1.37	0.00	6.64	0.30
Liaoning	39.96	0.01	33.28	0.39	0.28	4.09	0.34
Ningxia	4.30	0.47	3.27	0.00	0.00	0.00	0.38
Qinghai	1.79	0.40	0.25	0.00	0.00	0.00	0.39
Shaanxi	15.93	5.52	8.04	0.00	0.00	0.95	0.00
Shandong	86.48	33.43	46.06	0.02	0.15	0.84	0.81
Shanghai	1.30	0.14	0.04	0.00	0.00	1.10	0.00
Shanxi	21.81	3.11	16.92	0.11	0.60	0.00	0.47
Sichuan	45.26	3.30	13.78	0.00	0.00	14.74	5.65
Tianjin	3.17	0.84	2.06	0.00	0.00	0.24	0.01
Tibet	0.24	0.03	0.04	0.00	0.00	0.01	0.01
Xinjiang	37.41	7.53	11.74	0.00	0.00	0.67	0.17
Yunnan	21.95	0.97	11.78	0.00	0.00	5.29	1.65
Zhejiang	8.17	0.58	0.47	0.00	0.00	5.69	0.46
Total Amount of Residues (MT)	**1001.47**	**176.46**	**440.64**	**3.22**	**2.36**	**241.45**	**30.47**

Continued on next page

Province	Beans	Peanuts	Rapeseed	Sesame	Sunflower	Cotton
Anhui	2.29	1.36	2.27	0.20	0.00	0.47
Beijing	0.01	0.01	0.00	0.00	0.00	0.00
Chongqing	0.52	0.15	1.01	0.02	0.00	0.00
Fujian	0.10	0.00	0.00	0.00	0.00	0.00
Gansu	0.27	0.45	1.02	0.00	0.00	0.12
Guangdong	0.09	1.62	0.00	0.00	0.00	0.00
Guangxi	0.18	1.11	0.00	0.02	0.00	0.00
Guizhou	0.13	0.13	1.78	0.00	0.00	0.00
Hainan	0.01	0.17	0.00	0.00	0.00	0.00
Hebei	0.33	1.26	0.00	0.00	0.00	0.96
Heilongjiang	12.23	0.00	0.00	0.00	0.00	0.00
Henan	0.84	6.46	0.00	0.42	0.00	0.18
Hubei	0.58	1.18	4.37	0.32	0.00	0.61
Hunan	0.54	0.41	4.01	0.04	0.00	0.36
Inner Mongolia	2.92	0.00	0.00	0.00	4.14	0.00
Jiangsu	0.77	0.54	1.82	0.05	0.00	0.17
Jiangxi	0.48	0.70	1.38	0.99	0.00	2.58
Jilin	1.14	0.00	0.00	0.00	0.33	0.00
Liaoning	0.33	1.20	0.00	0.00	0.03	0.00
Ningxia	0.01	0.00	0.07	0.12	0.00	0.00
Qinghai	0.06	0.00	0.69	0.00	0.00	0.00
Shaanxi	0.19	0.14	1.01	0.00	0.00	0.09
Shandong	0.52	3.83	0.00	0.00	0.00	0.83
Shanghai	0.01	0.00	0.01	0.00	0.00	0.00
Shanxi	0.44	0.00	0.00	0.00	0.13	0.02
Sichuan	1.25	0.79	5.76	0.00	0.00	0.00
Tianjin	0.00	0.01	0.00	0.00	0.00	0.00
Tibet	0.04	0.00	0.12	0.00	0.00	0.00
Xinjiang	0.16	0.02	0.35	0.00	0.00	16.76
Yunnan	1.24	0.07	0.95	0.00	0.00	0.00
Zhejiang	0.46	0.08	0.41	0.00	0.00	0.02
Total Amount of Residues (MT)	**28.13**	**21.71**	**27.05**	**2.19**	**4.62**	**23.15**

Appendix VI. The scale of arable land distribution under technical potential (km^2).

Province	Total arable land (theoretical potential)	Arable land under technical potential
Anhui	89505	80135
Beijing	1737	1433
Chongqing	35758	5461
Fujian	23313	5466
Gansu	42293	15910
Guangdong	47847	30982
Guangxi	61347	33848
Guizhou	55422	4857
Hainan	8453	7439
Hebei	87398	70399
Heilongjiang	122940	107864
Henan	144250	123117
Hubei	79524	57715
Hunan	87170	48830
Inner Mongolia	75679	44663
Jiangsu	77450	75663
Jiangxi	55791	34002
Jilin	56791	45771
Liaoning	42199	27798
Ningxia	12646	7803
Qinghai	5584	2830
Shaanxi	42845	17623
Shandong	110265	87284
Shanghai	3402	3363
Shanxi	37677	21440
Sichuan	96899	22462
Tianjin	4690	4639
Tibet	2528	985
Xinjiang	57573	53281
Yunnan	71856	12367
Zhejiang	22906	14589
Total scale of arable land	**1663738**	**1070020**

Appendix VII. Arable land distribution under sustainable potential (km^2).

Province	Arable land Under legislative regulation	Arable land under weak soil erosion	Arable land under mild soil erosion	Arable land under moderate soil erosion
Anhui	79303	77791	1084	278
Beijing	1421	1370	23	25
Chongqing	5366	2437	1255	1424
Fujian	5396	5247	64	19
Gansu	15862	6641	2985	2401
Guangdong	30282	29017	631	320
Guangxi	33475	33141	269	16
Guizhou	4840	3182	1081	467
Hainan	7369	7256	89	14
Hebei	70126	62194	5063	2401
Heilongjiang	107534	74861	20128	11339
Henan	122537	109203	10828	2272
Hubei	56042	52027	2325	1137
Hunan	47844	45110	1196	1461
Inner Mongolia	44475	21917	10017	9479
Jiangsu	74601	73179	1346	24
Jiangxi	33379	27658	1003	1823
Jilin	45591	36049	5924	2652
Liaoning	27651	23135	3982	451
Ningxia	7741	5344	1062	848
Qinghai	2817	2124	416	201
Shaanxi	17549	11498	2726	1543
Shandong	86653	81533	1044	2588
Shanghai	3312	3296	0	0
Shanxi	21373	15350	2108	2171
Sichuan	22209	12760	7104	1902
Tianjin	4639	4577	33	3
Tibet	974	541	221	152
Xinjiang	53101	35362	7921	6290
Yunnan	12260	9264	1451	1357
Zhejiang	14372	14077	188	81
Total scale of arable land	**1060092**	**887140**	**93566**	**55139**

Appendix VIII. Existed biorefinery plant in Heilongjiang.

Project name	Capacity	Biomass consumption (year)	GIS location
Mishan CHP project	30MW	249000	131.874069,45.541496
Wudalianchi CHP project	30MW	25-300000	126.625956,48.493882
Miudanjiang CHP project	30MW	250000	129.635615,44.596104
Anning CHP project	30MW	250000	129.482851,44.34072
Lanxi CHP project	30MW	250000	126.303462,46.232394
Jixian CHP project	30MW	250000	131.140483,46.728377
Fangzheng CHP project	30MW	250001	128.834606,45.840112
Qitaihe CHP project	40MW	300002	130.531311,45.786099
Xinglong CHP project	30MW	250003	120.525401,36.452069
Yichun CHP project	40MW	300000	127.743633,46.971286
Haerbin CHP project	30MW	250000	126.945454,45.553758
Suibin CHP project	30MW	250000	131.852759,47.289116
Hailun CHP project	30MW	250000	126.97631,47.471847
Shengli farm CHP project	15MW	150000	133.871674,47.368236
Nongjiang farm CHP project	6MW	60000	126.727527,45.682652
Tonghe CHP project	30MW	250000	128.766793,45.993464
Nenjiang CHP project	30MW	250000	125.260042,49.2089
Qindeli farm CHP project	15MW	130000	133.162606,47.976273
Daxing farm CHP project	15MW	130000	132.880837,46.981703
Qianshao farm CHP project	15MW	130000	134.13641,47.99376
Jiameng CHP project	30MW	250000	130.389804,48.890999
Hegang CHP project	30MW	250000	130.179225,47.323227
Yian CHP project	30MW	250000	125.306279,47.893548
Dongxing CHP project	30MW	250000	127.871729,46.382746
Wangkui CHP project	30MW	250000	126.465727,46.832396
Tangyuan CHP project	30MW	250000	129.894867,46.711284
Longjiang CHP project	30MW	250000	123.184447,47.331913
Youyi CHP project	30MW	250000	131.79984,46.801681
Jiansanjiang qianjinchp project	30MW	250000	133.112852,47.544961
Mingshui CHP project	36MW	400000	125.877646,47.172619

Appendix IX. Candidate C financial breakdown for each feedstock availability.

Table 1. Cost breakdown for biomass feedstock with 20% availability.

20% availability (feedstocks density 57.28 t/km^2)	Scenario 1	Scenario 2	Scenario 3	Scenario 4	Scenario 5
Purchasing cost	**5.29**	**5.29**	**5.29**	**6.34**	**6.34**
Equipment cost	0.00	0.00	0.00	0.74	0.94
Maintain cost	0.00	0.18	0.34	0.01	0.14
Employee cost	0.00	0.35	0.39	0.53	0.77
Operation cost	0.00	0.04	0.04	0.03	0.03
Pre-treatment cost	**0.00**	**0.58**	**0.78**	**1.32**	**1.87**
Storage fixed cost	0.12	0.03	0.01	0.02	0.01
Facility cost	0.04	0.01	0.00	0.01	0.00
Storage variable cost	0.92	0.92	0.92	0.62	0.62
Storage cost	**1.08**	**0.96**	**0.94**	**0.65**	**0.64**
Transportation cost to collection point	0.98	0.40	0.49	0.64	0.74
Transportation cost to power station	0.00	0.00	0.00	0.01	0.00
Loading and unloading cost	0.28	0.56	0.56	0.53	0.53
Transportation cost	**1.26**	**0.97**	**1.06**	**1.18**	**1.28**
Ash disposal cost	**0.13**	**0.13**	**0.13**	**0.09**	**0.09**
Power station annual investment cost	1.73	1.73	1.73	1.73	1.73
Maintain cost in power plant	0.04	0.04	0.04	0.04	0.04
Salary and welfare cost	0.04	0.04	0.04	0.04	0.04
Power station cost	**1.82**	**1.82**	**1.82**	**1.82**	**1.82**
Total cost for power generation	**9.59**	**9.74**	**10.01**	**11.39**	**12.03**
Heating selling income	4.21	4.21	4.21	6.27	6.27
Power generation income	16.71	16.71	16.71	16.71	16.71
Power plant revenue	**20.92**	**20.92**	**20.92**	**22.98**	**22.98**
Power plant net profit	11.33	11.18	10.90	11.59	10.95
Net present value	84.17	83.07	80.76	78.13	77.47
Profitability index	**4.00**	**4.02**	**3.94**	**2.85**	**2.98**

Table 2. Cost breakdown for biomass feedstock with 40% availability.

40% availability (feedstocks density 114.57 t/km^2)	Scenario 1	Scenario 2	Scenario 3	Scenario 4	Scenario 5
Purchasing cost	**10.59**	**10.59**	**10.59**	**12.69**	**12.69**
Equipment cost	0.00	0.00	0.00	1.21	1.53
Maintain cost	0.00	0.36	0.69	0.27	0.47
Employee cost	0.00	0.71	0.78	1.01	1.06
Operation cost	0.00	0.08	0.09	0.05	0.05
Pre-treatment cost	**0.00**	**1.15**	**1.56**	**2.54**	**3.11**
Storage fixed cost	0.24	0.05	0.03	0.04	0.02
Facility cost	0.09	0.02	0.01	0.01	0.01
Storage variable cost	1.84	1.84	1.84	1.25	1.25
Storage cost	**2.17**	**1.91**	**1.88**	**1.30**	**1.27**
Transportation cost to collection point	1.96	0.57	0.65	0.91	1.05
Transportation cost to power station	0.00	0.01	0.00	0.01	0.00
Loading and unloading cost	0.56	1.13	1.13	1.06	1.06
Transportation cost	**2.53**	**1.70**	**1.79**	**1.98**	**2.11**
Ash disposal cost	**0.26**	**0.26**	**0.26**	**0.17**	**0.17**
Power station annual investment cost	2.82	2.82	2.82	2.82	2.82
Maintain cost in power plant	0.07	0.07	0.07	0.07	0.07
Salary and welfare cost	0.07	0.07	0.07	0.07	0.07
Power station cost	**2.95**	**2.95**	**2.95**	**2.95**	**2.95**
Total cost for power generation	**18.49**	**18.56**	**19.02**	**21.62**	**22.30**
Heating selling income	8.41	8.41	8.41	12.53	12.53
Power generation income	33.43	33.43	33.43	33.43	33.43
Power plant revenue	**41.84**	**41.84**	**41.84**	**45.96**	**45.96**
Power plant net profit	**23.35**	**23.28**	**22.82**	**24.34**	**23.66**
Net present value	178.90	177.72	173.76	197.05	193.93
Profitability index	**4.91**	**4.88**	**4.79**	**5.30**	**5.23**

Table 3. Cost breakdown for biomass feedstock with 60% availability.

60% availability (feedstocks density 171.85 t/km^2)	Scenario 1	Scenario 2	Scenario 3	Scenario 4	Scenario 5
Purchasing cost	**17.20**	**17.20**	**17.20**	**20.61**	**20.61**
Equipment cost	0.00	0.00	0.00	1.69	2.14
Maintain cost	0.00	0.59	1.12	0.43	0.76
Employee cost	0.00	1.15	1.26	1.31	1.39
Operation cost	0.00	0.13	0.15	0.09	0.09
Pre-treatment cost	**0.00**	**1.87**	**2.53**	**3.53**	**4.38**
Storage fixed cost	0.39	0.08	0.04	0.06	0.03
Facility cost	0.14	0.03	0.02	0.02	0.01
Storage variable cost	2.99	2.99	2.99	2.03	2.03
Storage cost	**3.52**	**3.11**	**3.05**	**2.10**	**2.07**
Transportation cost to collection point	3.32	0.74	0.89	1.21	1.38
Transportation cost to power station	0.00	0.01	0.00	0.01	0.00
Loading and unloading cost	0.92	1.83	1.83	1.72	1.72
Transportation cost	**4.24**	**2.59**	**2.73**	**2.94**	**3.10**
Ash disposal cost	**0.42**	**0.42**	**0.42**	**0.28**	**0.28**
Power station annual investment cost	3.96	3.96	3.96	3.96	3.96
Maintain cost in power plant	0.10	0.10	0.10	0.10	0.10
Salary and welfare cost	0.09	0.09	0.09	0.09	0.09
Power station cost	**4.15**	**4.15**	**4.15**	**4.15**	**4.15**
Total cost for power generation	**29.53**	**29.34**	**30.08**	**33.61**	**34.59**
Heating selling income	13.67	13.67	13.67	20.37	20.37
Power generation income	54.32	54.32	54.32	54.32	54.32
Power plant revenue	**67.99**	**67.99**	**67.99**	**74.69**	**74.69**
Power plant net profit	**38.46**	**38.65**	**37.91**	**41.07**	**40.09**
Net present value	299.66	300.38	293.93	335.48	330.88
Profitability index	**5.64**	**5.65**	**5.55**	**6.19**	**6.12**

Table 4. Cost breakdown for biomass feedstock with 80% availability.

80% availability (feedstocks density 229.14 t/km^2)	Scenario 1	Scenario 2	Scenario 3	Scenario 4	Scenario 5
Purchasing cost	**22.50**	**22.50**	**22.50**	**26.96**	**26.96**
Equipment cost	0.00	0.00	0.01	2.04	2.59
Maintain cost	0.00	0.77	1.46	0.56	1.00
Employee cost	0.00	1.51	1.65	1.55	1.65
Operation cost	0.00	0.17	0.19	0.11	0.11
Pre-treatment cost	**0.00**	**2.45**	**3.31**	**4.27**	**5.34**
Storage fixed cost	0.51	0.11	0.06	0.07	0.04
Facility cost	0.19	0.04	0.02	0.03	0.01
Storage variable cost	3.91	3.91	3.91	2.65	2.65
Storage cost	**4.61**	**4.06**	**3.99**	**2.75**	**2.70**
Transportation cost to collection point	4.30	0.84	0.99	1.37	1.56
Transportation cost to power station	0.00	0.01	0.00	0.01	0.00
Loading and unloading cost	1.20	2.40	2.40	2.25	2.25
Transportation cost	**5.50**	**3.25**	**3.39**	**3.63**	**3.82**
Ash disposal cost	**0.54**	**0.54**	**0.54**	**0.37**	**0.37**
Power station annual investment cost	4.77	4.77	4.77	4.77	4.77
Maintain cost in power plant	0.12	0.12	0.12	0.12	0.12
Salary and welfare cost	0.11	0.11	0.11	0.11	0.11
Power station cost	**5.01**	**5.01**	**5.01**	**5.01**	**5.01**
Total cost for power generation	**38.16**	**37.81**	**38.74**	**42.98**	**44.20**
Heating selling income	17.88	17.88	17.88	26.63	26.63
Power generation income	71.03	71.03	71.03	71.03	71.03
Power plant revenue	**88.91**	**88.91**	**88.91**	**97.67**	**97.67**
Power plant net profit	**50.75**	**51.10**	**50.17**	**54.68**	**53.47**
Net present value	398.71	400.40	392.35	448.45	442.61
Profitability index	**6.10**	**6.12**	**6.02**	**6.74**	**6.66**

Table 5. Cost breakdown for biomass feedstock with 100% availability.

100% availability (feedstocks density 286.42 t/km^2)	Scenario 1	Scenario 2	Scenario 3	Scenario 4	Scenario 5
Purchasing cost	**29.11**	**29.11**	**29.11**	**34.88**	**34.88**
Equipment cost	0.00	0.00	0.01	2.45	3.10
Maintain cost	0.00	1.00	1.89	0.72	1.29
Employee cost	0.00	1.95	2.14	1.85	1.98
Operation cost	0.00	0.22	0.25	0.15	0.15
Pre-treatment cost	**0.00**	**3.17**	**4.28**	**5.17**	**6.51**
Storage fixed cost	0.66	0.14	0.07	0.10	0.05
Facility cost	0.24	0.05	0.03	0.04	0.02
Storage variable cost	5.06	5.06	5.06	3.43	3.43
Storage cost	**5.96**	**5.26**	**5.16**	**3.56**	**3.50**
Transportation cost to collection point	5.66	0.99	1.16	1.58	1.86
Transportation cost to power station	0.00	0.01	0.01	0.01	0.01
Loading and unloading cost	1.55	3.11	3.11	2.91	2.91
Transportation cost	**7.21**	**4.10**	**4.27**	**4.51**	**4.77**
Ash disposal cost	**0.70**	**0.70**	**0.70**	**0.48**	**0.48**
Power station annual investment cost	5.72	5.72	5.72	5.72	5.72
Maintain cost in power plant	0.14	0.14	0.14	0.14	0.14
Salary and welfare cost	0.14	0.14	0.14	0.14	0.14
Power station cost	**6.00**	**6.00**	**6.00**	**6.00**	**6.00**
Total cost for power generation	**48.99**	**48.35**	**49.53**	**54.60**	**56.14**
Heating selling income	17.88	17.88	17.88	34.47	34.47
Power generation income	91.92	91.92	91.92	91.92	91.92
Power plant revenue	**109.80**	**109.80**	**109.80**	**126.39**	**126.39**
Power plant net profit	**60.81**	**61.45**	**60.27**	**71.79**	**70.25**
Net present value	477.58	481.53	471.23	590.79	583.03
Profitability index	**6.08**	**6.13**	**6.02**	**7.29**	**7.21**

Appendix X. Aspen simulation flowrate value.

Flow code	Flowrate (kg/hr)	Code	Flowrate (kg/hr)
801	403607.0	S24	6735.3
802	20000.0	S25	202.0
803	10000.0	S26	6533.3
S1	31.0	S27	6533.3
S2	350171.5	S28	1784.0
S3	375252.2	S29	1784.0
S4	375252.2	S30	1255.8
S5	349440.0	S31	528.3
S6	12009.1	S32	700.0
S7	375252.2	S33	20000.0
S8	391597.9	S34	20000.0
S9	391597.9	S35	21284.2
S10	30572.5	S36	1228.2
S11	375252.2	S37	361025.4
S12	350171.5	S38	5305.1
S13	25080.7	S39	10689.6
S14	350171.5	S40	374289.5
S15	350171.5	S41	374289.5
S16	121815.5	S42	26024.1
S17	228355.7	S43	27308.3
S18	29882.9	S44	2574.5
S19	0.4	S45	21284.2
S20	121815.5	S46	20290.5
S21	6735.3	S47	993.7
S22	115079.3	S48	375283.3
S23	0.9		

Appendix XI. Capital cost of Lignin extraction and By-product purification process.

Mechanical Equipment List												Scaled Installed Costs								
EQPT N		EQUIPMENT TITLE	VENDOR	MODEL	ESCRIPTIO	HP	MATERIAL	UOTE INF	NUM REQD	$	Year of Quote	Purch Cost in Base Yr	Scaling Variable	Scaling Val	Units	Scaling Exp	Inst Factor	New Val	Size Ratio	Scaled Purch Cost
V	601	Tank	UET Mixers		Side-mour	170 kW	316LSS	YES	1	$30,000	2020	30000	strm.a200.	252891	kg/hr	0.5	1.5	375283.3	1.483972	$36,546
V	602	Flash tank			23' x 48' - 110,000 ga		SS316	HGI databa	1	$511,000	2020	511000	strm.a200.	264116	kg/hr	0.7	2	375252.2	1.420786	$653,418
V	603	Decanter			13,750 gal 14' dia x 1:		SS	HGI databa	1	$103,000	2020	103000	strm.a500.	31815	kg/hr	0.7	2	1783.969	0.056073	$13,708
P	601	Transfer P			2152 GPM	125	316SS	HGI databa	1	$26,800	2020	26800	strm.501	488719	kg/hr	0.8	2.3	375252.2	0.767828	$21,694
P	602	Flash Tank	Viking		900 GPM,	75	316SS	HGI databa	1	$30,000	2020	30000	strm.a200.	204390	kg/hr	0.8	2.3	350171.5	1.713252	$46,151
P	603	Primary de	Megtec		10,000 gpr	200	316SS	Included w	1	INCLUDED	2020									
P	604	Secondary	Megtec		15 gpm	2	316SS	Included w	1	INCLUDED	2020									
P	605	Ethanol re	Megtec		150 gpm	15	316SS	Included w	1	INCLUDED	2020									
T	601	Primary dehydration column					316SS	Included w	1	INCLUDED	2020									
T	602	Secondary	Megtec		14' dia. x 76' tall, 32 t		316SS	Megtec Pr	1	$257,000	2020	257000	strm.a500.	30379	kg/hr	0.6	2.4	121815.5	4.009859	$591,304
T	603	Ethanol re	Megtec		14' dia. x 76' tall, 32 t		316SS	Megtec Pr	1	$3,407,000	2020	3407000	strm.a500.	30379	kg/hr	0.6	2.4	6735.3	0.221709	$1,379,883
T	604	Tertiary de	Megtec		4' dia, 6' high, 50 psig		316SS	Included w	1	INCLUDED	2020									
T	605	Furfural re	Megtec		4' dia, 6' high, 50 psig		316SS	Included w	1	INCLUDED	2020									
M	601	Waste Wa	UET Mixers		Side-mour	170 kW	316LSS	YES	1	$30,000	2020	30000	strm.a200.	252891	kg/hr	0.5	1.5	349440	1.381781	$35,265
E	601	Heatexcha	Mueller		29.9 MMBtu		304SS	HGI databa	1	$92,000	2020	92000	Heat.A200	7.5	Gcal/hr	0.7	2.2	16.11187	2.148249	$157,126
E	602	Heater	Mueller		29.9 MMBtu		304SS	HGI databa	1	$92,000	2020	92000	Heat.A200	7.5	Gcal/hr	0.7	2.2	13.40116	1.786822	$138,116
E	603	Waste Vap	Mueller		Copied H-201		304SS	HGI databa	1	$34,000	2020	34000	Heat.A200	-7.5	Gcal/hr	0.7	2.2	-189.743	25.29908	$326,326
E	604	Condenser	Megtec		S & T		316SS;CS	Included w	1	INCLUDED	2020									
																	By-products purification			$3,399,536
V	801	Filtrate Ta	UET Mixers		Side-mour	170 kW	316LSS	YES	1	$30,000	2020	30000	strm.a200.	252891	kg/hr	0.5	1.5	403607	1.595972	$130,122
V	802	Dryer Tank			13,750 gal 14' dia x 1:		SS	HGI databa	1	$103,000	2020	103000	strm.a500.	31815	kg/hr	0.7	2	47308.33	1.486982	$135,973
V	803	Filtrate Tank		0	13,750 gal 14' dia x 1:		SS	HGI databa	1	$103,000	2020	103000	STRM.A50	31815	kg/hr	0.7	2	21284.24	0.669	$77,738
C	801	Plant Air C	Rogers Ma	QNW752	400 SCFM	150 hp		HGI databa	1	$28,000	2020	28000	DRY101	83333	kg/hr	0.6	1.6	20000	0.240001	$11,893
M	801	In-line Mix	KOMAX		Kynar Lined - 600 gpn		SS304	Komax	1	$6,000	2020	6000	strm.a200.	136260	kg/hr	0.5	1	374289.5	2.746878	$9,944
M	802	In-line Mix	KOMAX		Kynar Lined - 600 gpn		SS305	Komax	1	$6,000	2020	6000	strm.a200.	136260	kg/hr	0.5	1	375283.3	2.75417	$9,957
P	801	Flash Tank	Viking		900 GPM,	75	316SS	HGI databa	1	$30,000	2020	30000	strm.a200.	204390	kg/hr	0.8	2.3	391597.9	1.915935	$50,469
P	802	Mixer Disc	Viking		900 GPM,	75	316SS	HGI databa	1	$30,000	2020	30000	strm.a200.	204390	kg/hr	0.8	2.3	374289.5	1.831252	$48,677
X	801	Pressure F	Larox	FFP 2512 - 384 sq. m fitration ar			SS316	from Larox	1	$312,997	2020	312996.5	strm.a500.	238612.5	kg/hr	0.8	1.7	391597.9	1.641146	$465,219
X	802	Pressure F	Larox	FFP 2512 - 384 sq. m fitration ar			SS316	from Larox	1	$3,294,700	2020	3294700	strm.a500.	31815	kg/hr	0.8	1.7	29882.85	0.939269	$3,133,632
T	801	Single-stag	Harrington Plastic		4000 gal.		HDPE	HGI databa	1	$1,520	2020	1520	strm.a500.	31815	kg/hr	0.7	3	40572.46	1.275262	$1,802
E	801	heater	Mueller		29.9 MMBtu		304SS	HGI databa	1	$92,000	2020	92000	Heat.A200	-7.5	Gcal/hr	0.7	2.2	-0.38717	0.051623	$11,555
E	802	Condenser	Mueller		Copied H-201		304SS	HGI databa	1	$34,000	2020	34000	Heat.A200	1.83	Gcal/hr	0.7	2.2	0.706242	0.385925	$17,459
																	Lignin extraction			$4,104,440

Reference

[1] Department for Business Energy and Industrial Strategy, UK ENERGY IN BRIEF 2021 in: E.a.I.S. Department for Business (Ed.) Digest of UK Energy Statistics, 2021.
[2] UNFCCC Authors, Glasgow Climate Pact, 2021.
[3] L. Pérez-Lombard, J. Ortiz, C.J.E. Pout, buildings, A review on buildings energy consumption information, Energy and buildings 40(3) (2008) 394-398.
[4] N. Scarlat, F. Fahl, E. Lugato, F. Monforti-Ferrario, J.J. Dallemand, Integrated and spatially explicit assessment of sustainable crop residues potential in Europe, Biomass bioenergy 122 (2019) 257-269.
[5] European Commission, Energy roadmap 2050, 2012. https://ec.europa.eu/energy/sites/ener/files/documents/2012_energy_roadmap_2050_en_0.pdf. (Accessed 18 December 2019).
[6] Centre For Renewable Energy Development, Renewable energy data book 2015, 2015.
[7] S.D. Ekşioğlu, A. Acharya, L.E. Leightley, S. Arora, Analyzing the design and management of biomass-to-biorefinery supply chain, Computers & Industrial Engineering 57(4) (2009) 1342-1352.
[8] M. Christopher, Logistics and Supply Chain Management: Strategies for Reducing Cost and Improving Service Financial Times: Pitman Publishing. London, 1998 ISBN 0 273 63049 0 (hardback) 294+ 1× pp, Taylor & Francis, 1999.
[9] N. Ishii, M. Ohba, A supply chain analysis and design method based on the value of information, Computer Aided Chemical Engineering, Elsevier2018, pp. 1591-1596.
[10] R.K. Oliver, M.D. Webber, Supply-chain management: logistics catches up with strategy, Outlook 5(1) (1982) 42-47.
[11] B. Sharma, R.G. Ingalls, C.L. Jones, A. Khanchi, Biomass supply chain design and analysis: Basis, overview, modeling, challenges, and future, Renewable and Sustainable Energy Reviews 24 (2013) 608-627.
[12] S. Gold, S. Seuring, Supply chain and logistics issues of bio-energy production, Journal of cleaner production 19(1) (2011) 32-42.
[13] A.A. Rentizelas, A.J. Tolis, I.P. Tatsiopoulos, Logistics issues of biomass: The storage problem and the multi-biomass supply chain, Renewable and sustainable energy reviews 13(4) (2009) 887-894.
[14] A.A. Rentizelas, A.I. Tolis, I.P. Tatsiopoulos, Combined Municipal Solid Waste and biomass system optimization for district energy applications, Waste Management 34(1) (2014) 36-48.
[15] J. Kim, M.J. Realff, J.H. Lee, Optimal design and global sensitivity analysis of biomass supply chain networks for biofuels under uncertainty, Computers & Chemical Engineering 35(9) (2011) 1738-1751.
[16] S.L.Y. Lo, B.S. How, W.D. Leong, S.Y. Teng, M.A. Rhamdhani, J. Sunarso, Techno-economic analysis for biomass supply chain: A state-of-the-art review, Renewable and Sustainable Energy Reviews 135 (2021) 110164.
[17] P. Fiedler, M. Lange, M. Schultze, Supply logistics for the industrialized use of biomass-principles and planning approach, 2007 International Symposium on Logistics and Industrial Informatics, IEEE, 2007, pp. 41-46.
[18] O. Sun, N. Fan, A review on optimization methods for biomass supply chain: models and algorithms, sustainable issues, and challenges and opportunities, Process Integration and Optimization for Sustainability (2020) 1-24.
[19] C.F.S. Gomes, H.G. Costa, G.G. de Souza, Abordagem estratégica para a seleção de sistemas erp utilizando apoio multicritério à decisão, Revista Produção Online 13(3) (2013) 1060-1088.
[20] S.H. Shuit, K.T. Tan, K.T. Lee, A. Kamaruddin, Oil palm biomass as a sustainable energy source: A Malaysian case study, Energy 34(9) (2009) 1225-1235.
[21] N.Z. Atashbar, N. Labadie, C. Prins, Modeling and optimization of biomass supply chains: A review and a critical look, IFAC-PapersOnLine 49(12) (2016) 604-615.

[22] E. Alakangas, C. Wiik, J. Rautbauer, L. Sulzbacher, G. Baumbach, D. Kilgus, D. Blumberga, J. Guscha, P. Grammelis, A. Malliopoulou, Classification of used wood in European solid biofuel standard: Fuel specification and classes (EN 14961-1), 18th European Biomass Conference and Exhibition, ETA-Florence Renewable Energies, 2010, pp. 1932-1939.
[23] E. Iakovou, A. Karagiannidis, D. Vlachos, A. Toka, A. Malamakis, Waste biomass-to-energy supply chain management: A critical synthesis, Waste management 30(10) (2010) 1860-1870.
[24] X. Zhu, X. Li, Q. Yao, Y. Chen, Challenges and models in supporting logistics system design for dedicated-biomass-based bioenergy industry, Bioresource technology 102(2) (2011) 1344-1351.
[25] S.M. Zahraee, N. Shiwakoti, P. Stasinopoulos, Biomass supply chain environmental and socio-economic analysis: 40-Years comprehensive review of methods, decision issues, sustainability challenges, and the way forward, Biomass and Bioenergy 142 (2020) 105777.
[26] A. Mirkouei, K.R. Haapala, J. Sessions, G.S. Murthy, A review and future directions in techno-economic modeling and optimization of upstream forest biomass to bio-oil supply chains, Renewable and Sustainable Energy Reviews 67 (2017) 15-35.
[27] A. Thorenz, L. Wietschel, D. Stindt, A. Tuma, Assessment of agroforestry residue potentials for the bioeconomy in the European Union, Journal of cleaner production 176 (2018) 348-359.
[28] D. Voivontas, D. Assimacopoulos, E. Koukios, Aessessment of biomass potential for power production: a GIS based method, Biomass and bioenergy 20(2) (2001) 101-112.
[29] B. Batidzirai, E. Smeets, A. Faaij, Harmonising bioenergy resource potentials—Methodological lessons from review of state of the art bioenergy potential assessments, Renewable and sustainable energy reviews 16(9) (2012) 6598-6630.
[30] A. Zyadin, K. Natarajan, P. Latva-Käyrä, B. Igliński, A. Iglińska, M. Trishkin, P. Pelkonen, A. Pappinen, Estimation of surplus biomass potential in southern and central Poland using GIS applications, Renewable and Sustainable Energy Reviews 89 (2018) 204-215.
[31] J. Singh, Overview of electric power potential of surplus agricultural biomass from economic, social, environmental and technical perspective—A case study of Punjab, Renewable and Sustainable Energy Reviews 42 (2015) 286-297.
[32] N.J. Glithero, P. Wilson, S.J. Ramsden, Straw use and availability for second generation biofuels in England, biomass and bioenergy. 55 (2013) 311-321.
[33] N. Scarlat, M. Martinov, J.-F. Dallemand, Assessment of the availability of agricultural crop residues in the European Union: potential and limitations for bioenergy use, Waste management 30(10) (2010) 1889-1897.
[34] D. McCartney, H. Block, P. Dubeski, A. Ohama, The composition and availability of straw and chaff from small grain cereals for beef cattle in western Canada, Canadian journal of animal science, 86(4) (2006) 443-455.
[35] T. Fischer, D. Byerlee, G. Edmeades, Crop yields and global food security: will yield increase continue to feed the world?, Australian Centre for International Agricultural Research (ACIAR)2014.
[36] E.M. Smeets, A.P. Faaij, I.M. Lewandowski, W.C. Turkenburg, A bottom-up assessment and review of global bio-energy potentials to 2050, Progress in Energy and combustion science 33(1) (2007) 56-106.
[37] N.S. Bentsen, C. Felby, B.J. Thorsen, Agricultural residue production and potentials for energy and materials services, Progress in energy and combustion science 40 (2014) 59-73.
[38] H. Liu, G. Jiang, H. Zhuang, K. Wang, Distribution, utilization structure and potential of biomass resources in rural China: with special references of crop residues, Renewable and sustainable energy reviews 12(5) (2008) 1402-1418.
[39] G.D.M. Dassanayake, A. Kumar, Techno-economic assessment of triticale straw for power generation, Applied energy 98 (2012) 236-245.
[40] C. Weiser, V. Zeller, F. Reinicke, B. Wagner, S. Majer, A. Vetter, D. Thraen, Integrated assessment of sustainable cereal straw potential and different straw-based energy applications in Germany, Applied energy 114 (2014) 749-762.

[41] F. Monforti, E. Lugato, V. Motola, K. Bodis, N. Scarlat, J.-F. Dallemand, Optimal energy use of agricultural crop residues preserving soil organic carbon stocks in Europe, Renewable and sustainable energy reviews 44 (2015) 519-529.
[42] M. Haase, C. Rösch, D. Ketzer, GIS-based assessment of sustainable crop residue potentials in European regions, Biomass Bioenergy 86 (2016) 156-171.
[43] B. Batidzirai, M. Valk, B. Wicke, M. Junginger, V. Daioglou, W. Euler, A. Faaij, Current and future technical, economic and environmental feasibility of maize and wheat residues supply for biomass energy application: Illustrated for South Africa, Biomass & Bioenergy 92 (2016) 106-129.
[44] A. Gojiya, D. Deb, K.K. Iyer, Feasibility study of power generation from agricultural residue in comparison with soil incorporation of residue, Renewable Energy 134 (2019) 416-425.
[45] J.K. Kurian, G.R. Nair, A. Hussain, G.V. Raghavan, Feedstocks, logistics and pre-treatment processes for sustainable lignocellulosic biorefineries: a comprehensive review, Renewable and Sustainable Energy Reviews 25 (2013) 205-219.
[46] K. Sahoo, S. Mani, L. Das, P.J.B. Bettinger, bioenergy, GIS-based assessment of sustainable crop residues for optimal siting of biogas plants, Biomass and bioenergy 110 (2018) 63-74.
[47] R. Lal, World crop residues production and implications of its use as a biofuel, Environment International 31(4) (2005) 575-584.
[48] R. Allmaras, R. Dowdy, Conservation tillage systems and their adoption in the United States, Soil Tillage Research 5(2) (1985) 197-222.
[49] S.J.W.p.S.Q.N.T.D.T.U.-N.R.C.S. Andrews, Crop residue removal for energy production: effects on soils and recommendations, (2006) 15.
[50] K.E. Giller, E. Witter, M. Corbeels, P. Tittonell, Conservation agriculture and smallholder farming in Africa: the heretics’ view, Field crops research 114(1) (2009) 23-34.
[51] Z. Liang, S. Chen, Y. Yang, R. Zhao, Z. Shi, R.V. Rossel, National digital soil map of organic matter in topsoil and its associated uncertainty in 1980's China, Geoderma 335 (2019) 47-56.
[52] T. Morato, M. Vaezi, A. Kumar, Assessment of energy production potential from agricultural residues in Bolivia, Renewable and Sustainable Energy Reviews 102 (2019) 14-23.
[53] C.E. Noon, M.J. Daly, GIS-based biomass resource assessment with BRAVO, Biomass Bioenergy Research 10(2-3) (1996) 101-109.
[54] H. Woo, M. Acuna, M. Moroni, M. Taskhiri, P. Turner, Optimizing the location of biomass energy facilities by integrating Multi-Criteria Analysis (MCA) and Geographical Information Systems (GIS), Forests 9(10) (2018) 585.
[55] S. Kim, S. Kim, J.R. Kiniry, Two-phase simulation-based location-allocation optimization of biomass storage distribution, Simulation Modelling Practice and Theory 86 (2018) 155-168.
[56] P. Moodley, C. Trois, Lignocellulosic biorefineries: the path forward, Sustainable Biofuels, Elsevier2021, pp. 21-42.
[57] K. Srirangan, L. Akawi, M. Moo-Young, C.P. Chou, Towards sustainable production of clean energy carriers from biomass resources, Applied energy 100 (2012) 172-186.
[58] C. Veluchamy, A. Kalamdhad, B. Gilroyed, Advanced pretreatment strategies for bioenergy production from biomass and biowaste, Handbook of environmental materials management (2018) 1-19.
[59] F. Abnisa, W.W. Daud, W. Husin, J. Sahu, Utilization possibilities of palm shell as a source of biomass energy in Malaysia by producing bio-oil in pyrolysis process, Biomass and Bioenergy 35(5) (2011) 1863-1872.
[60] M.R. Zakaria, S. Fujimoto, S. Hirata, M.A. Hassan, Ball milling pretreatment of oil palm biomass for enhancing enzymatic hydrolysis, Applied biochemistry and biotechnology 173(7) (2014) 1778-1789.
[61] S. Rezania, B. Oryani, J. Cho, A. Talaiekhozani, F. Sabbagh, B. Hashemi, P.F. Rupani, A.A. Mohammadi, Different pretreatment technologies of lignocellulosic biomass for bioethanol production: An overview, Energy 199 (2020) 117457.

[62] C. Martín, A. García, A. Schreiber, J. Puls, B. Saake, Combination of water extraction with dilute-sulphuric acid pretreatment for enhancing the enzymatic hydrolysis of Jatropha curcas shells, Industrial Crops and Products 64 (2015) 233-241.
[63] C.C. Santos, W. de Souza, C. Sant'Anna, M. Brienzo, Elephant grass leaves have lower recalcitrance to acid pretreatment than stems, with higher potential for ethanol production, Industrial Crops and Products 111 (2018) 193-200.
[64] S. Mirmohamadsadeghi, Z. Chen, C. Wan, Reducing biomass recalcitrance via mild sodium carbonate pretreatment, Bioresource technology 209 (2016) 386-390.
[65] N. Uppugundla, L. da Costa Sousa, S.P. Chundawat, X. Yu, B. Simmons, S. Singh, X. Gao, R. Kumar, C.E. Wyman, B.E. Dale, A comparative study of ethanol production using dilute acid, ionic liquid and AFEX™ pretreated corn stover, Biotechnology for biofuels 7(1) (2014) 1-14.
[66] C. Zhao, W. Ding, F. Chen, C. Cheng, Q. Shao, Effects of compositional changes of AFEX-treated and H-AFEX-treated corn stover on enzymatic digestibility, Bioresource technology 155 (2014) 34-40.
[67] P.C. Bergman, J.H. Kiel, Torrefaction for biomass upgrading, Proc. 14th European Biomass Conference, Paris, France, sn, 2005, pp. 17-21.
[68] A. Molino, S. Chianese, D. Musmarra, Biomass gasification technology: The state of the art overview, Journal of Energy Chemistry 25(1) (2016) 10-25.
[69] J. Shankar Tumuluru, S. Sokhansanj, J.R. Hess, C.T. Wright, R.D. Boardman, A review on biomass torrefaction process and product properties for energy applications, Industrial Biotechnology 7(5) (2011) 384-401.
[70] R.D. Wankhade, Biomass Gasification Technologies for Sustainability of Future Energy Demand, Renewable Energy and Green Technology: Principles and Practices (2021) 105.
[71] A. Uslu, A.P. Faaij, P.C. Bergman, Pre-treatment technologies, and their effect on international bioenergy supply chain logistics. Techno-economic evaluation of torrefaction, fast pyrolysis and pelletisation, Energy 33(8) (2008) 1206-1223.
[72] G. Maschio, C. Koufopanos, A. Lucchesi, Pyrolysis, a promising route for biomass utilization, Bioresource Technology;(United Kingdom) 42(3) (1992).
[73] R. Marsh, S. Hewlett, A.J. Griffiths, K.P. Williams, Advanced thermal treatment for solid waste-A waste manager's guide, (2007).
[74] A. Demirbaş, Biomass resource facilities and biomass conversion processing for fuels and chemicals, Energy conversion and Management 42(11) (2001) 1357-1378.
[75] A.V. Bridgwater, G. Evans, An assessment of thermochemical conversion systems for processing biomass and refuse, (1993).
[76] P.C. Badger, P. Fransham, Use of mobile fast pyrolysis plants to densify biomass and reduce biomass handling costs—A preliminary assessment, Biomass and bioenergy 30(4) (2006) 321-325.
[77] K.S. Ng, J. Sadhukhan, Process integration and economic analysis of bio-oil platform for the production of methanol and combined heat and power, Biomass and Bioenergy 35(3) (2011) 1153-1169.
[78] D. Abbas, R. Handler, B. Hartsough, D. Dykstra, P. Lautala, L. Hembroff, A survey analysis of forest harvesting and transportation operations in Michigan, Croatian Journal of Forest Engineering: Journal for Theory and Application of Forestry Engineering 35(2) (2014) 179-192.
[79] F. Mafakheri, F. Nasiri, Modeling of biomass-to-energy supply chain operations: Applications, challenges and research directions, Energy policy 67 (2014) 116-126.
[80] M.J. Bussemaker, K. Day, G. Drage, F. Cecelja, Supply chain optimisation for an ultrasound-organosolv lignocellulosic biorefinery: impact of technology choices, Waste and biomass valorization 8(7) (2017) 2247-2261.
[81] P.T. Lautala, M.R. Hilliard, E. Webb, I. Busch, J.R. Hess, M.S. Roni, J. Hilbert, R.M. Handler, R. Bittencourt, A. Valente, Opportunities and challenges in the design and analysis of biomass supply chains, Environmental management 56(6) (2015) 1397-1415.

[82] M.D. Berry, J. Sessions, R. Zamora-Cristales, Subregional comparison for forest-to-product biomass supply chains on the Pacific West Coast, USA, Applied Engineering in Agriculture 34(1) (2018) 157.
[83] y. Zhuang, y. Zhang, y. Tian, g. Wang, Research on the Application Mode of Industrialized Collection of Agricultural and Forestry Biomass in China, China engineering sciences 13(2) (2011) 101-106.
[84] B.S. How, S.L. Ngan, B.H. Hong, H.L. Lam, W.P.Q. Ng, S. Yusup, W.A.W.A.K. Ghani, Y. Kansha, Y.H. Chan, K.W. Cheah, An outlook of Malaysian biomass industry commercialisation: Perspectives and challenges, Renewable and Sustainable Energy Reviews 113 (2019) 109277.
[85] S.M. Zahraee, S.R. Golroudbary, N. Shiwakoti, P. Stasinopoulos, A. Kraslawski, Transportation system analysis of empty fruit bunches biomass supply chain based on delivery cost and greenhouse gas emissions, Procedia Manufacturing 51 (2020) 1717-1722.
[86] P.L. Eranki, B.D. Bals, B.E. Dale, Advanced regional biomass processing depots: a key to the logistical challenges of the cellulosic biofuel industry, Biofuels, Bioproducts and Biorefining 5(6) (2011) 621-630.
[87] L. Nunes, T. Causer, D. Ciolkosz, Biomass for energy: A review on supply chain management models, Renewable and Sustainable Energy Reviews 120 (2020) 109658.
[88] J.M.P. Cardoso, J.G. de Figueired Coutinho, P.C. Diniz, Embedded computing for high performance: Efficient mapping of computations using customization, code transformations and compilation, Morgan Kaufmann2017.
[89] A. Waldock, D. Corne, Multiple objective optimisation applied to route planning, Proceedings of the 13th annual conference on Genetic and evolutionary computation, 2011, pp. 1827-1834.
[90] J. Gorski, Multiple objective optimization and implications for single objective optimization, Universität Wuppertal, Fakultät für Mathematik und Naturwissenschaften ..., 2018.
[91] J. Kim, M.J. Realff, J.H.J.C. Lee, C. Engineering, Optimal design and global sensitivity analysis of biomass supply chain networks for biofuels under uncertainty, 35(9) (2011) 1738-1751.
[92] M.S. Roni, S.D. Eksioglu, K.G. Cafferty, J.J. Jacobson, A multi-objective, hub-and-spoke model to design and manage biofuel supply chains, Annals of Operations Research 249(1-2) (2017) 351-380.
[93] K.T. Malladi, O. Quirion-Blais, T. Sowlati, Development of a decision support tool for optimizing the short-term logistics of forest-based biomass, Applied Energy 216 (2018) 662-677.
[94] H. Chen, L. Amodeo, F. Chu, K. Labadi, Modeling and performance evaluation of supply chains using batch deterministic and stochastic Petri nets, IEEE Transactions on Automation Science and Engineering 2(2) (2005) 132-144.
[95] B. Bilgen, I. Ozkarahan, Strategic tactical and operational production-distribution models: a review, International Journal of Technology Management 28(2) (2004) 151-171.
[96] H. Ghaderi, M.S. Pishvaee, A. Moini, Biomass supply chain network design: an optimization-oriented review and analysis, Industrial crops and products 94 (2016) 972-1000.
[97] J. Ren, L. Dong, L. Sun, M.E. Goodsite, S. Tan, L. Dong, Life cycle cost optimization of biofuel supply chains under uncertainties based on interval linear programming, Bioresource technology 187 (2015) 6-13.
[98] I. Awudu, J. Zhang, Uncertainties and sustainability concepts in biofuel supply chain management: A review, Renewable and Sustainable Energy Reviews 16(2) (2012) 1359-1368.
[99] N.T. Albashabsheh, J.L.H. Stamm, Optimization of lignocellulosic biomass-to-biofuel supply chains with densification: Literature review, Biomass and Bioenergy 144 (2021) 105888.
[100] B. Theozzo, M.T. dos Santos, A MILP framework for optimal biorefinery design that accounts for forest biomass dynamics, Computers & Chemical Engineering 146 (2021) 107201.
[101] X. Guo, J. Voogt, B. Annevelink, J. Snels, A. Kanellopoulos, Optimizing resource utilization in biomass supply chains by creating integrated biomass logistics centers, Energies 13(22) (2020) 6153.

[102] L. Moretti, M. Milani, G.G. Lozza, G. Manzolini, A detailed MILP formulation for the optimal design of advanced biofuel supply chains, Renewable Energy 171 (2021) 159-175.
[103] H. Gunnarsson, M. Rönnqvist, J.T. Lundgren, Supply chain modelling of forest fuel, European journal of Operational research 158(1) (2004) 103-123.
[104] S.R. Poudel, M. Marufuzzaman, L. Bian, Designing a reliable bio-fuel supply chain network considering link failure probabilities, Computers & Industrial Engineering 91 (2016) 85-99.
[105] E. León-Olivares, H. Minor-Popocatl, O. Aguilar-Mejía, D. Sánchez-Partida, Optimization of the supply chain in the production of ethanol from agricultural biomass using mixed-integer linear programming (MILP): a case study, Mathematical Problems in Engineering 2020 (2020).
[106] M. Budzinski, M. Sisca, D. Thrän, Consequential LCA and LCC using linear programming: an illustrative example of biorefineries, The International Journal of Life Cycle Assessment 24(12) (2019) 2191-2205.
[107] Z. Liu, T. Qiu, B. Chen, A study of the LCA based biofuel supply chain multi-objective optimization model with multi-conversion paths in China, Applied Energy 126 (2014) 221-234.
[108] Y. Bai, X. Li, F. Peng, X. Wang, Y. Ouyang, Effects of disruption risks on biorefinery location design, Energies 8(2) (2015) 1468-1486.
[109] Z. Vazifeh, F. Mafakheri, C. An, Biomass supply chain coordination for remote communities: A game-theoretic modeling and analysis approach, Sustainable Cities and Society 69 (2021) 102819.
[110] J. Gong, F. You, Global optimization for sustainable design and synthesis of algae processing network for CO2 mitigation and biofuel production using life cycle optimization, AIChE Journal 60(9) (2014) 3195-3210.
[111] A. Singh, Y. Chu, F. You, Biorefinery supply chain network design under competitive feedstock markets: an agent-based simulation and optimization approach, Industrial & Engineering Chemistry Research 53(39) (2014) 15111-15126.
[112] N. Ayoub, R. Martins, K. Wang, H. Seki, Y. Naka, Two levels decision system for efficient planning and implementation of bioenergy production, Energy conversion and management 48(3) (2007) 709-723.
[113] H. Min, G. Zhou, Supply chain modeling: past, present and future, Computers & industrial engineering 43(1-2) (2002) 231-249.
[114] F. Latterini, W. Stefanoni, A. Suardi, V. Alfano, S. Bergonzoli, N. Palmieri, L. Pari, A GIS approach to locate a small size biomass plant powered by olive pruning and to estimate supply chain costs, Energies 13(13) (2020) 3385.
[115] F. Zhang, J. Wang, S. Liu, S. Zhang, J.W. Sutherland, Integrating GIS with optimization method for a biofuel feedstock supply chain, Biomass and bioenergy 98 (2017) 194-205.
[116] H. Jeong, H.L. Sieverding, J.J. Stone, Biodiesel supply chain optimization modeled with geographical information system (GIS) and Mixed-Integer Linear Programming (MILP) for the northern great plains region, Bioenergy Research 12(1) (2019) 229-240.
[117] J. Kim, M.J. Realff, J.H. Lee, C. Whittaker, L. Furtner, Design of biomass processing network for biofuel production using an MILP model, Biomass and bioenergy 35(2) (2011) 853-871.
[118] D.K. Brownell, J. Liu, Computer Model of Satellite Storage Locations for Herbaceous Biomass Handling, 2010 Pittsburgh, Pennsylvania, June 20-June 23, 2010, American Society of Agricultural and Biological Engineers, 2010, p. 1.
[119] M.S. Roni, D.N. Thompson, D.S. Hartley, Distributed biomass supply chain cost optimization to evaluate multiple feedstocks for a biorefinery, Applied Energy 254 (2019) 113660.
[120] S.F. Salleh, M.F. Gunawan, M.F.B. Zulkarnain, A. Halim, Modelling and optimization of biomass supply chain for bioenergy production, Journal of Environmental Treatment Techniques 7(4) (2019) 689-695.
[121] World Bioenergy Association, WBA global bioenergy statistics 2017, World Bioenergy Association: Stockholm, Sweden (2017).

[122] M. Aghbashlo, Z. Khounani, H. Hosseinzadeh-Bandbafha, V.K. Gupta, H. Amiri, S.S. Lam, T. Morosuk, M. Tabatabaei, Exergoenvironmental analysis of bioenergy systems: A comprehensive review, Renewable and Sustainable Energy Reviews 149 (2021) 111399.
[123] A.A. Rentizelas, J. Li, Techno-economic and carbon emissions analysis of biomass torrefaction downstream in international bioenergy supply chains for co-firing, Energy 114 (2016) 129-142.
[124] A. Mana, A. Allouhi, K. Ouazzani, A. Jamil, Feasibility of agriculture biomass power generation in Morocco: Techno-economic analysis, Journal of Cleaner Production 295 (2021) 126293.
[125] H. Ritchie, M. Roser, CO2 emissions, 2020. https://ourworldindata.org/co2-emissions. (Accessed 17-08 2021).
[126] S.H.M. Azhar, R. Abdulla, S.A. Jambo, H. Marbawi, J.A. Gansau, A.A.M. Faik, K.F. Rodrigues, Yeasts in sustainable bioethanol production: A review, Biochemistry and Biophysics Reports 10 (2017) 52-61.
[127] OECD-FAO Agricultural, OECD-FAO Agricultural Outlook 2010, 2010, p. 17.
[128] Renewable Fuel Association, ESSENTIAL ENERGY 2021 ethanol industry outlook, 2021.
[129] J. López-Linares, C. Cara, M. Moya, E. Ruiz, E. Castro, I. Romero, Fermentable sugar production from rapeseed straw by dilute phosphoric acid pretreatment, Industrial Crops and Products 50 (2013) 525-531.
[130] V.M. Nascimento, A. Manrich, P.W. Tardioli, R. de Campos Giordano, G.J. de Moraes Rocha, R.d.L.C. Giordano, Alkaline pretreatment for practicable production of ethanol and xylooligosaccharides, Bioethanol 1(open-issue) (2016).
[131] S. Nakanishi, V. Nascimento, S. Rabelo, I. Sampaio, T. Junqueira, G. Rocha, Comparative material balances and preliminary technical analysis of the pilot scale sugarcane bagasse alkaline pretreatment to 2G ethanol production, Industrial Crops and Products 120 (2018) 187-197.
[132] R. Bibi, Z. Ahmad, M. Imran, S. Hussain, A. Ditta, S. Mahmood, A. Khalid, Algal bioethanol production technology: a trend towards sustainable development, Renewable and Sustainable Energy Reviews 71 (2017) 976-985.
[133] D. Humbird, R. Davis, L. Tao, C. Kinchin, D. Hsu, A. Aden, P. Schoen, J. Lukas, B. Olthof, M. Worley, Process design and economics for biochemical conversion of lignocellulosic biomass to ethanol: dilute-acid pretreatment and enzymatic hydrolysis of corn stover, National Renewable Energy Lab.(NREL), Golden, CO (United States), 2011.
[134] D. Bbosa, M. Mba-Wright, R.C. Brown, More than ethanol: a techno-economic analysis of a corn stover-ethanol biorefinery integrated with a hydrothermal liquefaction process to convert lignin into biochemicals, Biofuels, Bioproducts and Biorefining 12(3) (2018) 497-509.
[135] D. Carrillo-Nieves, S. Saldarriaga-Hernandez, G. Gutiérrez-Soto, M. Rostro-Alanis, C. Hernández-Luna, A.J. Alvarez, H.M. Iqbal, R. Parra-Saldívar, Biotransformation of agro-industrial waste to produce lignocellulolytic enzymes and bioethanol with a zero waste, Biomass Conversion and Biorefinery (2020) 1-12.
[136] Ministry of ecology and environment, technical guideline for delineating source water protection areas, 2007.
[137] Seventh National People's Congress, Law of the Peoples Republic of China on Water and Soil Conservation, 2010.
[138] W.C.M. R.I. Papendick, Crop Management to Reduce Soil Erosion and Improve Soil Quality, USDA-Agricultural Research Service, Northwest. Sprinfield (VA), 1995.
[139] USDA NRCS Soil Quality Institute, Managing soil organic matter: The key to air and water quality., 2003.
[140] D. Simon, W.E. Tyner, F. Jacquet, Economic analysis of the potential of cellulosic biomass available in France from agricultural residue and energy crops, Bioenergy Research 3(2) (2010) 183-193.
[141] M. Valk, Availability and cost of agricultural residues for bioenergy generation; International literature review and a case study for South Africa, 2014.

[142] S. Liu, The Rule of Temporal and Spatial Distribution of Soil Organic Carbon of Cropland and Its Influencing Factors in China Jilin agriculture university 2016.
[143] S.A. El-Sayed, M. Khairy, Effect of heating rate on the chemical kinetics of different biomass pyrolysis materials, Biofuels 6(3-4) (2015) 157-170.
[144] H. Belyadi, E. Fathi, F. Belyadi, Hydraulic fracturing in unconventional reservoirs: theories, operations, and economic analysis, Gulf Professional Publishing2019.
[145] J. Zhang, J. Li, C. Dong, X. Zhang, A. Rentizelas, D. Shen, Comprehensive assessment of sustainable potential of agricultural residues for bioenergy based on geographical information system: A case study of China, Renewable Energy 173 (2021) 466-478.
[146] A.K. Mathew, A. Abraham, K.K. Mallapureddy, R.K. Sukumaran, Lignocellulosic biorefinery wastes, or resources?, Waste Biorefinery, Elsevier2018, pp. 267-297.
[147] K.T. Tan, K.T. Lee, A.R. Mohamed, Role of energy policy in renewable energy accomplishment: the case of second-generation bioethanol, Energy policy 36(9) (2008) 3360-3365.
[148] The National Center for Biotechnology Information, COMPOUND SUMMARY Furfural, 2021.
[149] The National Center for Biotechnology Information, COMPOUND SUMMARY Ethanol, 2021.
[150] The National Center for Biotechnology Information, COMPOUND SUMMARY Water, 2021.
[151] National Bureau of Statistics of China, Annual crop production in China, 2015. http://data.stats.gov.cn/easyquery.htm?cn=C01. (Accessed 18 Jun 2019).
[152] Ministry of Agriculture and Rural Affairs of the People's Republic of China, Notice of the General Office of the Ministry of Agriculture and Rural Affairs on Construction of the Stalks of Crop Straw Resources plantform, 2019. http://www.moa.cn/nybgb/2019/201902/201905/t20190518_6309472.htm. (Accessed 18 September 2019).
[153] L.S. Liu Xiaoyong, Temporal and spatial distribution characteristcs of crop straw nutrient resources and returning to farmland in China, Transactions of the Chinese Society of Agricultural Engineering 33(21) (2017) 1-19.
[154] S. Xue, I. Lewandowski, X. Wang, Z. Yi, Assessment of the production potentials of Miscanthus on marginal land in China, Renewable and Sustainable Energy Reviews 54 (2016) 932-943.
[155] Han Lujia; Yan Qiaojuan; Liu Xiaoyang, China's crop straw resources and its utilization status, Transactions of the Chinese Society of Agricultural Engineering 18(3) (2002) 87-91.
[156] J. Gao, A. Zhang, S.K. Lam, X. Zhang, A.M. Thomson, E. Lin, K. Jiang, L.E. Clarke, J.A. Edmonds, P.G. Kyle, An integrated assessment of the potential of agricultural and forestry residues for energy production in C hina, Gcb Bioenergy 8(5) (2016) 880-893.
[157] D. Jiang, D. Zhuang, J. Fu, Y. Huang, K. Wen, Bioenergy potential from crop residues in China: Availability and distribution, Renewable and sustainable energy reviews 16(3) (2012) 1377-1382.
[158] Resource and environment data cloud platform, Remote sensing monitoring data of China's land use status in 2015, 2015. http://www.resdc.cn/data.aspx?DATAID=184. (Accessed 16 Jun 2019).
[159] Resource and environment data cloud platform, 2015 China Provincial Administrative Boundary Data, 2015. http://www.resdc.cn/data.aspx?DATAID=200. (Accessed 16 Jun 2019).
[160] Resource and environment data cloud platform, Spatial distribution data of landform types in China (1:1 million), 2009. http://www.resdc.cn/data.aspx?DATAID=124. (Accessed 17 Jun 2019).
[161] Resource and environment data cloud platform, The spatial distribution data of soil erosion in China, 2010. http://www.resdc.cn/data.aspx?DATAID=259. (Accessed 17 Jun 2019).
[162] Food and Agriculture Organization of the United Nations, annual crop production in China, 2019. http://www.fao.org/faostat/en/#data/QC. (Accessed 18 Jun 2019).
[163] National Bureau of Statistics of China, The size of arable land size, 2015. http://data.stats.gov.cn/easyquery.htm?cn=C01. (Accessed 18 May 2019).
[164] Food and Agriculture Organization, Crop annual production in China, 2019. http://www.fao.org/faostat/en/#data/QC. (Accessed 18 Jun 2019).

[165] S. Visa, B. Ramsay, A.L. Ralescu, E. Van Der Knaap, Confusion Matrix-based Feature Selection, MAICS 710 (2011) 120-127.
[166] X. Deng, Q. Liu, Y. Deng, S. Mahadevan, An improved method to construct basic probability assignment based on the confusion matrix for classification problem, Information Sciences 340 (2016) 250-261.
[167] G.M. Foody, Status of land cover classification accuracy assessment, Remote sensing of environment 80(1) (2002) 185-201.
[168] J. Cohen, A coefficient of agreement for nominal scales, Educational Psychological measurement 20(1) (1960) 37-46.
[169] J.R. Landis, G.G. Koch, The measurement of observer agreement for categorical data, Biometrics (1977) 159-174.
[170] National Bureau of Statistics of China, Crop yield from 2010 to 2017, 2017. http://data.stats.gov.cn/search.htm?s=%E7%B2%AE%E9%A3%9F%E4%BA%A7%E9%87%8F%202014%E5%B9%B4. (Accessed 10 September 2019).
[171] J.K. Sjaak Van Loo, The Handbook of Biomass Combustion and Co-firing., Routledge London 2012.
[172] P.B. Prabir Basu, Biomass Gasification and Pyrolysis, Academic Press 2010.
[173] P. Breeze, Combined Heat and Power, Academic Press2018.
[174] China National Renewable Energy Centre, China Renewable Energy Technology Catalogue, 2014.
[175] C. Wang, D. Li, F. Wang, Q. Yang, Experimental study on the combustion characteristics of biomass pellets, Transactions of the Chinese Society of Agricultural Engineering 22(10) (2006) 174-177.
[176] Z. Yao, L. Zhao, M. Ronnback, H. Meng, J. Luo, Y. Tian, Comparison on characterization effect of biomass pellet fuels on combustion behavior, Transactions of the Chinese Society for Agricultural Machinery 41(10) (2010) 97-102.
[177] C. Wang, J. Pan, J. Li, Z. Yang, Comparative studies of products produced from four different biomass samples via deoxy-liquefaction, Bioresource technology 99(8) (2008) 2778-2786.
[178] L. Deng, J. Ye, X. Jin, D. Che, Transformation and release of potassium during fixed-bed pyrolysis of biomass, Journal of the Energy Institute 91(4) (2018) 630-637.
[179] L. Cuiping, W. Chuangzhi, H. Haitao, Chemical elemental characteristics of biomass fuels in China, Biomass and bioenergy 27(2) (2004) 119-130.
[180] H.-b. Zhao, Q. Song, X.-y. Wu, Q. Yao, Study on the transformation of inherent potassium during the fast-pyrolysis process of rice straw, Energy & Fuels 29(10) (2015) 6404-6411.
[181] R.-d. LI, B.-s. LI, T.-h. YANG, Y.-h. XIE, Liquefaction of rice stalk in sub-and supercritical ethanol, Journal of Fuel Chemistry and Technology 41(12) (2013) 1459-1465.
[182] J. Shen, S. Zhu, X. Liu, H. Zhang, J. Tan, The prediction of elemental composition of biomass based on proximate analysis, Energy Conversion and Management 51(5) (2010) 983-987.
[183] X. Li, F. Qu, D. Jiang, P. Zhu, Integrated benefits of power generation by straw biomass—A case study on the Sheyang Straw Power Plants in Jiangsu Province, China, Frontiers of Environmental Science & Engineering in China 3(3) (2009) 348-353.
[184] R. Yin, R. Liu, Y. Mei, W. Fei, X. Sun, Characterization of bio-oil and bio-char obtained from sweet sorghum bagasse fast pyrolysis with fractional condensers, Fuel 112 (2013) 96-104.
[185] H.-L. Yan, Z.-M. Zong, Z.-K. Li, J. Kong, Q.-X. Zheng, Y. Li, X.-Y. Wei, Sweet sorghum stalk liquefaction in supercritical methanol: effects of operating conditions on product yields and molecular composition of soluble fraction, Fuel Processing Technology 155 (2017) 42-50.
[186] L. Wei, S. Xu, L. Zhang, H. Zhang, C. Liu, H. Zhu, S. Liu, Characteristics of fast pyrolysis of biomass in a free fall reactor, Fuel Processing Technology 87(10) (2006) 863-871.
[187] A. Callejón-Ferre, B. Velázquez-Martí, J. López-Martínez, F. Manzano-Agugliaro, Greenhouse crop residues: energy potential and models for the prediction of their higher heating value, Renewable and sustainable energy reviews 15(2) (2011) 948-955.

[188] M. Wu, Q. Guo, G. Fu, Preparation and characteristics of medicinal activated carbon powders by CO2 activation of peanut shells, Powder technology 247 (2013) 188-196.
[189] X. Wang, H. Chen, H. Yang, J. Wang, F. Xin, The influence of alkali and alkaline earth metal compounds on pyrolysis of peanut shell, Asia‐Pacific Journal of Chemical Engineering 7(3) (2012) 463-468.
[190] Ministry of Agriculture press office, The comprehensive utilization rate of main crop stalks in China exceeds 80%. 2016. http://jiuban.moa.gov.cn/zwllm/zwdt/201605/t20160526_5151375.htm. (Accessed 18 September 2019).
[191] China Power News Network, National Bureau of Statistics: Power generation increased by 6.8% in 2018, 2019. http://www.cpnn.com.cn/zdyw/201901/t20190121_1118811.html. (Accessed 18 Jun 2019).
[192] E.M. Gucho, K. Shahzad, E.A. Bramer, N.A. Akhtar, G. Brem, Experimental study on dry torrefaction of beech wood and miscanthus, Energies 8(5) (2015) 3903-3923.
[193] Ministry of Agriculture press office,

The comprehensive utilization rate of main crop stalks in China exceeds 80%, 2016. http://jiuban.moa.gov.cn/zwllm/zwdt/201605/t20160526_5151375.htm. (Accessed 03-17 2018).
[194] L. FOSHAN DRAGON CHEM CO., 2021 China Supply High Quality Industry Calcium Lignosulphonate /Pure Lignin Price, 2021. https://www.alibaba.com/product-detail/-pure-Lignin-Price-Lignin-2021_1600186023460.html?spm=a2700.7724857.normal_offer.d_title.3d214b29YpXxCr&s=p. (Accessed 04-04 2021).
[195] L. Binzhou Chengli Building Materials Co., sodium naphthalene sulfonate/lignin/ammonium lignosulphonate for russia market, 2021. https://www.alibaba.com/product-detail/Sodium-Naphthalene-Sulfonate-lignin-ammonium-Lignosulphonate_60339087096.html?spm=a2700.7724857.normal_offer.d_title.77885cefXLJ0f3&s=p. (Accessed 04-04 2021).
[196] Ricca Chemical, Ethanol 50% (v/v) analytical reagent, 2021. https://us.vwr.com/store/product/4544538/ethanol-50-v-v-analytical-reagent. (Accessed 04-04 2021).
[197] Fisher Scientific, Aqua Solutions ETHANOL/WATER 50% 4LTR, 2021. https://www.fishersci.com/shop/products/ethanol-water-50-4ltr/NC9234243. (Accessed 04-04 2021).
[198] U.S. Department of Energy Office of Scientific and Technical Information, Oxygenated commodity chemicals from chemo-catalytic conversion of biomass derived heterocycles, 2018.
[199] Businessinsider, Ethanol PRICE Today, 2021. https://markets.businessinsider.com/commodities/ethanol-price. (Accessed 02-04 2021).
[200] L.R. Lynd, X. Liang, M.J. Biddy, A. Allee, H. Cai, T. Foust, M.E. Himmel, M.S. Laser, M. Wang, C.E. Wyman, Cellulosic ethanol: status and innovation, Current opinion in biotechnology 45 (2017) 202-211.
[201] Energy Information Administration, How much carbon dioxide is produced per kilowatthour of U.S. electricity generation?, in: E.I. Administration (Ed.) 2020.
[202] European Environment Agency, CO2 emission intensity, 2020.
[203] Y. Cortes-Peña, D. Kumar, V. Singh, J.S. Guest, BioSTEAM: A fast and flexible platform for the design, simulation, and techno-economic analysis of biorefineries under uncertainty, ACS Sustainable Chemistry & Engineering 8(8) (2020) 3302-3310.
[204] A. Rentizelas, I.C. Melo, P.N.A. Junior, J.S. Campoli, D.A. do Nascimento Rebelatto, Multi-criteria efficiency assessment of international biomass supply chain pathways using Data Envelopment Analysis, Journal of Cleaner Production 237 (2019) 117690.

[205] Energy Information Administration (EIA), What is the efficiency of different types of power plants?, in: T.U.S.E.I. Administration (Ed.) 2020.
[206] Z. Liu, Research on Potential Assessment And Industry Development of Biomass Power Generation in China, Chinese Academy of Agricultural Sciences (2015).
[207] M.K. Delivand, M. Barz, S.H. Gheewala, Logistics cost analysis of rice straw for biomass power generation in Thailand, Energy 36(3) (2011) 1435-1441.
[208] C. Ma, P. Zhu, Straw has a new utility, People, 2018.
[209] Alibaba, Biomass compresser price 2020. https://detail.1688.com/offer/560187430249.html?spm=a261b.2187593.1998088710.31.1fd871b2wDkKSI.
[210] Q. Zhang, D. Zhou, P. Zhou, H. Ding, Cost analysis of straw-based power generation in Jiangsu Province, China, Applied Energy 102 (2013) 785-793.
[211] China Longyuan power group corporation limited, Year report 2017, (2018).
[212] ceicdata, Oil Price after Adjustment: NDRC: Maximum Retail Price: Diesel: Heilongjiang, 2019.
[213] Mingyang city council, Mudanjiang Chenneng Biomass Power Generation Co., Ltd. Biomass Cogeneration Project in Yangming District, Mudanjiang City, 2019.
[214] B. Batidzirai, F. van der Hilst, H. Meerman, M.H. Junginger, A.P. Faaij, Optimization potential of biomass supply chains with torrefaction technology, Biofuels, Bioproducts and Biorefining 8(2) (2014) 253-282.
[215] Y. Yu, J. Bartle, C.-Z. Li, H. Wu, Mallee biomass as a key bioenergy source in Western Australia: importance of biomass supply chain, Energy & Fuels 23(6) (2009) 3290-3299.
[216] Economic Information DailyEconomic Information Daily, logistic issue in Upper Yangtze River Region, Economic Information Daily, 2018.
[217] F. Zhang, D. Johnson, M. Johnson, D. Watkins, R. Froese, J. Wang, Decision support system integrating GIS with simulation and optimisation for a biofuel supply chain, Renewable Energy 85 (2016) 740-748.
[218] y. Wang, Biomass power generation supply chain under the game situation

Cooperation model research, School of Economics and Management, Nanjing University of Aeronautics and Astronautics, 2011.
[219] M. Phanphanich, S. Mani, Impact of torrefaction on the grindability and fuel characteristics of forest biomass, Bioresource technology 102(2) (2011) 1246-1253.
[220] National grid, Energy interview minutes, 2019.
[221] tianqi.com, China's central heating start and end time, 2019. https://www.tianqi.com/news/231148.html.
[222] ecoscore.be, How to calculate the CO2 emission from the fuel consumption?, 2020. https://ecoscore.be/en/info/ecoscore/co2. (Accessed 31-08 2021).
[223] energy Information Administration (EIA), How much carbon dioxide is produced per kilowatthour of U.S. electricity generation?, 2020.